Energy Transfer in Hot Gases

U. S. Department of Commerce
National Bureau of Standards
Circular 523

UNITED STATES DEPARTMENT OF COMMERCE • Sinclair Weeks, *Secretary*
NATIONAL BUREAU OF STANDARDS • A. V. Astin, *Director*

Energy Transfer in Hot Gases

Proceedings of the NBS Semicentennial Symposium on
Energy Transfer in Hot Gases Held at the NBS on
September 17 and 18, 1951

National Bureau of Standards Circular 523
Issued March 10, 1954

For sale by the Superintendent of Documents, U. S. Government Printing Office
Washington 25, D. C. - Price $1.50 Buckram

Foreword

The Symposium on Energy Transfer in Hot Gases was the sixth in a series of 12 conferences held at the National Bureau of Standards during 1951, the year which marked the 50th anniversary of its establishment. The problems of radiation from flames and hot gases, and of basic chemical and physical mechanisms governing energy transfer in those media, are subjects of current interest in which several divisions of the National Bureau of Standards have been active.

These problems are of both theoretical and practical importance in a number of fields. The improvement of heating devices of all kinds, of jet motors, gas turbines, and internal-combustion engines, depends upon a fuller understanding of the detailed mechanisms of energy transfer and the combustion process. Much the same problems arise in widely diverse areas; for example, in high-speed aerodynamics and in the effects of solar radiation on the upper atmosphere. The production and utilization of high temperatures in chemical technology is increasing.

The generous cooperation of the Office of Naval Research in making this Symposium possible is gratefully acknowledged. The program of the Symposium was planned and conducted by E. F. Fiock and W. S. Benedict; A. M. Bass has edited the papers and prepared this volume.

A. V. Astin, *Director,*
National Bureau of Standards.

Contents

1. Processes of Electronic Excitation in Relation to Flame Spectra

By A. G. Gaydon[1]

Introduction

Those who have studied flame spectra are usually aware that there is evidence for marked departures from equilibrium in the radiation from at least some parts of some flames. Although these departures from equilibrium are important and may give us a lot of interesting information, for their full appreciation we should first consider the normal thermal processes of radiation, which are, after all, responsible for the main body of radiation from the hot interconal gases in flames.

The processes by which atoms and molecules are excited and caused to radiate will therefore be considered first. Prof. Laidler and Dr. Shuler [1][2] have given a very good review of radiation processes in flames. They have discussed a large number of specific mechanisms which may lead to the formation of molecules in excited electronic states, that is to chemiluminescence, and have greatly clarified our ideas on this subject. Their ideas and some of their data are used freely here, but the general approach to the subject will be very different as the basic processes rather than the specific mechanisms will be considered.

The Mechanism of Electronic Excitation

In most of our spectroscopic work we are familiar with excitation produced by free electrons. In discharge tubes and arcs the excitation is clearly caused by collisions by electrons that are accelerated in the electric field, but in flames the concentration of free electrons is expected to be relatively small, and there is no electric field to accelerate them. It is true that there is evidence that the concentration in flames of ions may be abnormally high, [2] especially in the reaction zone of organic flames, but it seldom exceeds 10^{12} ions/cm^3, so that usually a molecule makes more than a million collisions with other molecules for each collision with a free electron. Only a very small proportion of the free electrons will, in any case, possess sufficient kinetic energy to cause excitation, and the chance of the transfer of this energy to a relatively massive molecule is also very small. Thus we can eliminate the possibility of excitation by free electrons playing an important role in flame gases.

We must therefore consider the possibility of excitation by collision with other molecules. The principle of microreversibility may be applied to systems in equilibrium, and information about the deactivation of electronically excited molecules and atoms obtained from studies of the quenching of fluorescence may be used to tell us about the likelihood of the reverse process of excitation.

---

[1] Imperial College, London, S. W. 7, England.

[2] Figures in brackets indicate the literature references on p. 8.

One would not expect a collision with a relatively heavy inert atom easily to affect the orbits of the relatively light electrons attached to a molecule, and indeed the rare gases are found to be extremely inefficient in removing electronic excitation. It seems, however, that diatomic and polyatomic molecules may be relatively efficient at quenching of fluorescence, due presumably to the possibility of converting the electronic excitation energy into that of intramolecular vibration or rotation. The efficiency of quenching of fluorescence is, however, extremely variable. Studies of the deactivation of excited sodium atoms show that for rare gases the collision cross section is practically zero; for carbon monoxide it is about 28×10^{-16} cm^2, for ethylene 40×10^{-16}, but for methane only 0.11×10^{-16}. Thus we see that it varies very much from one molecule to another. This variation is best interpreted in terms of the collision complex momentarily formed between the excited sodium and the colliding molecule. The problem bears some resemblance to that of predissociation in a diatomic molecule. The collision complex may be visualized as having a number of potential energy surfaces corresponding to the various possible electronic configurations. At any instant during the collision, the state of the complex molecule may be represented by a point on one of these surfaces, the point moving over the surface with time. If this surface intersects another surface, then we have the possibility of a radiationless transition from the initial electronic configuration to that corresponding to the intersecting surface, and then on dissociation of the complex molecule we may find that one or both of the products are in different electronic states from those in which they were when they originally collided.

We thus visualize deactivation of an excited atom as due to a radiationless transition during the collision, the electronic excitation energy being converted into internal motion (i. e., vibration) of the colliding molecule. The reverse process of excitation will enable vibrational energy to be converted to electronic excitation. The likelihood of excitation will depend very much on the form and crossings of the potential surfaces of the collision complex, and the marked variation in quenching efficiency from molecule to molecule is understandable.

One important conclusion comes out of this qualitative discussion. If the temperature of a gas that is not in equilibrium is measured from the proportion of electronically excited atoms, i. e., by the spectrum-line reversal method, then this temperature may be more closely related to the average vibrational energy of the gas molecules, that is, to their effective vibrational temperature, than to their translational energy. This has probably not been realized before.

Vibrational Energy Lag in Flame Gases

This brings us to the possibility of lag in the equipartition of vibrational energy with that in other forms. In the past various strange effects in flames have been attributed to this cause, but we must examine the possibility rather critically. It seems that for some molecules, such as CO_2, the vibrational energy can only be converted into translational energy with difficulty and may occur on the average only after around 50,000 collisions; these observations are, however, made from measurements of ultrasonic dispersion in gases at or around room temperature. The majority of molecules probably pass on vibrational energy rather more easily than does CO_2, and also we shall expect the conversion of vibrational energy into translational energy, and vice versa, to become much easier at high temperature. At higher temperature kT (where k is the Boltzmann constant) will become of the same order as the vibrational energy, determined by the vibrational frequency ω, and thus, in flame gases, delays in equipartition of vibrational energy should be less important. If we allow an average of 1,000 collisions for the removal of excess vibrational energy and remember that in flame gases a molecule suffers about 10^9 collisions per second, equipartition of vibrational and translational energy may be expected in around 10^{-6} sec. Even the fastest laminar flames only have a burning velocity of about 10 m/sec. so any vibration lag should not be expected to persist for more than a distance of the order 1/100 mm. This figure should, perhaps, be corrected for expansion of the gases as they become heated in their passage through the reaction zone, and so be corrected to 1/10 mm. For slower flames with air, however, the distance should be much less.

The Effect of Radiative Disequilibrium

Most laboratory flames are optically thin and emit discontinuous radiation and thus do not approach the black-body condition where the radiation shows a continuous spectrum and is equal in amount to that given by the radiation laws for a body of unit emissivity. The radiation from the gas is not balanced by absorption of radiation.

The atoms and molecules in the flame will be subject to electronic excitation and deactivation by collision processes, and excited ones will also be deactivated by emission of radiation, but the reverse process of absorption of radiation will not occur to an appreciable extent. Now from the quenching of fluorescence we can get a measure of the amount of activation and deactivation by collision. From measurement of the absorption spectrum we can get the transition probability and from this the radiative lifetime. It is thus possible to compare the deactivation due to radiation with that due to collision processes.

This is best illustrated by a simple numerical example of sodium in an atmosphere of nitrogen at 2,000° K; this corresponds fairly closely to a flame with air and is of interest for the sodium-line reversal measurement of flame temperature. From the quenching of Na fluorescence by N_2 it can be shown that a sodium atom would suffer about 3.11×10^9 collisions per second [3] corresponding to a collision lifetime of 3.2×10^{-10} sec, while the free radiative lifetime is 1.6×10^{-8} sec. Thus the deactivation by radiation is about 2 percent of that due to collisions. Now we can use the usual Maxwell-Boltzmann distribution law to calculate the proportion of sodium atoms that should be in the excited state for equilibrium, and then assuming a 2 percent reduction in this population we can with the same law deduce the temperature to which this slightly reduced population would be equivalent. We find, in this way, a difference of 3.3°, so that if there is emission of radiation without reabsorption, the effective electronic excitation temperature for Na under these conditions would be 3.3° lower than the true gas temperature.

The Spectrum-Line Reversal Method of Measuring Temperature

In the familiar measurement of flame temperature by the sodium-line reversal method, a bright background source giving a continuous spectrum is placed behind the flame, an image of the source being thrown into the flame with a lens. The flame is colored with a little sodium, which may be introduced by spraying or other means, and an image of both background source and flame are then together thrown onto the slit of the spectroscope with a second lens. If the flame is the hotter the Na *D* lines are seen in emission, if the background source is hotter then the lines appear in absorption against the continuous spectrum. At the reversal point, the lines just disappear and this occurs when the brightness temperature of the background, which can be measured with an optical pyrometer, is equal to the flame temperature.

The essential measurement is the comparison of the strength of absorption and emission, and the result is really that temperature which would, in complete equilibrium, correspond to the actual ratio of populations of excited and unexcited Na atoms. If loss of excited atoms by emission of radiation occurs, the temperature will depart slightly from the true flame temperature, but the measurement should still correctly give the ratio of the populations.

We have seen that with sodium in N_2 at 1 atm and 2,000° K, an optically thin flame will have an effective excitation temperature which is 3.3° too low. Now in making a temperature measurement by the reversal method, it is usual to put sufficient sodium into the flame to give a fairly strong line, so that it can be seen in absorption. Under these conditions the flame is not optically thin for the central wavelength of the lines. However, even under these conditions the Na atoms in the outer layers of the flame, which are dominant for an optically thick flame, emit over an angle of 4π and only receive radiation from an angle of 2π, so that we may still expect about half the simply calculated error. Also the wings of the spectrum lines, for which the flame is still optically thin, will show the full effect. An error of about 2° is therefore to be expected at atmospheric pressure. This is for a flame consisting mainly of nitrogen; rather different results will be expected for gases of different composition; thus the radiation losses would be very much more serious in an atmosphere of methane, which is relatively inefficient for collision excitation and deactivation. Atoms other than Na will also behave quantitatively differently. Also in flames at reduced pressure the difference between the true flame temperature and the effective electronic excitation temperature will be greater.

The Temperature Distribution in Flames

The simple Bunsen-type flame may be considered as divided into three regions: I, the inner cone, or reaction zone; II, the interconal gases above this inner cone; and III, the outer cone, which is really a diffusion flame. Spectroscopic studies of diffusion flames by Wolfhard and Parker [4] show that there are few if any departures from thermal equilibrium in this type of flame. Similarly, there is not much reason to doubt that the interconal gases will be in fairly good thermal and chemical equilibrium; there may be a few exceptions, especially in flames of near-limit mixtures and for establishment of the $2\ NO \rightleftarrows N_2 + O_2$ equilibrium. Thus for the main body of the flame, covering regions II and III, there should not be any great difficulty in defining and measuring the temperature.

The maximum flame temperature, as measured by the sodium-line reversal method, in the interconal gases is usually close to the theoretically calculated value. Lewis and von Elbe [5] have shown some excellent plots of the temperature distribution in flames, using a rectangular burner viewed edge on, with the center only of the flame colored with sodium. The general results are rather as one might expect; for weak mixtures, with excess air, the highest temperature is attained above the inner cone in the center of the flame; for rich mixtures, however, the temperature through the interconal gases is fairly uniform, with temperature maxima on each side in the region of the outer cone or diffusion flame. There are, however, some interesting and unexplained features about these temperature plots. With the weak mixture, for a natural-gas–air flame, the full maximum temperature is not attained immediately above the inner cone, but only at a distance of from 6 to 10 mm higher up. A similar plot for a weak natural-gas–oxygen flame also has a rather unusual form, but of a different type. In this case we have a thin region just above the inner cone where the measured temperature is about 150° above the theoretical maximum flame temperature.

These effects have never been satisfactorily explained. They are not peculiar to the observations of Lewis and von Elbe; many authors have obtained similar results. It does not seem as though they can easily be explained as due to a lag in vibrational excitation. Too low a temperature by the sodium-line reversal method would, as already suggested, probably indicate a deficiency of vibrational energy; in the flame with air the departure from equilibrium persists for 6 to 10 mm, whereas vibrational lag should only persist for perhaps 0.01 mm in this rather slow flame. Persistence of free atoms is a more likely cause of the delay in reaching the full temperature in the air flames. Combustion processes proceed mainly by bimolecular reactions, but the recombination of free atoms usually requires three-body collisions and is therefore less rapid. The full flame temperature cannot be attained until after the completion of the large heat release due to the recombination of free atoms formed in the reaction zone. If the recombination were, however, to occur with Na atoms as third body, then it might result in a form of chemiluminescence and lead to too high a temperature.

Detailed Study of the Reaction Zone

In the reaction zone, or flame front, corresponding to region I, the inner cone of the Bunsen flame, we cannot expect chemical equilibrium and perhaps not thermal equilibrium. Studies of temperature by optical means and of emission spectra are, however, important for telling us about the state of the reacting gases. The difficulty of making measurements is mainly the extreme thinness of the reaction zone. In optical measurements it is necessary to use sufficient optical aperture to fill the instrument, e. g., a spectrograph. Thus even if a flame with a long, flat reaction zone is developed for use, it is still difficult to examine the spectrum of the zone alone without the light also traversing a relatively thick region of interconal gases. Thus with an optical aperture of $F/10$ and a flame, such at that of oxy-acetylene, with a reaction zone 1/50 mm thick the maximum usable length of reaction zone is only 1/5 mm. Long, flat reaction zones are therefore of little use unless very small apertures can be used, and this can only be done by using very small images of the flame and by sacrificing speed in photography. It is also difficult in practice to keep such flames sufficiently steady (to 1/50 mm) and to focus sharply to this accuracy.

A technique developed by Dr. Wolfhard and the author [6] is to make use of the much thicker reaction zones obtained with flames at low pressure. Flames may be run down to well below 1/100 atm, and the reaction zone then becomes over 1 cm thick, so that quantitative measurements become possible. The great strength of the emission from the reaction zone compared with that from the interconal gases immediately above it should be stressed. This is true for OH radiation as well as for the visible bands of C_2, CH, etc.

In the oxyhydrogen flame the OH radiation is relatively weak and there is no clear difference in the radiation from the reaction zone and that from the burnt gases. With the addition of only 0.75 percent of acetylene the emission from the reaction zone is increased by a factor of about 20, while that from the burnt gases is not altered. This is shown by published photographs [7] in which the addition of the acetylene reduced the exposure for comparable blackening from 2 hr to 6 min. It is also very obvious that there is a change in the appearance of the OH band due to its much higher effective rotational temperature in the flame containing acetylene. This marked increase in OH emission and the change from a normal to a very high rotational temperature in hydrocarbon flames appears indisputable evidence of chemiluminescent excitation of OH in these low-pressure flames.

The disequilibrium in the reaction zone can also be examined using the spectrum-line reversal method. For work at low pressure it is easier to introduce either iron carbonyl or lead ethyl than sodium. With lead ethyl in an acetylene-air flame at low pressure we find [8] that, against the background of the carbon arc the resonance line of Pb at 2,833 A appears in absorption, but that other neighboring lines of Pb remain in emission even against this very bright background, which has a temperature of about 3,800° K. This is further qualitative proof of the disequilibrium in the reaction zone. More quantitative evidence is obtained by measuring the reversal temperature for various lines. These results have been published in detail [8]. Lines of low excitation energy (below about 18,000 cm^{-1}) give a temperature near that to be expected for the flame gases, around 2,000° K. As soon, however, as we come to lines with higher excitation energy we find an excessive population in the upper electronic state. For lines of Fe in the ultraviolet the reversal temperature reaches about 3,500° K for the acetylene-air flame. We may express this in terms of the relative populations in the excited electronic states and for the most highly excited Fe lines the population in the excited state is found to be of the order of a million times greater than for a temperature of 2,000° K, the value given by the Na lines.

These results are for acetylene-air flames, but most organic flames show similar effects. Formaldehyde, carbon monoxide, and hydrogen do not, however, show the abnormal excitation effect. While the effect is only measurable at low pressure. it appears to occur as well at 1 atm. Flames containing a little Fe show a much fuller development of the Fe lines in the inner cone than in the interconal gases.

Predissociation

In some band spectra there is an abrupt termination of the branches of the rotational fine structure. It is due to the possibility of a radiationless transition from certain energy levels to other levels of a state that is unstable. In complete equilibrium the radiationless transition to the unstable state, followed by dissociation of the molecule, will be balanced by the reverse process, association of two atoms on collision to form a molecule in the unstable state, which then undergoes radiationless transition to the stable state. Under nonequilibrium conditions of excitation, however, there will be a depopulation of the levels affected by the predissociation and lines arising from such levels will show as weakened lines or may be entirely absent from the emission spectrum. The observation of breaking-off of rotational structure in a band system can therefore be made to serve as a sensitive test for the existence or otherwise of equilibrium in the excitation conditions.

In flames the normal appearance of the 3,900–A band of CH is with a marked predissociation in the highest rotational levels of the (0,0) band and in rather lower levels of the (1,0) band. Dr. Durie [9], working in my laboratory, has found that flames of rich mixtures of hydrogen to which a little ethylene or other hydrocarbon have been added show further lines of the structure, the normal predissociation being absent or at least much weaker. This presumably indicates a closer approach to equilibrium in this flame, and therefore that there are departures from equilibrium in the excitation of CH in ordinary flames.

Recently a weak predissociation has been observed by Dr. Wolfhard and the author [10] in the rotational levels of the $v'=2$ and $v'=3$ states of OH, and this has been confirmed by Dr. Broida and Dr. Shuler and forms the subject of a paper in this volume. This predissociation has the apparent effect of modifying the vibrational structure. In some low pressure flames the (2,1) band of OH is accentuated, while in some flames of hydrogen with air at atmospheric pressure the (3,2) as well as the (2,1) band is enhanced [7]; the explanation of this has been discussed in detail [10]. Here the main point is to stress that observations of such effects can tell us about departures from equilibrium in reacting gases.

Summary

Observations of flame spectra and most optical methods of temperature measurement depend on electronic excitation. This occurs not by collision with free electrons but by collision with molecules carrying energy as internal vibrational energy. The spectrum-line reversal method of temperature measurement gives basically the electronic excitation temperature; if equilibrium is not established this is likely to be closer to the vibrational than to the translational temperature of the gas.

In small flames, lack of radiative equilibrium must lead to a small error in temperature measurements by the reversal method. For Na in a flame with air the error is only about 2°. Temperature anomalies above the inner cones of flames are unlikely to be due to vibrational lag; they may be due to the persistence of free atoms. Thermal equilibrium is not maintained in the reaction zones of organic flames. Effective rotational temperatures for OH bands are much too high, the radiation from the zone is very much greater than from the interconal gases, and measurements of excitation temperature by the spectrum-line reversal method for lines in the ultraviolet come very high. The causes of this abnormally high excitation are unknown. It is suggested that observations of predissociation of band systems such as CH in flames may serve as a sensitive test for the existence or otherwise of thermal equilibrium.

In conclusion, I express my sincere thanks to the National Bureau of Standards for the invitation to attend the Symposium. I am also very grateful to those who have extended such warm hospitality to me during this visit.

References

[1] K. J. Laidler and K. Shuler, Chem. Rev. **48**, 153 (1951).
[2] H. F. Calcote, Third Symposium on Combustion, Wisconsin 1948, p. 245.
[3] A. G. Gaydon and H. G. Wolfhard, Proc. Phys. Soc. [A] **65**, 19 (1952).
[4] H. G. Wolfhard and W. G. Parker, Proc. Phys. Soc. [A] **62**, 722 (1949); **65**, 2 (1952).
[5] B. Lewis and G. von Elbe, J. Chem. Phys. **11**, 75 (1943).
[6] A. G. Gaydon and H. G. Wolfhard, Proc. Roy. Soc. [A] **194**, 169 (1948); **199**, 89 (1949); **201**, 561 (1950); **201**, 570 (1950).
[7] A. G. Gaydon and H. G. Wolfhard, Rev. inst. franc. pétrole et Ann. combustibles liquides **4**, 405 (1949).
[8] A. G. Gaydon and H. G. Wolfhard, Proc. Roy. Soc. [A] **205**, 118 (1951).
[9] R. A. Durie, Proc. Phys. Soc. [A] **65**, 125 (1952).
[10] A. G. Gaydon and H. G. Wolfhard, Proc. Roy. Soc. [A] **208**, 63 (1951).

2. Studies of Some Polyatomic Flame Bands[1]

By George A. Hornbeck * and Robert C. Herman [2]

Introduction

It has been known for many years that bands with complex structure are found in the spectra of flames of ammonia, carbon monoxide, hydrogen, and hydrocarbons burning with air or oxygen [1].[3] Some investigators have suggested that the α-bands of the ammonia-oxygen flame spectrum are emitted by the NH_2 radical, that the so-called CO flame bands are emitted by carbon dioxide, that the long wavelength complex bands in the hydrogen-oxygen flame spectrum are emitted by water, and that the hydrocarbon flame bands are emitted by the HCO radical. The photographic infrared bands of the hydrogen-oxygen flame were provisionally assigned by Kittagawa [2] to the vibration-rotation spectrum of water, which assignment was subsequently verified by Gaydon [1] and recently by Benedict, [3] who is making a complete rotational analysis of many of the water bands. Although there is considerable evidence in support of the suggested emitters of the other flame bands, there has never been a complete analysis of these spectra. A complete spectral analysis of such flame bands has been difficult because of (a) the complexity of electronic polyatomic spectra; (b), the fact that the best conditions for obtaining most of these flame bands have been with sources of weak intensity, thereby precluding the feasibility of obtaining high dispersion spectrograms; and, (c), the frequent overlapping of rotational structure by diatomic spectra. The purpose of this paper is to describe a method for obtaining these flame bands that virtually eliminates the effect of overlapping diatomic spectra and provides a source of sufficient intensity to permit high dispersion spectrograms. Several electronic band systems are briefly discussed, and evidence for identifying their emitters is given. Special emphasis is placed on the spectrum of the so-called hydrocarbon flame bands.

Experimental

There is no characteristic spectrum that one can associate with the flame of a given fuel. It has been shown that the spectrum is very dependent on flame conditions, principally the fuel-oxygen ratio and the temperature [4]. Adjusting the fuel-oxygen ratio can raise or lower the temperature, while significantly lower temperatures can be

---

[1] The work described herein was supported by the U. S. Navy Bureau of Ordnance.
[2] Applied Physics Laboratory, The Johns Hopkins University, Silver Spring, Md.
[3] Figures in brackets indicate the literature references on p. 18.
* Present address National Bureau of Standards.

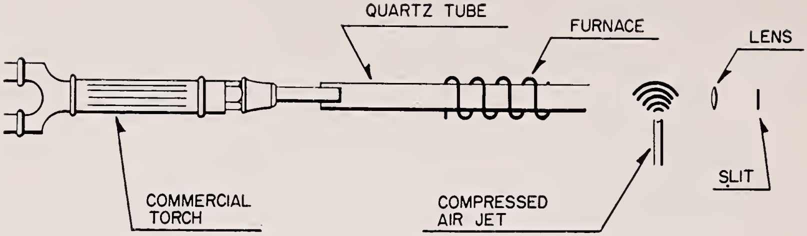

FIGURE 2.1. *Schematic diagram of low temperature burner used for high oxygen-fuel ratios.*

produced by the introduction of such diluents as nitrogen, carbon dioxide, and the inert gases [5]. The authors have found that electronic polyatomic flame bands are obtained best in a flame with the fuel-oxygen ratio quite small; i. e., of the order of 0.01 to 0.05. In order to stabilize a flame with such a lean mixture it is necessary to employ a flame holder of rather large orifice. An easily constructed burner that satisfies the requirement of large orifice and high mass flow is shown in figure 2.1. This burner consists of a commercial acetylene torch feeding into a quartz tube of 1 in. inside diameter and 8 in. long. The torch tip is cut off and the mixing baffle removed in order to permit gas flow up to 100 liters per minute. The quartz tube is fitted to the torch over a teflon bushing and the joint is completed with a high-temperature sealing compound such as alundum or water glass. In place of the furnace that is indicated in figure 2.1, a bunsen burner can be used to obtain a hot annular area on which the flame stabilizes. The burner or the furnace can be removed once the flame inside the quartz tube is established. Since the flame is viewed end on, it is essential that the optical elements in front of the burner be protected from the hot exhaust gases by a jet of compressed air near the open end of the quartz tube.

Hydrocarbon Flame Bands

Two densitometer tracings of spectrograms from acetylene-oxygen flames are shown in figure 2.2. The top tracing is from a flame with acetylene and oxygen in stoichiometric proportions burning from an ordinary commercial torch. All of the prominent band structure in the spectral region shown has been identified as due to the diatomic species given in table 2.1. The lower tracing is from an acetylene flame burning with a fuel-oxygen ratio of about 0.025, using the burner shown in figure 2.1. All the bands other than the 3064A OH band belong to a system usually referred to as the "hydrocarbon flame bands." This system was first observed by Vaidya [6] in the inner cone of a split burner using ethylene and air. His source intensity was very low and necessitated exposures of long duration (~50 hours) to obtain spectrograms of adequate density. Vaidya found that he could not arrange these bands into a single vibrational scheme, nor did the frequencies associated with these bands agree with those known for the diatomic molecules found in hydrocarbon flames. He therefore concluded that the emitter of this band system was a polyatomic molecule or radical. In an effort to obtain significant vibra-

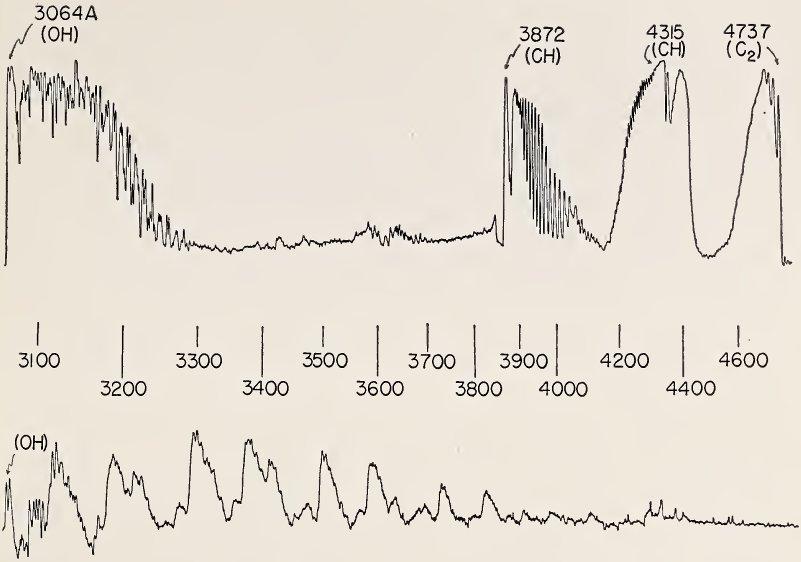

FIGURE 2.2. *Densitometer tracings of oxyacetylene flame spectra taken at medium quartz dispersion to compare "hot" flame (above) to "cool" flame (below).*

tional frequencies most of the bands were fitted into a vibrational array that suggested frequencies of 1,072 cm^{-1} and 1,960 cm^{-1}. Since his spectrum did not appear to show any vibrational structure similar to that in the fluorescence or absorption spectra of formaldehyde, which possesses similar vibrational frequencies, Vaidya was led to attribute the bands to the HCO radical. He offered in support of this hypothesis the comparison of his spectra with that of the isoelectronic NO molecule which has vibrational frequencies of 1,029 cm^{-1} and 1,889 cm^{-1}. In 1951 Vaidya continued his investigation by means of the isotope effect, burning deuterated acetylene with atomic oxygen [7]. This work demonstrated that the emitter contained at least one hydrogen atom. On the basis of these measurements he made new vibrational quantum number assignments. By extending the spectrum further into the ultraviolet he observed a new set of bands, which he correlates with the bending of the HCO radical. Finally, by an approximate treatment of HCO as a diatomic molecule, assuming that the HC group moves as a unit, Vaidya attempted to

TABLE 2.1.

Species	Transition	Name of band system
C_2	$^1\Pi_g \rightarrow {}^1\Pi_u$	Deslandres-D'Azambuja.
C_2	$B^3\Pi_g \rightarrow {}^3\Pi_u$	Fox-Herzberg.
C_2	$A^3\Pi_g \rightarrow {}^3\Pi_u$	Swan.
OH	$^2\Sigma^+ \longrightarrow {}^2\Pi$	OH bands.
O_2	$^3\Sigma^-_u \rightarrow {}^3\Sigma^-_g$	Schumann-Runge.
CH	$^2\Sigma^+ \longrightarrow {}^2\Pi$	3143A system.
CH	$^2\Sigma^- \longrightarrow {}^2\Pi$	3900A system.
CH	$^2\Delta \rightarrow {}^2\Pi$	4315A system.

calculate the mass factor, and thereby the reduced mass of the emitter. In spite of these efforts the identity of the emitter has not been established with certainty. It appears that this failure stems in part from the insufficient knowledge obtained from measurements of these bands at low dispersion.

Apart from Vaidya's investigations there has been little progress in the analysis of these bands, and because of the low intensity of earlier flame sources, a study of the rotational structure of these bands has been impractical. The work of Dyne and Style [8] on the fluorescence of formaldehyde in which they obtained the hydrocarbon flame bands by exciting formaldehyde with ultraviolet light suggests that the emitter is HCO, but it does not preclude other possible emitters, in particular formaldehyde itself. Unfortunately, the intensity of Dyne and Style's source was also quite weak and did not permit high-dispersion studies.

The improved source for the hydrocarbon flame bands that was described earlier in this paper also does not have sufficient intensity to permit the use of grating spectrographs with ultimate dispersion and resolving power, but it has been satisfactorily used with spectrographs of ~150,000 resolving power. A large number of spectrograms have been taken of this relatively low temperature burner on spectrographs of various dispersions, and plates have been obtained involving fewer bands of this system than reported by Vaidya. The individual bands involve lower J values than those from the higher temperature source used by Vaidya, and most of the bands are entirely free of overlapping diatomic structure, permitting more accurate measurements to be made. Table 2.2 contains measurements of the band heads that appear under the low temperature conditions of the flame in the tube type burner. This group of bands constitutes the "A" band progressions in Vaidya's work. There is an appreciable difference between Vaidya's measurements and ours. With the higher dispersion (4 A/mm) in the experiments reported here, it was possible to observe more accurately the true heads of these bands that lie to the short wavelength side of the apparent heads at low dispersion.

Very little significance can be attached to a vibrational array of polyatomic bands involving only two quantum numbers. However, it is interesting to note that all but the last five of the bands in table 2.2 can be fitted into an array that offers fairly smooth vertical and horizontal differences. The two vibrational frequencies obtained with this arrangement are 1,782 and 2,851 cm^{-1}. It should be noted that 1,782 cm^{-1} is very close to the characteristic frequency of $C{=}O$, while 2,851 cm^{-1} lies within the range of the valence vibration of the C—H bond (2,800 to 3,300 cm^{-1}). This arrangement of the bands is presented in table 2.3.

One of the significant features in the gross structure of these bands that is emphasized by the use of the lower-temperature flame source, is the appearance of what may be quadratic K structure (see fig. 2.4). If the assignment of HCO as the emitter is correct, then the observed K structure precludes HCO from being linear. However, if the structure is due to multiplicity and is not K structure, the emitter need not be bent. Spectrographs of very high resolving power may be needed to satisfactorily answer this question.

Another suggestive feature of this spectrum is the alternation of single and double bands throughout the entire spectrum except for

TABLE 2.2. *Hydrocarbon flame bands*

Wavelength			
A	*cm*$^{-1}$	*A*	*cm*$^{-1}$
3824.15	26142.23	2945.73	33937.55
2729.91	26802.72	2857.78	34981.96
2588.49	27858.96	2794.67	35771.84
4501.59	28550.38	2748.67	36369.57
3377.10	29608.44	2714.49	36828.43
3298.27	30310.25	2664.43	37520.33
3186.07	31377.63	2618.60	38176.96
3114.87	32094.77	2535.76	39424.07
3014.46	33163.83		

TABLE 2.3. *Possible array for some hydrocarbon flame bands.*

Wavelength		
cm^{-1}	*cm*$^{-1}$	*cm*$^{-1}$
26142.23	-----------	-----------
(1716.73)	-----------	-----------
27858.96	-----------	-----------
(1749.48)	-----------	-----------
29608.44	(2799.98)	26802.72
(1769.19)	-----------	(1747.66)
31377.63	(2827.25)	28550.38
(1786.20)	-----------	(1759.87)
33163.83	(2853.58)	30310.25
(1818.13)	-----------	(1784.52)
34981.96	(2887.19)	32094.77
(1846.47)	-----------	(1842.28)
36828.43	(2890.88)	33937.55

the last five bands listed in table 2.2. It is possible that the single bands are electronic parallel bands consisting of a number of subbands disposed in the manner of Q branches, each of which has P, Q, and R branches, while the double bands may be perpendicular bands with the subbands disposed about the origin in the manner of P and R structure, with each subband possessing P, Q, and R branches.

Spectrograms with good resolution indicate that there are two bands of the hydrocarbon flame band system that offer the best possibilities for studies of the rotational structure. These are the bands at 3377 and 3014 A. The 3377A band is shown in figure 2.3. The lines that were measured are numbered and the wavelengths in A and cm^{-1} in vacuum are given in table 2.4. It is obvious from the densitometer tracing in figure 2.3 that complete resolution was not achieved in this spectrogram. However, we have recently obtained plates with considerably improved resolution that should permit study of the rotational structure.

Another approach we have used in trying to determine the emitter of the hydrocarbon flame bands has been to obtain the spectrum of the acetylene-d flame bands at both low and medium dispersion. This spectrum is compared with the hydrocarbon flame bands taken on a medium quartz prism spectrograph in figure 2.4. There is no simple or regular shift caused by the deuterium substitution, and the deuterocarbon bands are very different in character and particularly more diffuse than the bands from the acetylene-h flame. In fact, the extreme diffuseness of the deuterocarbon bands made reproducible measurements of the bands very difficult. The reason for this is not easily understood in view of the 95 percent purity of the deuterated acetylene

TABLE 2.4. *3377–A hydrocarbon-flame band*

Line	Wavelength		Line	Wavelength		Line	Wavelength	
	A	cm^{-1}		*A*	cm^{-1}		*A*	cm^{-1}
1	3375.21	29619.34	51	3400.55	29398.59	101	3426.65	29174.70
2	3376.45	29608.44	52	3400.81	29396.33	102	3427.05	29171.30
3	3376.75	29605.83	53	3401.15	29393.43	103	3427.38	29168.50
4	3377.26	29601.31	54	3401.50	29390.43	104	3427.79	29164.95
5	3377.62	29598.13	55	3402.58	29381.06	105	3428.35	29160.23
6	3378.08	29594.11	56	3402.87	29378.58	106	3429.12	29153.65
7	3378.46	29590.86	57	3403.48	29373.33	107	3429.71	29148.68
8	3378.86	29587.35	58	3404.33	29365.98	108	3430.30	29143.61
9	3379.29	29583.56	59	3404.78	29362.07	109	3430.85	29138.94
10	3379.84	29578.72	60	3405.51	29355.83	110	3431.42	29134.11
11	3380.11	29576.36	61	3406.26	29349.30	111	3431.94	29129.68
12	3380.43	29573.57	62	3406.84	29344.37	112	3432.31	29126.54
13	3380.94	29569.09	63	3407.11	29341.96	113	3433.08	29120.00
14	3381.38	29565.26	64	3407.35	29339.92	114	3433.77	29114.18
15	3381.75	29562.00	65	3407.98	29334.49	115	3434.49	29108.06
16	3382.28	29557.39	66	3408.14	29333.12	116	3435.12	29102.72
17	3382.86	29552.36	67	3408.62	29328.99	117	3435.89	29096.24
18	3383.12	29550.03	68	3408.86	29326.93	118	3437.20	29085.10
19	3383.73	29544.74	69	3409.26	29323.52	119	3437.37	29083.74
20	3384.02	29542.20	70	3409.76	29319.21	120	3437.96	29078.71
21	3384.77	29535.69	71	3410.13	29316.01	121	3438.64	29072.93
22	3385.42	29529.99	72	3411.54	29303.88	122	3439.48	29065.90
23	3386.40	29521.43	73	3411.76	29302.01	123	3440.50	29057.26
24	3387.02	29516.08	74	3412.04	29299.59	124	3441.12	29052.01
25	3387.56	29511.36	75	3412.60	29294.83	125	3441.52	29048.67
26	3388.21	29505.69	76	3413.50	29287.04	126	3441.85	29045.84
27	3388.96	29499.14	77	3414.72	29276.63	127	3442.37	29041.48
28	3389.60	29493.58	78	3414.94	29274.72	128	3442.95	29036.54
29	3390.06	29489.53	79	3415.52	29269.79	129	3443.74	29029.90
30	3390.62	29484.73	80	3416.30	29263.04	130	3444.24	29025.66
31	3391.48	29477.21	81	3416.87	29258.19	131	3445.15	29018.00
32	3391.80	29474.41	82	3417.22	29255.18	132	3445.68	29013.60
33	3392.07	29472.06	83	3417.84	29249.90	133	3446.24	29008.83
34	3392.38	29469.39	84	3418.26	29246.33	134	3446.91	29003.24
35	3392.93	29464.63	85	3418.92	29240.64	135	3447.56	28997.74
36	3393.35	29461.00	86	3419.65	29234.40	136	3448.38	28990.82
37	3393.74	29457.61	87	3420.46	29227.49	137	3448.98	28985.77
38	3394.39	29451.93	88	3420.99	29222.99	138	3449.79	28978.98
39	3395.36	29443.57	89	3421.17	29221.40	139	3450.16	28975.86
40	3395.96	29438.35	90	3421.60	29217.76			
41	3396.66	29432.31	91	3421.94	29214.87			
42	3396.81	29430.98	92	3422.79	29207.60			
43	3397.49	29425.07	93	3423.15	29204.50			
44	3397.90	29421.57	94	3423.47	29201.81			
45	3398.25	29418.48	95	3423.80	29198.97			
46	3398.78	29413.95	96	3424.08	29196.54			
47	3399.09	29411.20	97	3424.29	29194.81			
48	3399.34	29409.10	98	3424.59	29192.25			
49	3399.72	29405.74	99	3425.02	29188.54			
50	3400.02	29403.16	100	3425.89	29181.15			

[1] See fig. 2.3.

TABLE 2.5. *Prominent gross structure in deuterocarbon-flame bands*

Wavelength			
A	cm^{-1}	*A*	cm^{-1}
2481.00	40294.24	3260.90	30657.58
2548.85	39221.55	3274.75	30527.93
2602.83	38408.28	3345.95	29878.36
2672.90	37401.41	3366.63	29694.79
2735.93	36539.84	3384.76	29535.71
2760.71	36212.02	3441.74	29046.76
2820.49	35444.41	3461.88	28877.77
2907.49	34383.86	3479.35	28732.81
2928.84	34133.22	3558.12	28096.77
2984.01	33502.23	3580.03	27924.82
3004.10	33278.17	3602.20	27752.95
3014.99	33158.00	3686.67	27117.06
3091.50	32342.63	3708.27	26959.14
3103.00	32217.55	3801.08	26300.91
3175.62	31480.86	3823.02	26149.92
3189.89	31339.98	3942.41	25358.10
3207.16	31171.21	3967.40	25198.32
3250.19	30758.56		

reported earlier [4]. For the sake of completeness approximate positions for the most prominent structure are given in table 2.5.

The above discussion may serve to emphasize the complexities that are encountered in attempting to understand the spectrum of the hydrocarbon flame bands and indicates the necessity of additional study before any assignment of an emitter for the hydrocarbon-flame bands can be made with certainty.

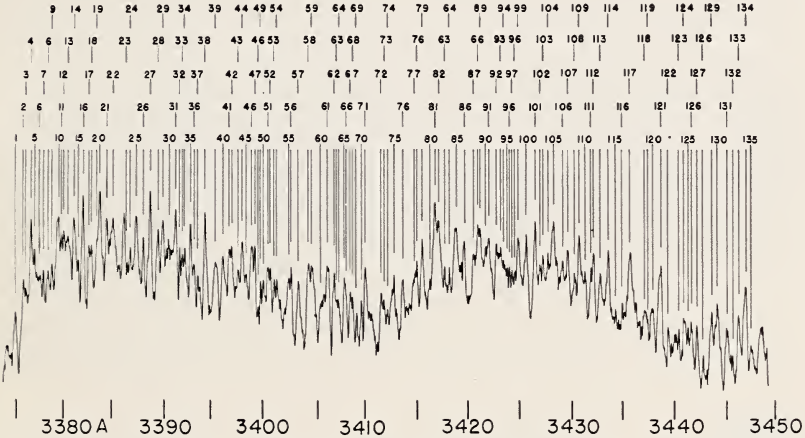

FIGURE 2.3. *The 3377 A hydrocarbon flame band at 4 A/mm.*

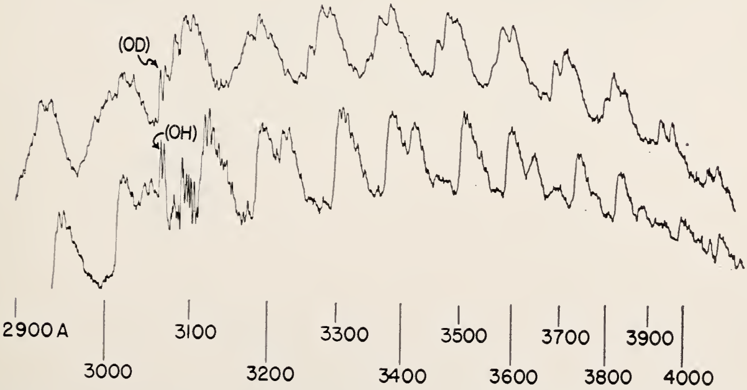

FIGURE 2.4. *Comparison of hydrocarbon flame bands with deuterocarbon flame bands obtained from the* C_2D_2—O_2 *flame at medium quartz dispersion.*

The α-Bands of Ammonia

Many years ago Rimmer [9] investigated the spectrum of the ammonia-oxygen flame with the view of identifying a large number of lines in the solar spectrum that had been attributed to ammonia. Included in his studies was an extended band spectrum that was named the "α-bands" by Eder and Valenta [10]. Rimmer described the spectrum as consisting of about 3,000 closely packed lines, both sharp and diffuse.

In order to minimize the difficulties of overlapping diatomic spectra and the vibration-rotation water spectrum that is known to exist in the spectral region covered by the α-bands, a spectrogram was obtained of the ammonia-oxygen flame with the low temperature burner. A densitometer tracing of the spectrum of the usual ammonia-oxygen flame together with one from the low temperature burner is shown in figure 2.5. Although the spectrum of the latter flame was a considerable improvement over the spectrum of the flame at higher temperature, the complexities are still too great to attempt an analysis. Herzberg and Ramsay [11] have recently obtained the α-bands in absorption by irradiating ammonia in a flash-photolysis apparatus. They have made progress toward a complete analysis of the spectrum, and have already established with certainty that the emitter of the α-bands of ammonia is the free NH_2 radical.

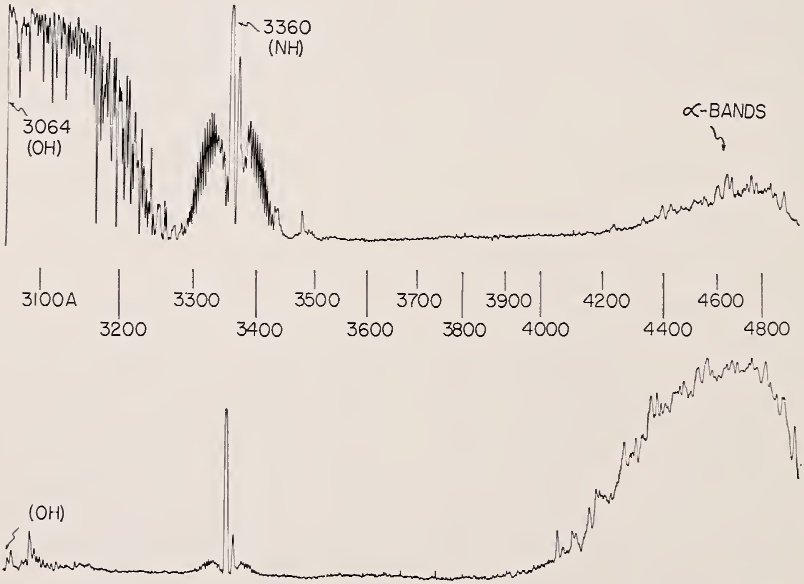

Figure 2.5. *Comparison of the ammonia-oxygen flame spectrum (above) with the cool flame spectrum at medium quartz dispersion.*

CO Flame Bands

Another polyatomic band system that has received much attention by flame investigators is the so-called CO flame band system. Among the first to study these bands from a carbon monoxide-oxygen flame source were Weston, [12, 13] Kondratjew, [14] and Gaydon [15, 16]. All of these investigators reported that this band spectrum is very complex and shows no obvious regularity, and that the diffuseness of the structure prevented accurate measurements. Several attempts were made to fit the bands into a vibrational array. The grouping of the differences obtained in this manner suggested some regularity, and the frequency values indicated CO_2 as being the most likely emitter of this spectrum. However, the electronic spectrum of CO_2 has never been satisfactorily analyzed or even identified. In the work of Mrozowski [17] on a discharge in CO_2, the bands analyzed have been shown to be those of CO_2^+.

In order to obtain the CO flame bands in good contrast with the ever present continuum, previous investigators resorted to low pressure burners, which generally give sources of low intensity. The low temperature burner now makes it possible to obtain good CO-flame band spectra on high dispersion instruments because of its relatively high intensity. A carbon monoxide-oxygen spectrum from a low pressure burner is compared with one from a low temperature burner in figure 2.6. Densitometer tracing (A) was obtained from a low pressure burner and required a 4-hour exposure; tracing (B) is from the low temperature burner on the same spectrograph employing the same slit width, and was obtained with an exposure of 10 minutes; finally, tracing (C) is the CO-flame spectrum obtained from a hydro-

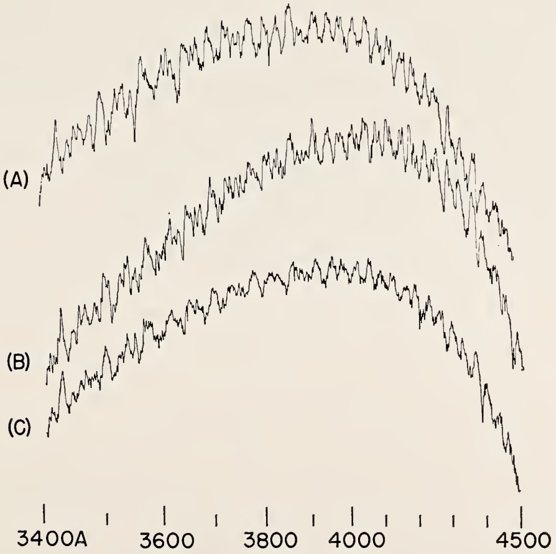

Figure 2.6. *The CO-flame bands at medium quartz dispersion.*
A, Low pressure burner; (B), low temperature burner; (C), H_2+O_2 flame with CO_2 diluent.

gen-oxygen flame, operating at atmospheric pressure, to which was added a large amount of carbon dioxide. If there is twice as much CO_2 as H_2 in such a flame, the "temperature" is so low as to permit a thick-skinned individual to hold his hand in it. It is of interest to note that at higher dispersion (~4 A/mm) many of the CO flame bands appear to degrade to the violet. This is in contrast to the behavior at low dispersion where all bands appear to degrade to the red. Frequently, adjacent bands appear to be doublets at low dispersion because they degrade in opposite directions. These observations lend support to our contention that high resolution is required in order to unravel and interpret flame spectra properly.

Conclusion

The work described above indicates the importance of using low-temperature-high-intensity sources for the study of polyatomic flame spectra. The suppression of diatomic spectra and the higher resolution possible because of lower temperature and higher intensity have revealed many hitherto obscure features in polyatomic flame bands. It is hoped that studies such as these together with the results of investigations of flame dynamics may eventually lead to an understanding of the kinetic mechanisms and the molecular species involved in flames.

References

[1] A. G. Gaydon, Spectroscopy and combustion theory (Chapman and Hall, London, 1948).
[2] T. Kitagawa, Proc. Imp. Acad. Tokyo **12**, 281 (1936).
[3] W. S. Benedict and E. K. Plyler (see paper 8, p. 57).
[4] G. A. Hornbeck and R. C. Herman, Ind. Eng. Chem. **43**, 2739 (1951).
[5] R. C. Herman, G. A. Hornbeck, and K. J. Laidler, Science **112**, 497 (1950).
[6] W. M. Vaidya, Proc. Roy. Soc. [A] **147**, 513 (1934).
[7] W. M. Vaidya, Proc. Phy. Soc. (London) **64**, 428 (1951); G. M. Murphy and L. Schoen, J. Chem. Phys. **19**, 380, 1214 (1951).
[8] P. S. Dyne and D. W. G. Style, Disc. Faraday Soc. **2**, 159 (1947).
[9] W. B. Rimmer, Proc. Roy. Soc. **103**, 696 (1923).
[10] Atlas Typischen Spektren, Wien, p. 10 (1911).
[11] G. Herzberg and D. A. Ramsay, J. Chem. Phys. **20**, 347 (1952).
[12] F. R. Weston, Proc. Roy. Soc. [A] **109**, 177 (1925).
[13] F. R. Weston, Proc. Roy. Soc. [A] **109**, 523 (1925).
[14] V. Kondratjew, Z. Phy. **63**, 322 (1930).
[15] A. G. Gaydon, Proc. Roy. Soc. [A] **176**, 505 (1940).
[16] A. G. Gaydon, Proc. Roy. Soc. [A] **182**, 286 (1944).
[17] S. Mrozowski, Phys. Rev. **60**, 730 (1941).

3. Emission Spectra of Polyatomic Free Radicals

By P. J. Dyne [1]

Considerable interest has been maintained in the spectroscopic study of free radicals as it affords a powerful method for their detection and for detailed study of their structure. A number of band systems are found in flames, discharges, and other sources, which are assigned to polyatomic free radicals. The positive identification of the emitter of these band systems is, however, a difficult and often controversial matter.

The arguments that are used for identification are generally circumstantial. They depend upon assumptions made about the chemical species present in the flame or discharge and about the methods of excitation of these species. The validity of these assumptions is, practically always, open to discussion. It is relevant to point out here that ultraviolet spectroscopy only detects electronically excited species. These may or may not constitute a significant kinetic concentration in the flame or discharge. More precise evidence for identification could be obtained from a detailed analysis of the spectrum, but so far little progress has been made along these lines. The main difficulty is that of obtaining these spectra with sufficient intensity for high dispersion studies. The subsequent analysis is likely to be very difficult, and success is only likely to be obtained in a few favourable cases.

The purpose of this paper is to discuss some particular experiments and their results as examples of these general conclusions.

In a fluorescence method of excitation used by Terenin [1],[2] Terenin, and Neujmin [2], and Dyne and Style [3] we have one of the simplest excitation mechanisms. Circumstantial arguments for the assignment of band systems have, in this case, considerable weight. The method is essentially photochemical. A molecule A—B, where A and B are atoms or groups, can be photochemically dissociated to give electronically excited products. Thus,

$$\mathrm{A{-}B} + h\nu \rightarrow \mathrm{A} + \mathrm{B}^*, \tag{1}$$

which may be followed by

$$\mathrm{B}^* \rightarrow \mathrm{B} + h\nu'. \tag{2}$$

---

[1] National Research Council, Ottawa, Canada.

[2] Figures in brackets indicate the literature references on p. 22.

Process 2 will give rise to a fluorescence due to the "B" atom or radical. Such processes have been studied extensively by Terenin, examples being

$$NaI + h\nu \rightarrow Na(^2P) + I, \qquad (3)$$

$$Na(^2P) \rightarrow Na(^2S) + h\nu, \qquad (4)$$

the "D" lines of sodium being emitted in process 2. If Schumann radiation is used for excitation, processes like

$$H_2O + h\nu \rightarrow H + OH(^2\Sigma) \qquad (5)$$

$$OH(^2\Sigma) \rightarrow OH(^2\Pi) + h\nu \qquad (6)$$

can be observed, the fluorescence spectrum being the OH band at λ3064. The apparatus used is shown schematically in figure 3.1. A light source, chosen for its intensity in the region λ1300 to λ1400, is at A. For nearly all experiments a hydrogen arc was used. Radiation from the light sources passes along a glass tube B that serves to concentrate the light beam through a thin fluorite window C. It is estimated that light of wavelength as short as λ1280 is active in some instances. For this reason, it is essential that the fluorite is of the best quality and that the window is perfectly clean. The vapor under investigation is pumped continuously through the fluorescence cell at a pressure of a few tenths of a millimeter. The fluorescence is observed along the axis 0–0′ through the quartz window F.

The fluorescences are very weak. With the apparatus of the type described here the emission of the OH band from H_2O, which is the most intense fluorescence observed, requires an exposure of 10 minutes on a *f*/1.8 quartz spectrograph to give a reasonably exposed band head. Other fluorescences, which consisted of band systems, required exposures of 4 to 6 hours. The difference in intensity is mainly due to the fact that in one case the whole of the intensity of the fluorescence is concentrated in one band head and that in the other case the intensity is spread over many diffuse bands. The fluorescences being discussed here have therefore the same order of *total* intensity and are therefore processes with comparable quantum efficiency.

Let us suppose that a fluorescence can be excited from a molecule A—B, and further that photochemical studies show that the molecule is likely to split at, say, the A—B bond. [See eq 1 and 2.] As in

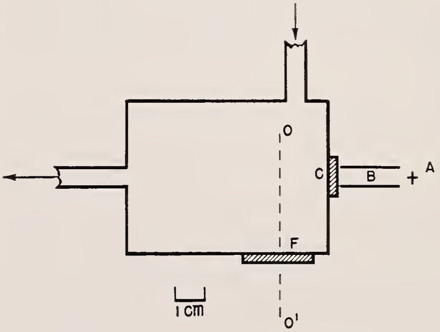

FIGURE 3.1. *Apparatus for observing fluorescence.*

A, Source; B, glass tube; C, fluorite window; F, quartz window.

most practical cases the group A is a hydrogen atom, the spectrum observed can be assigned to the B radical if we assume that the excitation mechanism is as given in eq 1 and 2. In the cases to be mentioned here this is certainly the most probable mechanism.

Conclusions based on this type of argument have been criticized on the ground that the possibility of secondary reactions has been neglected. It is suggested that the radicals or atoms formed initially may react to give new species. These may, in turn, be re-excited by the irradiation and the observed fluorescence may be due to quite another molecule or radical from that formed initially.

These possibilities are discounted by these arguments. Firstly, in all the cases mentioned here radiation shorter than λ1500 is required for the excitation. Because of the high energy of these quanta, processes like [1], the production of excited radicals, are almost certainly occurring. Secondly, these fluorescences are of the same order of total intensity and correspond to processes of similar efficiency. Therefore any secondary processes, occurring subsequent to the primary photochemical act, must have an overall efficiency very close to unity for the secondary "fluorescence" to be observed at all. This is unlikely. Thirdly, the low pressure and the flow conditions in the fluorescence cell do not favor any secondary reactions.

At the National Research Council, Ottawa, we have been developing a discharge source for polyatomic radicals capable of giving sufficient intensity for high dispersion studies. A normal discharge through an organic vapor will give spectra of diatomic species; e. g., C_2, CH, CO, almost exclusively. The conditions appear to be too violent for the excitation of polyatomic species. The experimental problem is to moderate the condition in the discharge sufficiently to prevent the large scale formation and excitation of diatomic molecules. In an ordinary discharge tube the largest potential gradient, and hence the most violent excitation is in the vicinity of the electrodes. A high-frequency electrodeless discharge was therefore chosen for this work because the conditions are uniform throughout the region of excitation and are therefore easier to control. It was found that polyatomic species are excited in the higher pressure ranges, at about 0.1 mm, near the pressure at which this particular discharge is extinguished. The reason for this may be seen by this rather elementary argument. The energy available at an electron molecule impact will, in a steady field, be proportional to the free path of the electron. This will be determined by the pressure because a decrease of pressure will increase the free path between nonelastic collisions and hence increase the excitation energy. These conditions, combined with a high flow rate through the tube, removing decomposition products, are favorable in several specific cases for the excitation of polyatomic species. The results, in many cases, duplicate those found by Schüler [4], who used a specially designed glow-discharge tube for the same purpose.

A new band system was observed in a high-frequency discharge of this type in acetylene. This is described in more detail elsewhere [5]. The system consists of a complex series of bands lying between $\lambda\lambda$2400 and 2900. The bands are mostly degraded to the red and are often double headed. These facts and the existence of short progressions with spacings of 1,050 cm^{-1} and 1,900 cm^{-1} are points of similarity with the known ultraviolet absorption spectrum of acetylene, which lies to the short wavelength side of the emission system. The emitter could be acetylene itself or the radical C_2H. If it were possible to examine the bands under sufficient resolution, a decision could be made between these two possibilities. Acetylene, being linear and symmetric, would show an intensity alternation in its fine structure; the radical C_2H would not.

The excitation of the hydrocarbon flame bands in fluorescence from formaldehyde has been already reported [3] and mentioned in the preceding paper by Dr. Herman and Mr. Hornbeck. It is sufficient to say that this observation is entirely consistent with the assignment of this system to the HCO radical. Were it not for the structure observed in these bands by Herman and Hornbeck one would take this observation as a proof. The possibilities of secondary processes mentioned in criticism of this conclusion have already been discussed. From this evidence, then, we can conclude with reasonable certainty that either HCO or formaldehyde itself is the emitter of these bands [7].

It is relevant to point out here that the assignment of the "α" band of ammonia to the radical NH_2 rests on similar evidence [8]. Terenin and Neujmin [2] report its excitation in fluorescence in ammonia. They assume that the mechanism is

$$NH_3+h\nu\rightarrow NH_2^*+H \tag{7}$$

$$NH_2^*\rightarrow NH_2+h\nu' \tag{8}$$

Terenin and Neujmin also observed a visible fluorescence excited in formic acid. This consisted of a series of diffuse bands degraded to the red lying between λλ3400 and 4400. It is also possible to excite this band system from formic acid in a discharge of the type described in this paper. Details of this band system, which was not described by Terenin and Neujmin, will be published elsewhere. It has also been found possible to excite this spectrum in a discharge through ethyl formate, HCOOEt. This and similar work on deuterated compounds [6] shows that the emitter is not formic acid itself but a radical derived from it, either HCO or HCO_2. The fact that under the dispersion of a large quartz instrument no resolution into fine structure is observed, even though the bands seem sharp, suggests a heavy molecule. This and the previous evidence about the hydrocarbon flame bands might lead one to suggest that this system is due to HCO_2.

To generalize from these results, which may be taken as fairly typical of this field, it can be said that as we are generally restricted to circumstantial arguments the amount of precise, unequivocal, spectroscopic data on polyatomic free radicals is small.

The author wishes to acknowledge helpful discussions he has had on these topics with Dr. G. Herzberg, F. R. S.

References

[1] A. Terenin, Z. Physik **37,** 98 (1926).
[2] A. Terenin and H. Neujmin, Acta Physico Chimica U. S. S. R. **5,** 465 (1936).
[3] P. J. Dyne and D. W. G. Style, Discussions of Faraday Soc. **2,** 159 (1947).
[4] H. Schüler, Chemische Technik. **15,** 99 (1942).
[5] P. J. Dyne, Can. J. Phys. **30,** 79 (1952).
[6] P. J. Dyne and D. W. G. Style, J. Chem. Soc. 2122 (1952).
D. W. G. Style and J. C. Ward, J. Chem. Soc. 2124 (1952).
[7] See D. A. Ramsay, J. Chem. Phys. **21,** 960 (1953).*
[8] See G. Herzberg and D. A. Ramsay, J. Chem. Phys. **20,** 347 (1952).*
*References 7 and 8 were added in proof.

4. Distributions of OH Rotational Intensities in Flames

By Herbert P. Broida [1]

Intensity distributions of rotational lines in the (0,0) band of the $^2\Sigma \rightarrow {}^2\Pi$ electronic transition of OH in a variety of flames have been obtained with a high-resolution grating monochromator. Various parts of the flames have been observed. These spectra have been used to investigate thermal equilibrium in the hot gases and to measure rotational "temperatures." Flames of stoichiometric mixtures of various fuels with oxygen have been studied systematically. Preliminary investigations of flames using up to 90 percent diluent have been made. Hydrocarbon flames burning in a slot burner with a long observable path through the reaction gave an abnormal distribution of OH rotational intensities similar to that obtained in a discharge through water vapor.

Introduction

One is a little dismayed by the comment of Dr. Gaydon [1] [2] that it is impossible to obtain quantitative spectroscopic data from the reaction zone of flames at atmospheric pressure. Presumably he was only referring to the great difficulty of such measurements. All measurements reported in this paper were obtained at atmospheric pressure.

The work described is part of a long-range program at the National Bureau of Standards designed to obtain information about basic physical and chemical processes in flames and hot gases. This afternoon in paper number 8 [2], Dr. Benedict will discuss some results of the infrared aspect of the project while this paper deals mainly with ultraviolet radiation and particularly with emission from electronically excited OH. Studies of CH and C_2 are in a very preliminary stage.

In the visible and ultraviolet regions of the spectrum use of photoelectric detection, rather than photographic detection, considerably simplifies the measurement of radiation intensity. Line intensities are read directly as distances above the background without the time consuming tasks of plate processing and calibrating. In addition, photoelectric detection makes it possible to measure smaller amounts of absorbed radiation. Only under conditions of extremely weak or very rapid emission is the photographic technique essential.

Experimental

As orientation toward better understanding of results to be presented, figure 4.1 is a photographic reproduction of a flame burning under carefully controlled conditions [3]. A flame of a stoichiometric mixture of dry methane and air is shown in this figure. The diameter of the nozzle opening is 12.5 mm. This nozzle has been designed to give uniform gas velocity across the burner. Tube burners of 0.5

---

[1] National Bureau of Standards, Washington, D. C.

[2] Figures in brackets indicate the literature references on p. 34.

FIGURE 4.1. *Flame of a stoichiometric mixture of methane and air burning above a 12.5-mm diameter nozzle.*

The nozzle has been designed to give a uniform gas velocity over the entire opening.

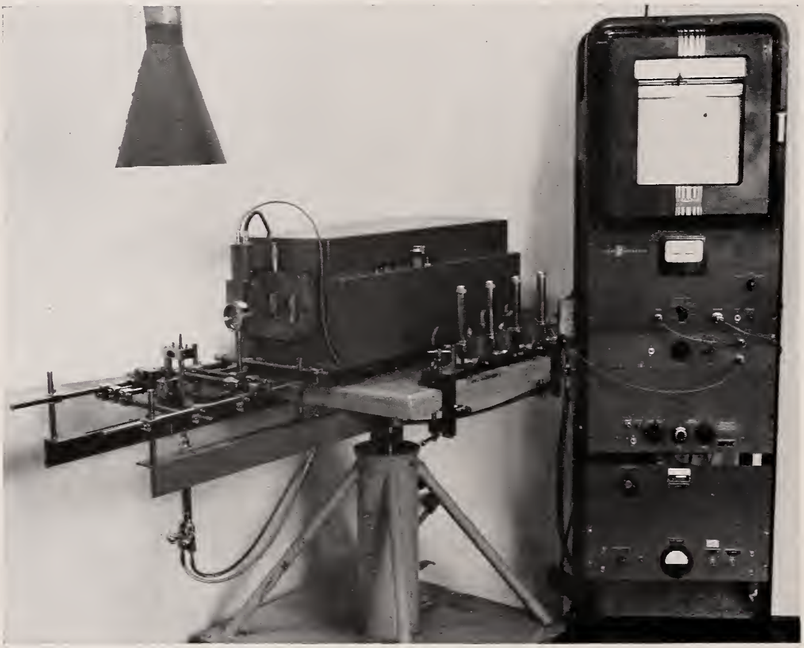

FIGURE 4.2. *Apparatus showing the monochromator, the spectral recording equipment, and an acetylene-oxygen flame.*

and 1.5 mm have been used for the faster burning oxygen mixtures. The thin, intense cone is called the reaction zone or the inner cone. Hot gases beyond the reaction zone are faintly visible. In a case of this sort, where there is not a diffusion flame, I do not think these hot gases should be called either the "outer cone" or the "interconal gases." Such terminology does not aid the understanding of the phenomena.

A systematic group of spectroscopic observations have been made of various portions of several flames. Any attempt to observe the reaction can be confused by contributions to the measured intensities from the hot gases outside the reaction zone. In order to separate the contributions from the two regions, we have made observations from the base of the flame to 40 mm beyond the base. Slits as small as 0.007 by 0.3 mm have been used.

The major portion of this spectroscopic work has been done with the apparatus pictured in figure 4.2. This is a photoelectric scanning monochromator built by the Research Department of Leeds and Northrup Co. and loaned on a field-trial basis to the High Temperature program at the National Bureau of Standards. The optical equipment is compact and measures only 30 by 35 by 85 cm. The flame is focused on the entrance slit of the monochromator with a simple quartz lens. A 90,000-line grating is the dispersing element. By rotating the grating it is possible to scan through the spectrum from 1,750 to 7,000 A. Using a narrow slit (0.007 mm) we have been able to achieve a resolving power ($\lambda/\Delta\lambda$) of some 55,000. This means that we have resolved lines separated by approximately 0.05 A in the region of 3,000 A. A 1–P28 photomultiplier is used as the detecting element. The output from the phototube is amplified by a stable d-c amplifier and put into a pen recorder. Intensity is plotted in one direction on the chart paper while wavelength is plotted in the other direction. Both scales are linear. Racks and pinions have been used to move the flame horizontally and vertically for observations of different regions of the flame.

Figure 4.3 shows a typical spectrum of the electronic transition of

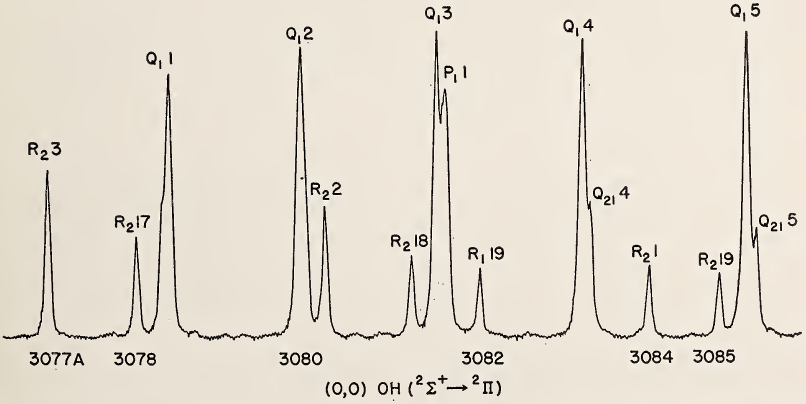

FIGURE 4.3. *Part of the emission spectrum of the 0,0 band of the* $^2\Sigma\rightarrow{}^2\Pi$ *transition of OH from a hydrogen-oxygen flame.*

This tracing shows both high and low *K* lines of the R_2 branch.

OH. This chart was selected because it illustrates the instrumental possibilities and shows the rotational lines used for our measurements of intensity. The emission was from the inner cone of a hydrogen-oxygen flame about 1.5 mm below the tip. Both low and high members of the R_2 branch of the 0,0 transition can be seen. On such a chart as this, it is easy to find lines of equal intensity for use in determining the rotational temperature.

Methods of Measuring Rotational Temperature

For rotational equilibrium, the intensity due to a transition from a rotational level, K, having energy, E_K, is given by

$$I_K = C A_K e^{-(E_K/kT)} \tag{1}$$

where A_K includes the transition probability of the particular transition, the statistical weight, and the frequency factor; k is the Boltzmann constant; T is the rotational temperature; and C depends upon the concentration of OH and is constant for a particular electronic and vibrational transition.

Rotational temperature can be obtained from the distribution of intensities among the various rotational transitions by plotting log (I_K/A_K) as a function of E_K. This plot is a straight line for an equilibrium distribution. The temperature is found from the reciprocal slope of the line. Dieke and Crosswhite [4] have emphasized that self-absorption of the stronger lines can so seriously affect the measured intensity distribution that this method is not always usable. Figure 4.4 is included to illustrate the effect of self-absorption. The data were obtained by observing the inner cone of an acetylene-oxygen flame. There is also some contribution to the measured intensities from the hot gases outside the reaction zone. In this case there definitely are two separate lines. A "temperature" of 4,150° K is found from the slope of the larger K values while 1,360° K is found from the smaller K values. The "break" in the curve is due entirely

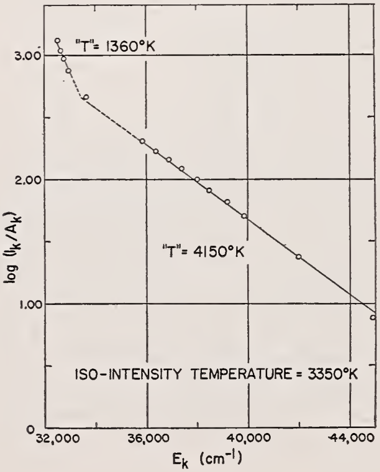

FIGURE 4.4. *Plot of log (I_K/A_K) versus E_K for the R_2 branch of OH from the inner cone of an acetylene-oxygen flame.*

The most intense lines in the neighborhood of $K=7$ are reduced in intensity more than 50 percent by self-absorption.

to self-absorption and the measured "temperature" is not an indication of the temperature of the flame. If a longer flame path is observed, the absorption is increased and the difference in the slopes becomes greater.

The isointensity method of temperature determination is not affected by absorption within the flame provided the temperature is uniform. This is so because to the first approximation lines of equal intensity are equally absorbed. It follows therefore that this method can be used to determine the temperature under conditions in which the log plot of figure 4.4 is inapplicable. It follows from eq 1 that for lines of equal intensity,

$$A_{X'}/A_X = e^{(E_{X'} - E_X)/kT} \tag{2}$$

and

$$T = \frac{E_{X'} - E_X}{k \log_e (A_{X'}/A_X)} \tag{3}$$

Figure 4.5 is a plot of the intensities versus the K values of the various transitions using the same data as plotted in figure 4.4 After finding lines of equal intensity, the temperature can be read from graphs prepared from eq 3. The isointensity temperatures for the first five K values are marked on figure 4.5. A mean temperature of 3,340° K is obtained. Rotational equilibrium is indicated by the agreement of the various temperatures.

Shuler [5] has modified this isointensity method in a way which makes it somewhat more appealing and which indicates whether or not the distribution corresponds to that of an equilibrium. Equation 2 is used and values of $E_{X'} - E_X$ for isointensity pairs are plotted against log (AX'/A_X). Figure 4.6 is such a plot using the same data as plotted in figures 4.4 and 4.5. The straight line passing through

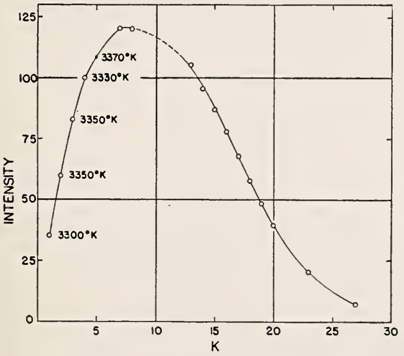

FIGURE 4.5. *Intensity distribution of the R_2 branch of OH as a function of K value.*

This data is the same as that used in figure 4.4. Temperatures corresponding to various isointensity pairs are shown on the graph.

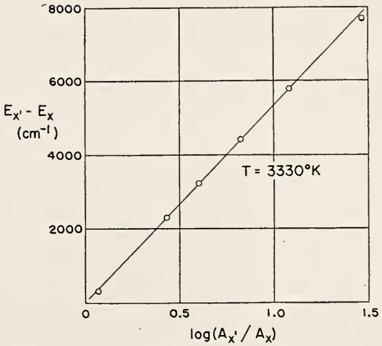

FIGURE 4.6. *Plot of $E_{X'} - E_X$ versus log $(A_{X'}/A_X)$ in the R_2 branch using the same data as that of figures 4.4 and 4.5.*

The straight line is indicative of a Boltzmann distribution of rotational energy. The temperature obtained from the slope is shown on the graph.

the origin indicates rotational equilibrium and a temperature of 3,330° K is found from the slope. However, no significance should be given to the 10° difference between this value and that previously given. A small difference in the isointensity pairs (fig. 4.5) or in the slope (fig. 4.6) can easily amount to 10°. Day-to-day reproducibility of temperature measurements was of the order of ±1.5 percent (50°).

In this work we have used a combination of these three methods to measure rotational temperature. The temperature can also be found from the line of maximum intensity. Although this method is rather insensitive, it is useful for an order of magnitude determination. Differentiation of eq 1 with respect to K shows that at maximum intensity the corresponding value of $K_{\max}$ is approximately related to the temperature by [6]

$$T=2\,Bhc\,K^2_{\max}/k \qquad (4)$$

where [4] $B=16.98\ cm^{-1}$ for the $^2\Sigma$ state of OH, h is Planck's constant and c is the velocity of light. Figure 4.5 shows that the maximum intensity for the R_2 branch occurs between $K=7$, and $K=8$, corresponding to a temperature between 2,600 and 3,400° K.

Results

Emission spectra have been obtained from various portions of flames of hydrogen, of acetylene, of methane, and of propane burning with oxygen. These results are described in more detail elsewhere [7].

Figure 4.7, showing values obtained from an acetylene-oxygen flame with a stoichrometric mixture, is representative of such measurements. In the upper graph, OH rotational temperatures are plotted as a function of distance above the base of the flame. The lower graph shows the change in measured intensity of the $R_2(3)$ line of the 0,0 transition of OH. The position of the tip of the inner cone is marked. There is a somewhat smaller decrease in temperature beyond the inner cone than might be expected from the cooling effect of the surrounding gases. The rate of decrease is about 5° C in each millimeter. However, from the tip of the inner cone to the base the rotational tempera-

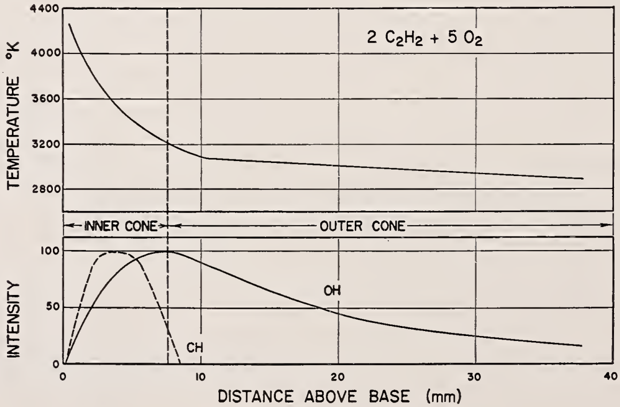

FIGURE 4.7. *Acetylene-oxygen flame, stoichiometric mixture.*

Rotational temperatures of OH and relative intensities of OH and CH each normalized to the respective maximum intensity, plotted as a function of distance above the burner.

ture rises rapidly, reaching a value near 4,250° K near the base of the flame. Since the thickness of the hot gases surrounding the reaction zone is quite small near the base, this high temperature is probably characteristic of the reaction zone. Near the tip of the inner cone there is a thicker region of hot gases contributing to the measured intensity. The abnormally high temperature of the reaction zone indicates that OH is formed in the excited state during the reactions. An interesting, but still unexplained point is that all positions seemingly give a Boltzmann distribution of rotational intensities.

Another interesting point is the manner in which the abnormal "temperature," if we call the temperature of the hot gas normal, continues beyond the tip of the inner cone about 2 mm. One might assume that this is due to a lifetime of some sort. It turns out that the time taken to reach the "equilibrium temperature" is of the order of 10^{-6} seconds. This is the same time as the lifetime of excited OH [8] and it is possible to assume that the continuation of the abnormal temperature beyond the inner cone is caused by the long life of the excited OH. If this is true, it means that something of the order of 10,000 collisions are not effective in quenching this abnormal rotational distribution.

We find that the decrease in OH intensity (lower part of fig. 4.7) beyond the reaction zone is wholly attributable to the decrease in temperature. In the inner cone the high measured temperatures would indicate that the intensity should increase from the tip to the base of the flame. However, it seems certain that the major part of the measured intensity is from the hot gases surrounding the reaction zone. Unfortunately the temperature measurements are not accurate enough for making a determination of the relative contribution from each region.

The "dashed" curve of figure 4.7 shows the observed relative intensity of the 3,143 A band of CH. The intensity drops rapidly at

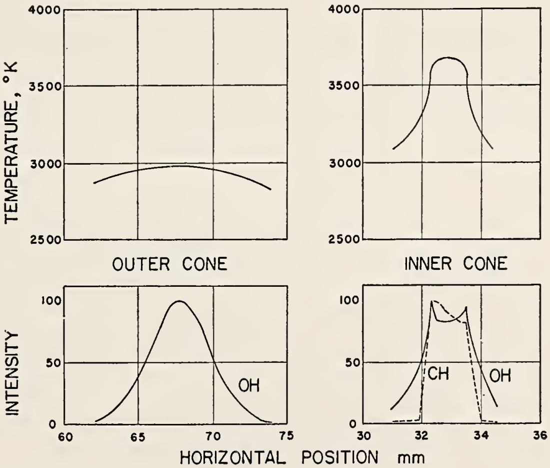

Figure 4.8. *Acetylene-oxygen flame, stoichiometric mixture.*

Rotational temperatures and relative intensities of OH normalized to the maximum intensity, plotted as a function of distance across the hot gases. The horizontal distance is measured on a millimeter scale with the zero arbitrarily set.

the tip of the inner cone. In hydrocarbon-oxygen flames near stoichiometric, excited CH has been observed only in the inner cone.

Figure 4.8 shows the measured OH temperatures and relative intensities found by scanning through the region of the inner cone just above the base of the flame.

Similar measurements have been made with flames of hydrogen, of methane, and of propane burning with oxygen. In all cases the same type of characteristics were observed. However, only the acetylene flames show such a high abnormal temperature. Table 4.1 summarizes the measured rotational temperatures and compares the measured values with Na line reversal temperatures and calculated adiabatic temperatures.

Previously [13] we completed some experiments with methane-air flames which showed some interesting results. Figure 4.9 shows a plot of log (I_K/A_K) versus E_K for the R_2 branch of OH emitted from the inner cone of a methane-air flame with a stoichiometric mixture. The circle points are for clearly resolved rotational lines and the square points are those for which there was some overlapping. The lines have been drawn only through the good points. In this case we again find two separate lines with a "break" in the logarithmic plot. With absorption measurements, it was possible to make certain that this effect was not due to self-absorption. An interesting thing here, which will be discussed by Dr. Penner in the next paper [14], is that this same type of break has been observed in emission from low-pressure flames.

We assumed that the intensity distribution is caused by two separate distributions of OH, one at a relatively high "temperature" and the other at a low "temperature." If that is the case, then it is possible to extrapolate to low K values the measured intensities at high K values, subtract from the total intensities and plot the distribution of the low "temperature" OH. The "temperatures" of these two distributions are 5,200° K and 1,550° K.

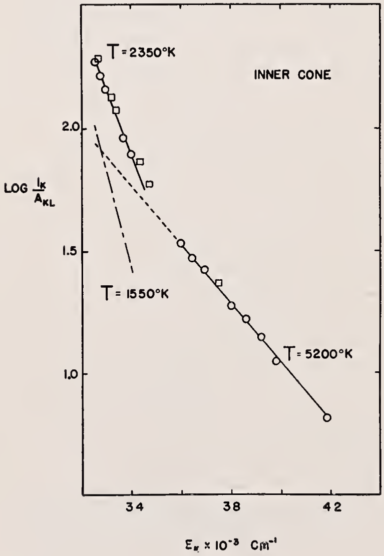

FIGURE 4.9. *Plot of log* (I_K/A_K) *versus* E_K *for the* R_2 *branch of* OH *in the inner cone of a flame with a stoichiometric mixture of methane and air.*

The "break" in the curve is not caused by self-absorption. The intensity of OH emission from the hot gases above the inner cone is less than 1/25 of that in the inner cone.

TABLE 4.1. *Flame temperatures*

Fuel	Mixture $\frac{F/O_2}{(F/O_2)_{\text{stoich.}}}$	Measured OH rotational temperature				Na line reversal [9]	Calculated equilibrium temperature
		Base	Tip	5 mm above tip	24 mm above tip		
		° *K*	° *K*	° *K*	° *K*	° *K*	° *K*
H_2	1.0 stoichiometric	3, 000	2, 750	2, 700	2, 600	2, 750	3, 100[10]
	0.66 lean	2, 950	2, 625	2, 600	2, 575	2, 750	2, 825
	2.0 rich	2, 950	2, 775	2, 740	2. 610	2, 710	2, 920
C_2H_2	1.0 stoichiometric	4, 250	3, 170	3. 020	2, 950	3, 300	3, 320[11]
	0.5 lean	4, 100	2, 780	2, 750	2, 750	3, 200	3, 080
	2.0 rich	4, 100	3, 180	3, 060	2, 940	3, 400	3, 400
CH_4	1.0 stoichiometric	3, 200	2, 800	2. 750	2, 700	[1] 3, 150	3, 060[12]
C_3H_8	1.0 stoichiometric	3, 300	2, 825	2, 800	2, 750	------	----------

[1] Natural gas.

Figure 4.10 again shows the OH spectrum, but in this case an absorption spectrum from the same methane-air flame is superimposed above the emission spectrum. In this case it is quite easy to see that the "temperature" of the excited state is much higher than the ground state because higher quantum transitions occur in emission. In figure 4.11, log I_K/A_K is plotted for absorption by OH in both the inner cone and the hot gases beyond the inner cone. In each case there is a straight line indicating thermal equilibrium. The two temperatures agree quite well and are of the order of 2,000° K. This is some 100° to 150° less than the calculated adiabatic values. The measured OH concentration also agrees well with the calculated value.

Work is progressing at the present time on a more extended program to investigate the effect of diluents. Acetylene, hydrogen, and methane are the fuels being used, and helium, argon, and nitrogen are the diluents. A range of diluent from zero to 90 percent will be used with stoichiometric mixtures of fuel and oxygen [16].

With increasing diluent concentration we find increasingly larger abnormal rotational "temperatures." This type of behavior is similar to that observed by Dr. Gaydon [11] at low pressure. Also, in a manner similar to that at low pressure we find that the intensity of an acetylene flame with large concentrations of diluent as compared to a hydrogen flame is greatly in excess of that to be expected from the difference of adiabatic temperatures. Another similarity of

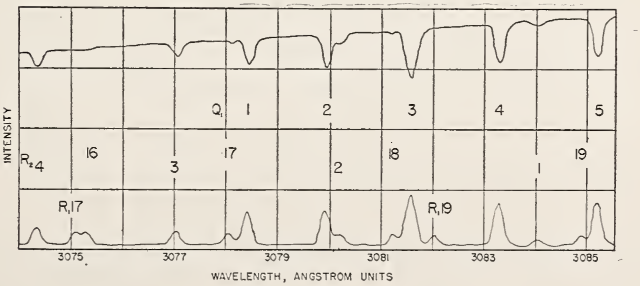

FIGURE 4.10. *Absorption and emission spectra of* OH *from a methane-air flame of stoichiometric mixture.*

The upper curve is absorption. The resolved lines of various branches are marked.

FIGURE 4.11. *Plots of log* (I_K/A_K) *versus* E_K *for the* R_2 *branch in absorption with a stoichiometric mixture of methane and air.*

The upper line is from the hot gases above the reaction zone; the lower line is from the inner cone.

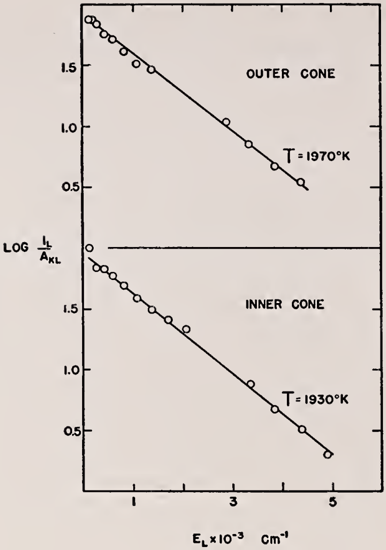

flames with large concentrations of diluent to flames at low pressure is that the intensity of the inner cone is very much stronger than that of the hot gases surrounding the inner cone. At high diluent concentration there is very little emission from the hot gases as compared to that from the reaction zone.

In an attempt to overcome the effect of the surrounding hot gases on measurements of the inner cone, a slot burner has been constructed. It is easier to show a picture of the burner than to try to describe it. Figure 4.12 shows such a burner. The slot is water cooled and has dimensions of 50 by 0.07 mm.

Figure 4.13 shows the rotational intensity distribution of OH as observed in an acetylene-oxygen flame with a stoichiometric mixture in this burner. Relative intensities of the R_2 branch are plotted as a function of the K value. The lower curve was obtained by sighting in the long direction 2 mm above the reaction zone. The maximum appears quite flat. This is due partly to the relative scale and partly to the great amount of self-absorption which is of the order of 95 percent in the more intense lines. Nevertheless, the measured isointensity is 3,000° K which compares well with that obtained in the usual round torch. The lines marked (x10) has a tenfold increased scale and was obtained by sighting through the reaction zone in the narrow direction. In this direction the thickness of the hot gases above the reaction zone is of the order of 1 mm. Using the isointensity method a rotational temperature of 3,700° K is found; this is in agreement with the measured values shown in figure 4.7.

The upper curve of figure 4.13 was obtained from the intensity measurements obtained by sighting through the long direction of the reaction zone. This intensity distribution is quite different than any previously observed in flames and is similar to that observed in discharges through water vapor [15]. The isointensity temperature as measured by various pairs of equal intensity increases with increasing

FIGURE 4.12. *Water-cooled slot burner with a slot of 0.076 by 50 mm.*

The flame is a stoichiometric mixture of methane and oxygen.

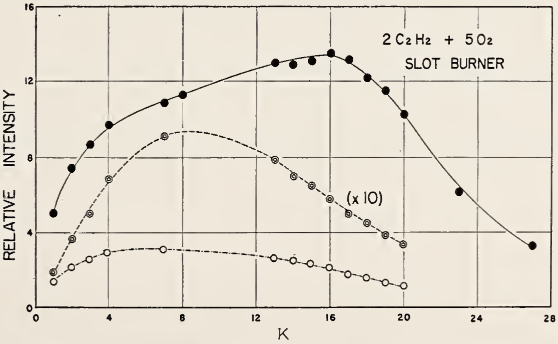

FIGURE 4.13. *Plot of intensities of the R_2 branch of* OH *as a function of K value from an acetylene-oxygen flame.*

The lower curve plots the measured intensities of the hot gases above the reaction zone viewed in the long direction. The middle curve plots the measured intensities multiplied by a factor of 10 of the inner cone viewed in the short direction. The upper curve plots the measured intensities in the inner cone viewed in the long direction.

K. This indicates a lack of equilibrium and thus no temperature exists. However, if it is assumed that a "temperature" can be obtained from the position of maximum intensity, using eq 4 and $K_{\max}=16$, a "temperature" of 13,600° K is found. A similar abnormal distribution was found in flames burning with propane, but the abnormality was not found in flames with hydrogen. As yet no adequate interpretation of this non-Boltzmann distribution has been possible [17].

Conclusions

These determinations of temperatures of rotation of OH in various flames have shown the need for extreme caution before drawing conclusions from the observations. In particular, it is necessary to know the conditions under which the flame is burning—the gas mixture, the type of burner, and the part of the flame observed.

There appears to be a nonequilibrium distribution of energy and intensity of OH in the reaction zone of most of the flames observed. This is especially apparent in flames with acetylene and in flames with large amounts of diluent. Above the reaction zones, OH appears to be in rotational equilibrium.

One of the most striking observations is that the addition of diluents to flames has somewhat the same effect on the rotational distribution of OH as going to low pressure.

References

[1] A. G. Gaydon (see paper 1, p. 1).
[2] W. S. Benedict (see paper 5, p. 35).
[3] F. R. Caldwell, H. P. Broida, and J. Dover, Ind. Eng. Chem. (1951).
[4] G. H. Dieke and H. M. Crosswhite, The ultraviolet bands of OH, Bumblebee Series Report No. 87 (Bur. Ord., USN, 1948).
[5] K. E. Shuler, J. Chem. Phys. **18,** 1466–70 (1950).
[6] G. Herzberg, Molecular spectra and molecular structure I, 2d ed., p. 125 (D. Van Nostrand Co., Inc., New York, 1950).
[7] H. P. Broida and G. T. Lalos, J. Chem. Phys. **20,** 1466–1471 (1952).
[8] O. Oldenberg and F. F. Rieke, J. Chem. Phys. **6,** 439–447 (1938).
[9] H. H. Lurie and G. W. Sherman, Ind. Eng. Chem. **25,** 404–409 (1933).
[10] H. P. Broida and K. E. Shuler, J. Chem. Phys. 20, 168–174 (1952).
[11] A. G. Gaydon and H. G. Wolfhard, Proc. Roy. Soc. [A] **194,** 169–184 (1948).
[12] F. Ruegg, private communication.
[13] H. P. Broida, J. Chem. Phys. **19,** 1383–1390 (1951).
[14] S. S. Penner (see paper 5, p. 35).
[15] T. Horie, J. Phys. Soc. Japan **1,** 6 (1946); E. R. Lyman, Phys. Rev. **53,** 379 (1938); **56,** 466 (1939).
[16] W. R. Kane and H. P. Broida, J. Chem. Phys. **21,** 347–354 (1953).
[17] H. P. Broida, J. Chem. Phys. **21,** 1165–1169 (1953).

5. Spectroscopic Studies of Low-Pressure Combustion Flames[1]

By S. S. Penner, M. Gilbert, and D. Weber[2]

A large metal duct with suitable accessory equipment has been constructed for spectroscopic investigations on two-dimensional, low-pressure flames.[3] The apparatus represents an improvement over the design used by Gaydon and Wolfhard,[4] as larger and more stable flames are obtained. Furthermore, the inlet duct is rectangular, thus providing larger and better defined isothermal regions than can be obtained with cylindrical burners. Spatial explorations of the flame are facilitated by use of the periscopic arrangement shown in figure 5.1. Excellent spatial resolution is obtained at the expense of loss of light intensity. This loss is, however, not serious since long exposures (24 hours or more) can be performed without difficulty.

Spectroscopic studies are being carried out by use of a Perkin-Elmer Model 12C infrared spectrometer provided with complete crystal optics and auxiliary photoelectric receivers for study in the near-infrared region.[5] Preliminary emission studies have been carried out with a 1.5-meter grating spectrograph with a theoretical resolving power of 48,800. Further studies will be performed with improved instrumentation.

Several emission spectra from the luminous zone of a propane-oxygen flame burning at a pressure of 5 mm have been obtained. A complete rotational analysis, using the compilation of Dieke and Crosswhite,[6] has been carried out for the Q_1, Q_2, P_1, P_2, and R_2 branches of the (0,0) transitions of the $^2\Sigma \rightarrow {}^2\Pi$ band system of OH. Representative data are shown in figures 5.2 and 5.3 where the abscissa represents the rotational energy of the initial state (i. e., the excited state in emission studies) and the ordinate equals the logarithm of the peak intensity of lines divided by the product of the transition probability and the fourth power of the frequency corresponding to the indicated transition. In agreement with the results reported by Gaydon and Wolfhard (see footnote 4), the lower rotational states (roughly up to $K=11$) of the upper energy level indicate rotational temperatures

---

This paper presents the results of one phase of research carried out at the Jet Propulsion Laboratory, California Institute of Technology, under Contract No. W 33-038-ac-4320 sponsored by the Department of the Air Force, Air Materiel Command.

[2] Jet Propulsion Laboratory, California Institute of Technology, Pasadena, Calif.

[3] M. Gilbert, The investigation of low-pressure flames, Report No. 4-54, Pasadena: Jet Propulsion Laboratory, (Aug. 30, 1949).

[4] A. G. Gaydon and H. G. Wolfhard, Proc. Roy. Soc. (London) [A] **194,** 169 (1948); [A] **199,** 89 (1949); [A] **201,** 561 (1950); [A] **201,** 570 (1950); [A] **202,** 118 (1951).

[5] S. S. Penner, J. Chem. Phys. **19,** 272, 1434 (1951).

[6] G. H. Dieke and H. M. Crosswhite, The ultraviolet bands of OH, fundamental data, Bumblebee Series Report No. 87, Silver Spring, Md.; Applied Physics Laboratory, Johns Hopkins University, November 1948.

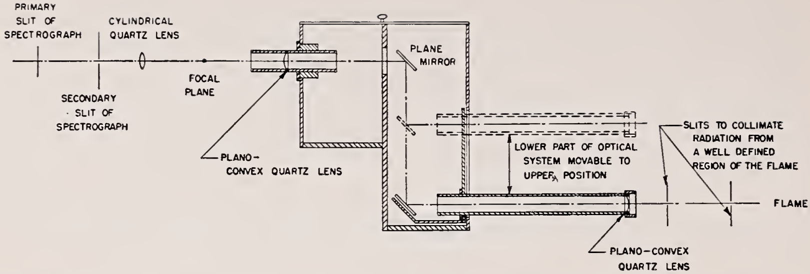

FIGURE 5.1. *Schematic drawing of optical system used to obtain spatial resolution of low-pressure combustion flames.*

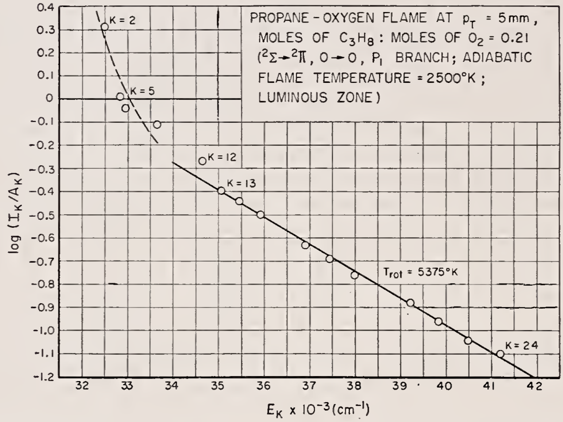

FIGURE 5.2. *Representative plot used for the determination of rotational temperatures of* OH *(P_1 branch).*

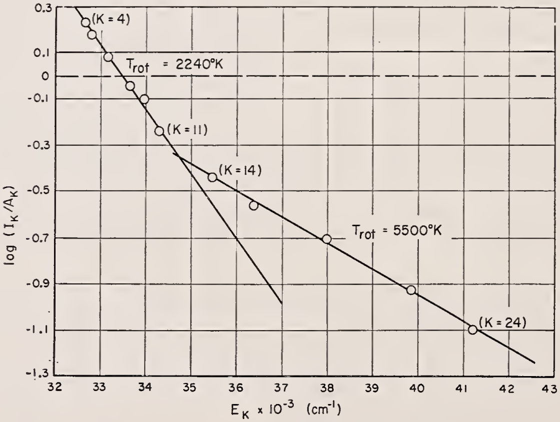

FIGURE 5.3. *Curve for determination of rotational temperature of* OH *(P_2 branch).*

somewhat lower than the adiabatic flame temperaturs (which is 2,500° K in the present case). On the other hand, the upper rotational states indicate abnormal rotational excitation and temperatures of 5,500° K to 8,000° K, depending on the position of the luminous zone that is being examined and on the branch for which a rotational analysis is performed. The interpretation of the experimental results described in figures 5.2 and 5.3 can be shown to imply the validity of the relation

$$1-\exp\,[-(P_\nu)_{\max}\,X]\simeq(P_\nu)_{\max}\,X,$$

where $(P_\nu)_{\max}$ is the maximum value of the spectral absorption coefficient for a given spectral line and X represents the optical density of the emitter. Calculations of appropriate values of $(P_\nu)_{\max}\,X$ for representative flames, using the *f*-values of Oldenberg et al.,[7] show that the expansion is probably not valid. Hence it follows that the observed "anomalous intensity distributions" may be the result of invalid interpretation of experimental data. This matter will be considered in greater detail in a subsequent publication.

A preliminary rotational analysis of the CH spectrum shows a reasonably normal rotational distribution, in agreement with the work of Gaydon and Wolfhard (see footnote 4).

Experimental studies in absorption and emission, with improved spectroscopic apparatus, are continuing.

---

[7] O. Oldenberg and F. F. Rieke, J. Chem. Phys. **6,** 439 (1938); R. J. Dwyer and O. Oldenberg, J. Chem. Phys. **12,** 351 (1944).

6. Studies of Emission and Absorption in Flames

By G. H. Dieke and H. M. Crosswhite [1]

Spectroscopic data are obtained as emission or absorption (or sometimes a simultaneous combination of both) intensity measurements, which may be obtained either photographically or by one of the radiant-flux detectors, which in the experiments discussed here was an electron photomultiplier tube. Because of the nonlinearities and other difficulties, the photographic plate is best used as an indicator only. The fundamental experiments which involve quantitative measurements of spectral intensities should be done photoelectrically whenever possible.

The interpretation of the data requires information in addition to intensity evaluations themselves. The measured intensity of a given spectrum line is determined in general by its transition probability, the excitation conditions in the light source and the amount of reabsorption along the path between the light source and measuring apparatus. A knowledge of any two of these will allow one to describe the third. In the study of flame spectra one is usually interested in determining the energy-level distribution of emitters in the light source. This requires the (relative) transition probabilities and the (relative) reabsorption coefficients for the lines considered. In some cases, such as for the rotational distribution within the ultraviolet OH bands, it is possible to calculate the first theoretically. The second must be accounted for by separate experiments.

Extensive measurements of this spectrum were made in this laboratory a number of years ago, and computations were made for the rotational transition probabilities corresponding to these data.[2] These tabulations have been in use for over 4 years, and we have become confident in the reliability of the results. Quite often, however, the data do not represent a uniquely defined temperature, which may be due to several conditions. There may, of course, be more than one temperature, since more than one excitation region may be in the line of sight. This causes the low-energy part of the distribution curve to have a steeper slope than otherwise. A more trivial cause, but one difficult to eliminate photographically, is that of the continuous background (fig. 6.1). The strong lines, which lie in the middle region, are less affected by the addition of the continuum than the weaker ones, and there is a systematic upbending of the ends. The isointensity method, however, will still work, since it depends on selection of lines affected by the continuum in the same way. Figure 6.2 shows the distributions encountered for temperatures of 1,000° and 3,000° K. At 1,000° the intensity of

---

[1] The Johns Hopkins University, Baltimore, Md.

[2] G. H. Dieke and H. M. Crosswhite, The ultraviolet bands of OH. Fundamental data. Bumblebee Report No. 87, The Johns Hopkins University (1948).

R_2 (1) falls halfway between that of R_2 (9) and R_2 (10), while at 3,000° it is between R_2 (19) and R_2 (20), which by interpolating between lines gives an accuracy usually of 50° or better. However, since this is only a two-point technique, one does not have the assurance that the temperature actually exists from this information alone.

The third phenomenon which produces a similar effect in appearance is that of self-absorption. Figure 6.3 shows this effect as it appears in four different size burners. Curve D does not need much correcting, but even for this small absorption, measurable errors would be made in using the slope of the high lines as the criterion. The absorption becomes progressively worse, however, as the OH intensity is increased. The lower curves of each pair represent the data as obtained, and the upper set those after correction. This correction has been made assuming uniform excitation in the light source. In this case the reabsorption depends only on the intensity of the spectrum line, which may be large either because of a large transition probability or a large concentration. These matters have been discussed in some detail by Cowan and Dieke.[3] The general form of this curve is exponential for weak intensities, but the value for strong lines depends somewhat on the line shape and slit widths used. Because the OH intensities are a little inflexible, these studies were continued, using Fe I lines obtained by injecting iron carbonyl, $Fe(CO)_5$, into the flame, as has been done by Gaydon. This is a volatile liquid that evaporates rapidly enough at room temperatures to give convenient Fe contamination of the fuel. The Fe spectrum is rich in lines of a wide variety of energy and intensity levels, and the concentration is easily changed by mixing with uncontaminated fuel. The carbonyl does not change the character of the combustion appreciably, and the Fe data are remarkably consistent with that for OH. Figure 6.4 shows an absorption curve similar to that discussed above for the case of the resonance lines around 3700 A. The relative intensities were measured in a low concentration flame, then in one 10 times stronger (as measured by the behavior of the weak lines), and in a high-concentration case 4.5 times stronger again. It is possible to plot the relative amount of light lost to reabsorption in terms of a parameter p, which is proportional to the number of absorbing atoms N_a, the frequency ν, and the transition probability B_ν, of the spectral line in question:

$$p \alpha \nu B_\nu N_a. \tag{1}$$

The shape of the characteristic curve thus obtained may depend somewhat on the experimental conditions used, but it should be independent of the particular line chosen, except as indicated in eq 1.

The intensity of I_0 of a line measured under conditions of negligible self-absorption will be proportional to the number N_e of emitting atoms, the frequency ν, and transition probability A_ν of the line:

$$I_0 \alpha \nu A_\nu N_e \alpha \nu^4 B_\nu N_e \tag{2}$$

---

[3] R. D. Cowan and G. H. Dieke, Self-absorption of spectrum lines. Rev. Mod. Phys. 20, 418–455 (1948).

Substituting for B_ν in (1), we get

$$p \alpha \frac{I_0}{\nu^3} \cdot \frac{N_a}{N_e}. \tag{3}$$

Both N_a and N_e depend on the temperature, which may or may not be the same for each. If the absorber is at a different temperature, or as is more usual, the temperature along the absorbing path varies in an indeterminate manner, the absorption behavior of the lines will depend strongly on their electronic origin. This has been found to be particularly true in arclike sources.

If, however, the source is uniformly excited and there are no cooler vapors between the source and the spectrograph, the self-absorption behavior will be considerably simplified. In this case we may rewrite (2) as

$$p \alpha \frac{I_0}{\nu^3} e^{\frac{h_\nu}{hT}}. \tag{4}$$

For lines of the same wavelength region, the reabsorption will be determined by I_0 alone, for a given temperature. Figures 6.4 and 6.5 show the results for this case, which is the Fe I spectrum as seen in the outer cone of a standard oxypropane burner. Figure 6.4 indicates that the absorption is uniquely determined by the I_0 value, but this would be true whether or not there was uniform excitation, as nearly homologous lines were used. Figure 6.5 shows, however, that this condition still holds with lines about 7,500 cm^{-1} apart (again at the same wavelength). This has the happy result that the matching techniques will still work, even with appreciable self-absorption, to the degree of approximation that this condition of uniform excitation is met.

A more sensitive test of whether or not the self-absorption behavior is independent of the electronic origin of the lines is to examine the line shapes under high dispersion. If completely uniform excitation conditions hold, the intensity distribution should have a maximum that is just the black-body intensity at that temperature and wavelength. Figure 6.6 shows the appearance of these lines. The $a\,^5\text{D}$ lines (marked D) have nearly the same maximum for I_0 values over 10 times different. If the nonuniformity was appreciable, the N_a/N_e ratio for the $a\,^5\text{F}$ line 3734 (marked F) would be higher than that for the resonance group. The uniformity is not perfect, however, since the strongest lines do show the dip in the center characteristic of self-reversal, which occurs only in sources with appreciable difference between emission and absorption temperatures. This, however, is not serious in this case if the integrated line intensity is used.

If lines of appreciably different wavelength are used, results as illustrated by figure 6.7 are obtained. Since the ν^3 correction has been made, the residual shift should be, according to (4), just the Boltzmann factor, from which the temperature can be calculated. In this case it is about 2700° ±100°, agreeing with the OH determination.

Since in this case both the reabsorption and excitation conditions are known, it is possible to calculate the relative transition probabilities of all the iron lines involved. This information can then be used in a more customary manner to examine the behavior of other light sources.

Even in flames it may happen, however, that self-reversal may occur if there is a strong temperature gradient along the line of sight.

Figure 6.8 shows a spectrum of the OH head at 3064 under high dispersion. The upper spectrum is unreversed, with relative intensities as indicated below, while the lower spectrum, taken from a large acetylene torch viewed end on, exhibits complete reversal for the stronger lines, such as R_1 (6). Self-absorption, but not self-reversal, can occur in a uniformly excited source. It is possible, however, to have a nonuniform source without self-reversal as such occurring. If two sources are viewed in tandem, the first being a very bright one with sharp lines and the second a cool one with relatively broad lines, absorption of the first in the second can occur; and if the sharp lines can be considered as monochromatic with respect to the absorbing lines, the absorption curve will have the shape shown in figure 6.9. Very weak lines are little affected, intermediate lines moderately so but the strongest lines may even disappear. Figure 6.10 shows the spectrum of such an arrangement. The upper spectra are, respectively, the absorber alone, both together, and the hollow cathode source, alone. The absorber is an oxypropane torch with appreciable iron-carbonyl contamination. It can be seen that the line at 3719 is weaker than 3707, which has an I_0 value some 100 times less. All lines labeled are those ending on the ground multiplet $a\,^5$D. Other higher lying lines, even some rather strong ones, are little affected. This absorption may also be taken as a measure of the transition probabilities. It will be particularly sensitive for the stronger lines because of the large slope; and because of the doubling back in intensities, matching techniques are feasible.

If a flame source shows signs of nonuniform excitation and it is still desirable to attempt some self-absorption corrections, it is sometimes possible to measure the transmission of the flame directly with a system of tandem sources similar to the above, which will at least give limits to the possible self-absorption. If sufficient absorption is present, the distribution over the absorbing states may be measured as shown in figure 6.11 for a typical case (outer cone of ethylene-oxygen-carbon dioxide flame). If sufficient symmetry is present, it may also be possible to convert these measurements into corrections for the emission lines, shown in figure 6.12 for this case. Notice that the P_1 lines, inherently stronger than the R_2 lines, fall below the latter in the uncorrected case but coincide after correction. It is also worth remarking that a high-lying line of a given intensity shows measurably less absorption than a low line of the same intensity, since the absorbing region is at a considerably lower temperature (2520°) than the emitting (3900°), which in this case disallows the use of the isointensity system.

Transition probability determinations have also been made recently for the case of CH. Some of the higher lines, particularly in the 3900 band, are markedly weaker than would be expected from the theoretical calculations. If the 4315 band is also examined it is found that one branch, from the $^2\Delta^+$ levels, gives a Boltzmann-like distribution, while the $^2\Delta^-$ behaves similarly to the 3900 lines, also of negative symmetry. If high enough dispersion is used, enough of the 4315 R lines may be measured to give a temperature plot from which corrections may be made for the 3900 lines (fig. 6.13), which are useful with considerably lower dispersion. These values may be used in other flames such as the ethylene flame discussed above for additional information from the reaction zone (see fig. 6.14).

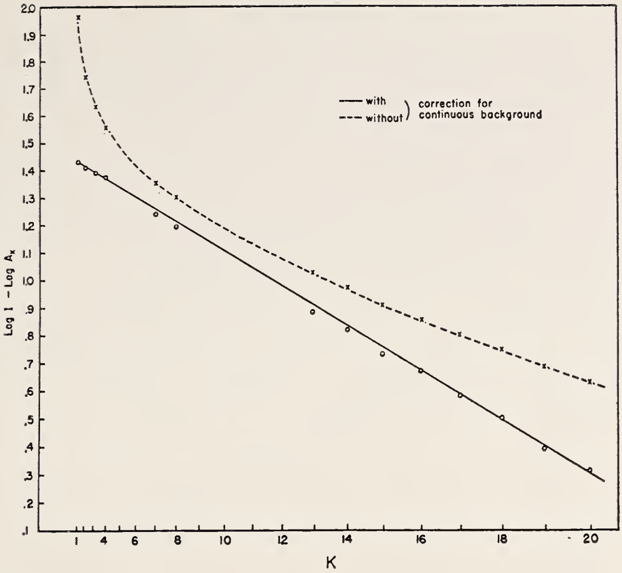

Figure 6.1. *Effect of continuous background on distribution plot.*

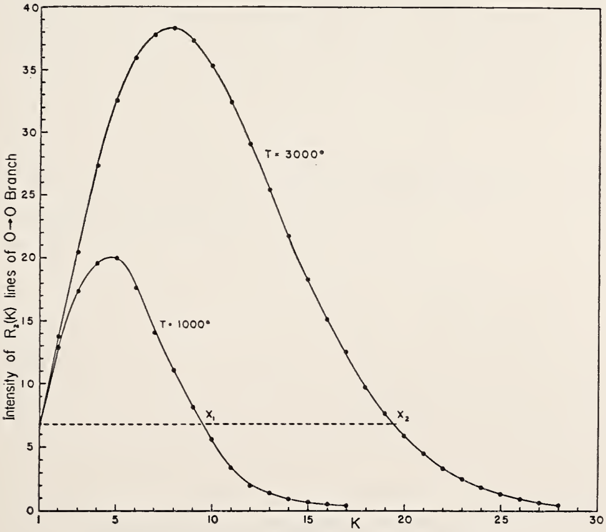

Figure 6.2. OH *intensity distributions.*

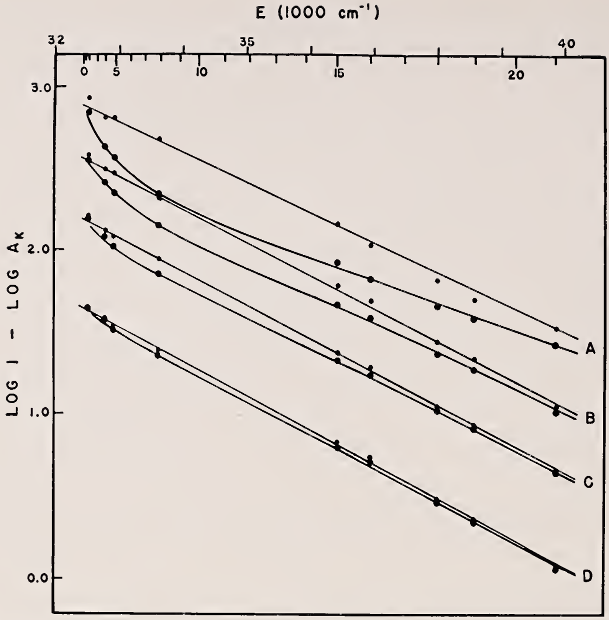

Figure 6.3.—*Effect of self-absorption on* OH *distribution plots*

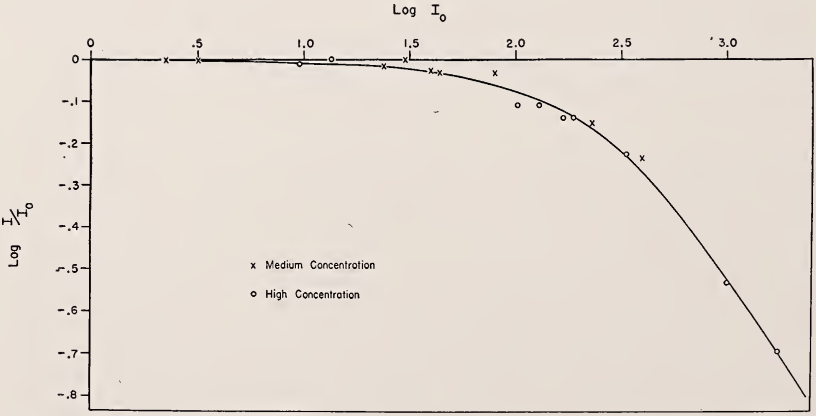

Figure 6.4. *Self-absorption of* Fe *lines in flames. Concentration dependence.*

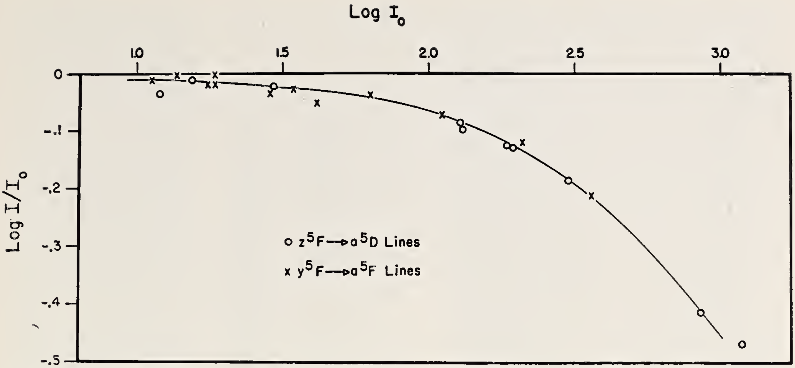

FIGURE 6.5. *Self-absorption of* Fe *lines in flame. Energy level dependence.*

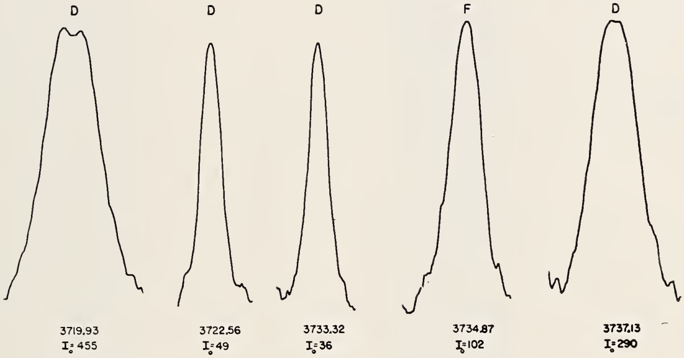

FIGURE 6.6. *The flame lines under high dispersion.*

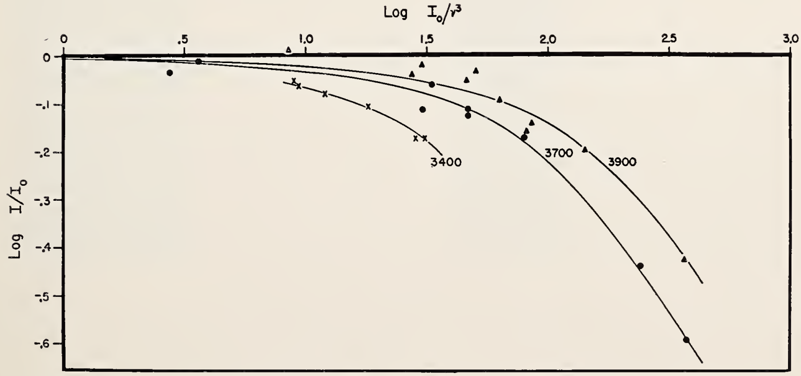

FIGURE 6.7. *Self-absorption of* Fe *lines in flame. Wavelength dependence.*

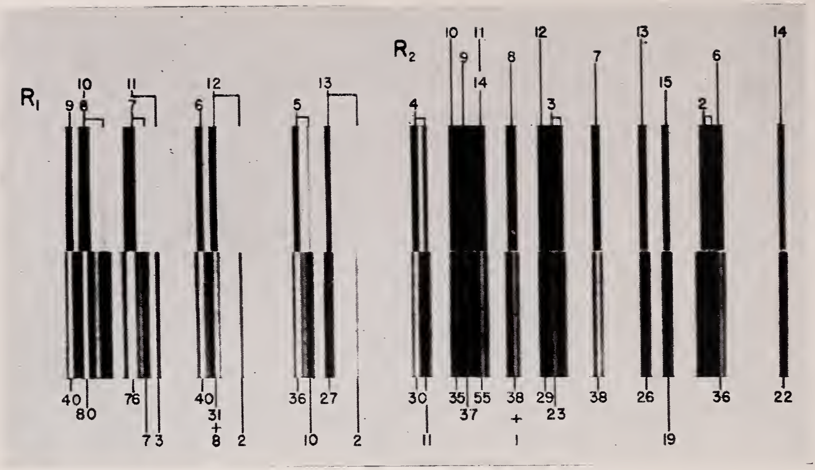

FIGURE 6.8. *Self-reversal of OH lines.*

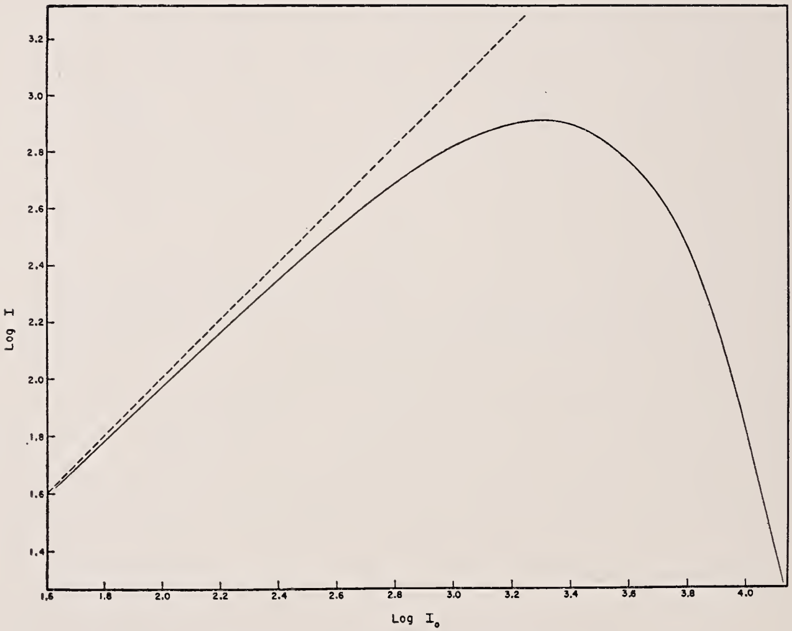

FIGURE 6.9. *Exponential self-absorption.*

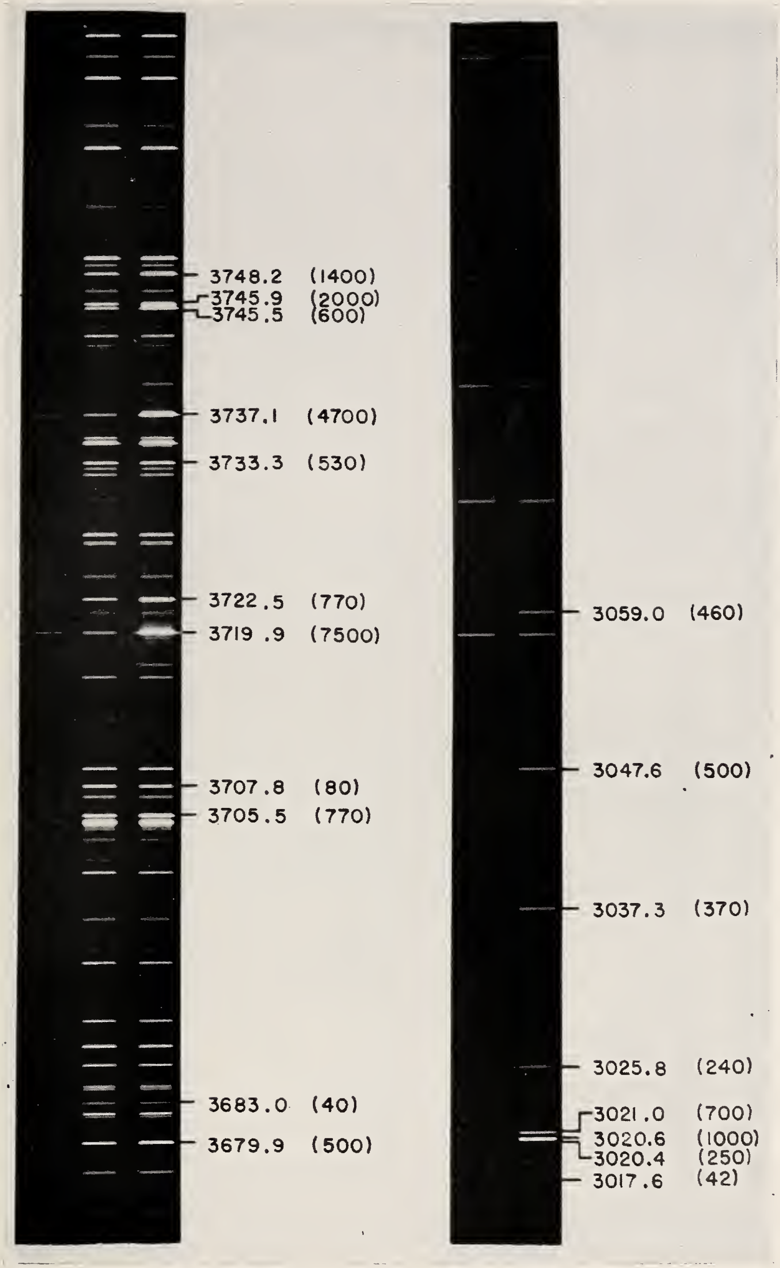

FIGURE 6.10. *Tandem* Fe *sources.*

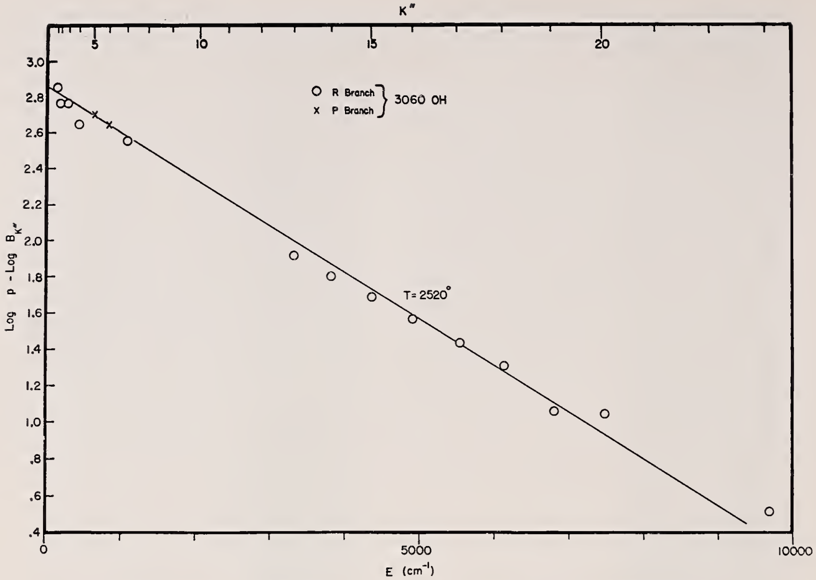

FIGURE 6.11. OH *absorption distribution in ethylene flame.*

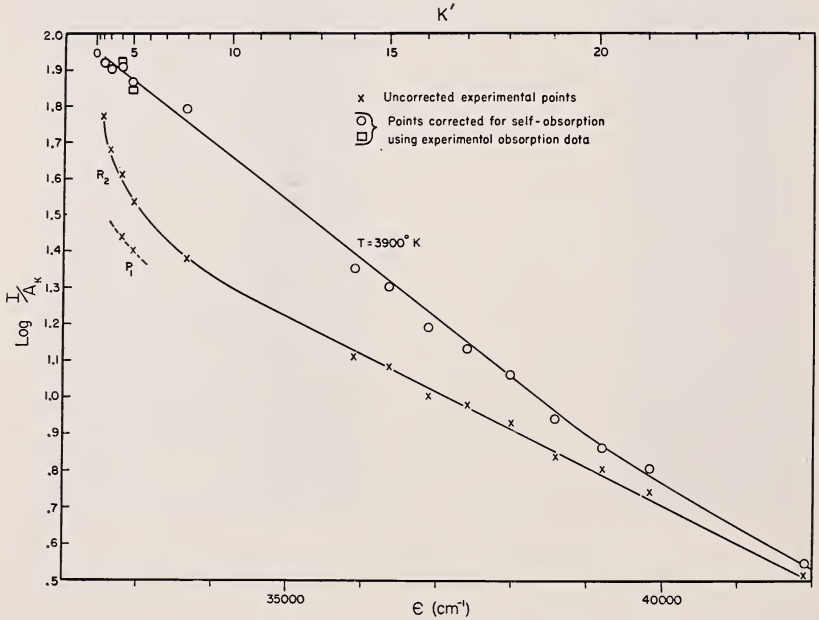

FIGURE 6.12. OH *distribution in ethylene flame corrected for nonuniform absorption.*

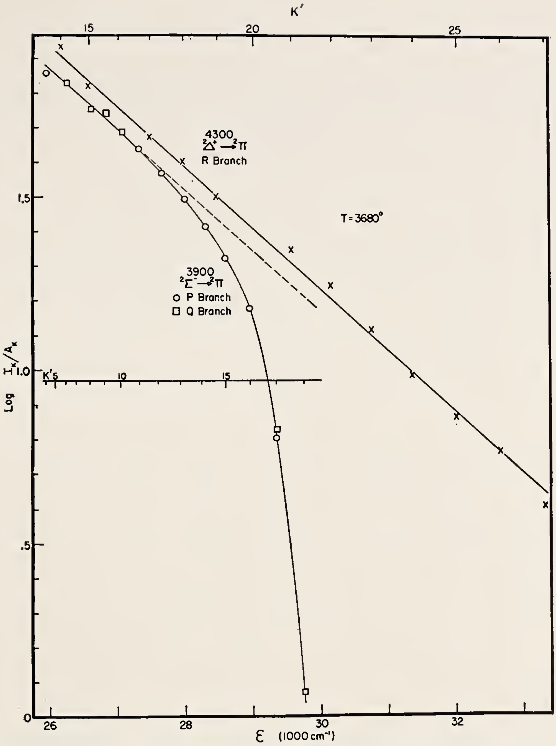

FIGURE 6.13. *Acetylene flame* CH *distributions uncorrected for predissociation.*

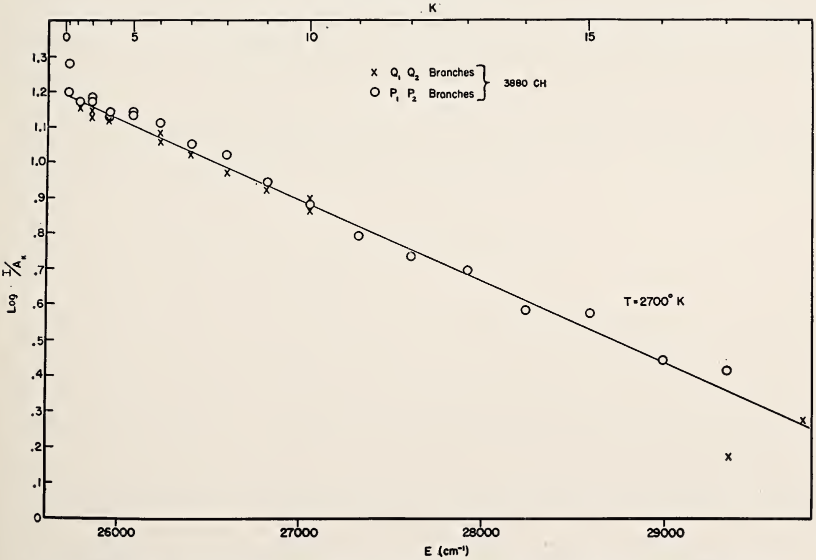

FIGURE 6.14. CH *distribution in ethylene flame corrected for predissociation.*

7. Energy Distribution of CO Molecules in CO —O_2 Flames*

By Shirleigh Silverman [1]

The energy distribution in CO—O_2 flames has been studied in the CO harmonic region at 2.3μ, under moderately high resolution (slit width $\sim$0.8 cm^{-1}). "Temperature" profiles were obtained for an essentially two-dimensional flame. In the cooler regions near the orifice, the rotational and vibrational "temperatures" are equal. The vibrational "temperature" seems to correspond to thermochemical values throughout the flame profile. On the other hand, in the outer cone rotational "temperatures" are higher than the adiabatic flame temperatures. Introduction of CO_2 or N_2 as a diluent into the fuel system is effective in establishing vibration-rotation equilibrium, with CO_2 being especially effective.

Among the various reasons for making spectroscopic observations on radiating gases is the fact that such observations may lead to increased knowledge concerning the reaction kinetics of such systems. In particular, intensity measurements under favorable circumstances permit one to study the energy distribution among the various modes of excitation for a given molecule or radical by application of the Maxwell-Boltzmann equation. Spectroscopically the molecules most suitable for accurate intensity measurements are diatomic, with a $^1\Sigma$ ground state and a fairly small moment of inertia. In addition, if one is interested primarily in the internal modes of rotation and vibration, the infrared vibration-rotation bands should lie in a region of negligible atmospheric absorption. Furthermore, it is also required that there be sufficient resolution to separate a large number of the individual rotation lines within various vibration bands.

Intensity measurements on the infrared (nonelectronic) bands will determine whether or not there is a Boltzmann distribution for either or both of the vibrational and rotational modes, provided one knows the transition probabilities for the various energy states that are involved.

In those cases where there is a Boltzmann distribution, one can stipulate the corresponding temperature parameter. The following possibilities exist (T_R=rotational temperature, T_V=vibrational, and T_C=thermochemical):

Complete Boltzmann distribution and equipartition:

1. $T_R=T_V=T_C$ equilibrium.
2. $T_R=T_V\neq T_C$ equipartition but nonequilibrium.

Partial-Boltzmann distribution and nonequipartition:

1. $T_R\neq T_V=T_C$ vibrational equilibrium—rotational nonequilibrium.
2. $T_V\neq T_R=T_C$ vibrational nonequilibrium—rotational equilibrium.

---

*This work was supported by the U. S. Navy Bureau of Ordnance under Contract NOrd-7386.

[1] Applied Physics Laboratory, The Johns Hopkins University, Silver Spring, Md.

3. $\neq T_R \neq T_V \neq T_C$ vibrational nonequilibrium—rotational nonequilibrium.

Non-Boltzmann distribution for one-mode and nonequipartition:

1. $T_R \neq k$ (not constant for different vibrational states):		Rotational Nonequilibrium
(a) $T_V = T_C$	vibrational equilibrium	
(b) $T_V \neq T_C$	vibrational nonequilibrium	
2. T_R does not exist:		
(a) $T_V = T_C$	vibrational equilibrium	
(b) $T_V \neq T_C$	vibrational nonequilibrium	
3. T_V does not exist:		Vibrational Nonequilibrium
(a) $T_R = T_C$	rotational equilibrium	
(b) $T_R \neq T_C$	rotational nonequilibrium	
(c) $T_R \neq k$	rotational nonequilibrium	
4. T_V and T_R both nonexistent—nonequilibrium		

During a recent investigation of the CO spectrum in the harmonic region of 2.3μ,[2] it was noted that there was an apparent lack of equilibrium between the vibrational and rotational energy modes for the CO molecules excited in a CO-oxygen flame as well as in some hydrocarbon-oxygen flames. Both the vibrational and rotational distributions for CO seemed to be Boltzmann-like, but were characterized by different "temperatures." It was not possible to arrive at any specific conclusions since the geometry of the flame was such that the spectrometer slit passed radiation from regions of all parts of the flame source. It was felt worthwhile to pursue this matter further with a view to attempting to get a detailed picture of the spatial variation in energy distribution throughout a simple flame.

For this purpose an ideal flame would be a two-dimensional one of infinitesimal thickness, with a well-defined linear reaction zone. In practice this can be approximated by burning from a vertical slot that is oriented in such a way that the brush of the flame is parallel to the plane of the slit jaws. With good optics and an aperture of about *F*:6.0 it is possible to image a thin slice of such a flame on the slit, and one can scan the flame spatially by imaging a succession of slices on the slit. For the current experiments a CO-oxygen flame was chosen as our emission source of hot CO for several reasons: (1) the thermochemical calculations were available for various fuel-oxygen ratios, (2) the CO concentration is large and therefore the emission is intense enough for accurate intensity measurements, (3) the flame velocity is low, so it is possible to maintain large and steady mass flows without danger of flashback, and (4) the spectrum of the flame is relatively simple, since there are only two radiating species: namely, CO and CO_2 (H_2O formed from contaminant H_2 is a relatively minor emitter).

The burner consisted of a channel 5 cm long and 1 by 30 mm in cross section milled out of a massive block of brass, which was water

---

[2] E. K. Plyler, W. S. Benedict, and S. J. Silverman, J. Chem. Phys. **20**, 175 (1952).

cooled. The gases were premixed in a commercial torch butt, which was brazed to the channeled brass block. The whole assembly was mounted on a bar that could be translated by a rack and pinion in a direction parallel to the plane of the slit jaws. At atmospheric pressure the burner supported a very steady flame when the mass flows were as large as 10 liters per minute. The reaction zone was V-shaped in cross section, and the apex of the V formed a line in space that was straight within better than 1 mm. It was found possible to focus on the slit a segment of the flame as close to the orifice as 1 to 2 mm. The volume element of the flame radiating into the slit is that determined by the slit width, ~0.1 mm, and the aperture angle, which was 10°. All spectral observations were limited to the $\Delta v=2$ vibration-rotation bands of CO. By restricting these measurements to the harmonic region, there are no self-absorption corrections to be made since emission for the various lines is sufficiently low. A portion of a typical spectrum taken at a resolution of about 0.8 cm^{-1} is shown in figure 7.1. Such spectra were observed for a number of slices of flame, all parallel to the plane of the burner orifice, ranging from 1 to 20 mm distance from the orifice. These spectra were obtained for flames burned from stoichiometric mixtures, rich mixtures, and rich mixtures to which a small amount of H_2 had been added to increase the flame speed.

The rotational energy distributions were studied by plotting log I_j/A_j versus E_j/kT, where the A_j's are the transition probabilities and the values E_j were obtained from the reference given in footnote 2. The vibrational energy distributions were obtained by plotting

$$\frac{\log I_j^{n+2\rightarrow n}}{|M|^2(\nu_j^{n+2\rightarrow n})^4} \text{ versus } \frac{E_j^{n+2\rightarrow n}}{kT},$$

where $I_j^{n+2\rightarrow n}$, $\nu_j^{n+2\rightarrow n}$ and $E_j^{n+2\rightarrow n}$ refer to the jth lines in the various $\Delta v=2$ bands. The vibration transition probabilities, $|M|^2$, are taken from the results of Crawford and Dinsmore.[3]

---

[3] B. L. Crawford, Jr., and H. L. Dinsmore, J. Chem. Phys. 18, 983 (1950).

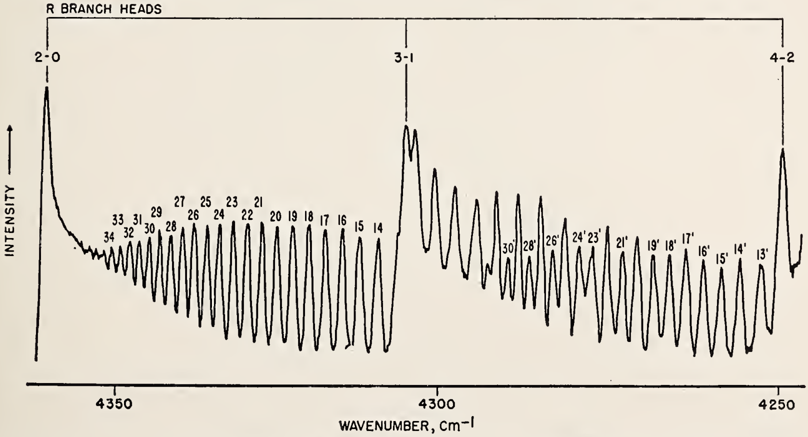

FIGURE 7.1. *Typical emission spectrum of* CO *in the overtone region at about 4,300 cm^{-1}.*

Slit width is 0.8 cm^{-1}.

In all cases it was found that the vibrational intensities so plotted gave lines that were fairly straight. Values of T were calculated for each value of J, and these were then averaged. From the vibrational data, the evidence is that a Boltzmann distribution exists for this mode throughout the flame.

The rotational data were also quite self-consistent in general. No significant differences were detected in the rotational distributions for the different vibration-rotation bands for a given flame setting; i. e., the rotational distribution is uniform for the different vibrational levels. It was also noted that in the cooler regions of the flame the rotational distribution seemed to be in equilibrium with the vibrational mode whereas in hotter regions of the flame, there was definitely nonequipartition of energy. In all cases, the rotational "temperatures" were determined by the best straight-line fit in the plot of log I_j/A_j versus E_j/kT, with the knowledge that in the hotter regions of the flame there is a faint suggestion of non-Boltzmann distribution in the direction of excess excitation of upper states. In addition the rotational temperatures were checked by observing the position of J_{max}.

Figures 7.2, 7.3, and 7.4 show typical "temperature" versus flame position plots for stoichiometric ($2CO+O_2$), fuel rich ($4CO+O_2$), and fuel rich ($4CO+O_2$), plus 5 percent H_2 flames, respectively. In addition, CO_2 and N_2 were added as diluents to the oxygen and

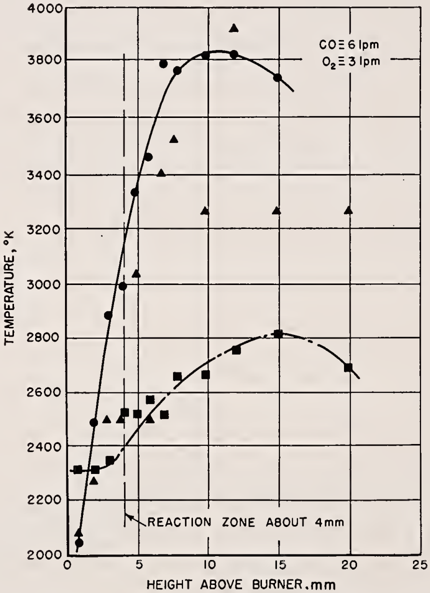

FIGURE 7.2. *"Temperature" distribution for a flame with gas composition of* 6 $CO+3$ O_2.

●, $\ln \frac{I}{A}$ versus $\frac{E}{kT}$; ▲, T versus $B\left(\frac{J_{\max}+\frac{1}{2}}{0.59}\right)^2$;

■, $\ln \frac{I}{|M|^2\nu^4}$ versus $\frac{E}{kT}$.

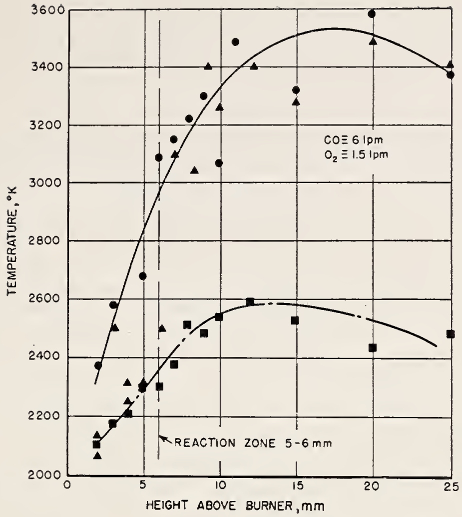

FIGURE 7.3. *"Temperature" distribution for a flame with gas composition* 6 $CO+1.5\ O_2$.

●, ln $\frac{I}{A}$ versus $\frac{E}{kT}$; ▲, T versns $B\left(\frac{J_{\max}+\frac{1}{2}}{0.59}\right)^2$;

■, ln $\frac{I}{|M|^2\nu^4}$ versus $\frac{E}{kT}$.

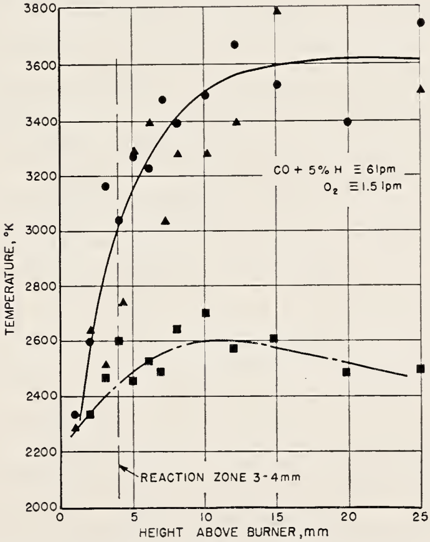

FIGURE 7.4. *"Temperature" distribution for a flame with gas composition* 6 $(0.95\ CO+0.5\ H_2)+1.5\ O_2$.

●, ln $\frac{I}{A}$ versus $\frac{E}{kT}$; ▲, T versus $B\left(\frac{J_{\max}+\frac{1}{2}}{0.59}\right)^2$;

■, ln $\frac{I}{|M|^2\nu^4}$ versus $\frac{E}{kT}$.

observations were made at a point 10.0 mm beyond the reaction zone. These results are shown in table 7.1, together with the mole concentrations of CO and CO_2 for an equilibrium system at the calculated temperature.

Table 7.1

Gas mixture	Temperature			Molar composition at T_c	
	Calculated	Rotational	Vibrational	CO_2	CO
	°K	°K	°K		
6 CO+1.5 O_2	2, 850	3, 400±10%	2, 550±10%	2. 59	3. 41
6 CO+1.5 O_2+1.3 CO_2	2, 625	2, 500	2, 300	4. 18	3. 12
6 CO+1.5 O_2+1.3 N_2	2, 680	2, 750	2, 400	2. 63	3. 37

The following may be noted:

1. The vibrational "temperatures" are approximately the same as thermochemically calculated values.

2. In the cooler regions of the flame, that is, the region near the orifice, there is vibrational-rotational equilibrium and equipartition.

3. In the hotter regions of the flame, (a) assuming a Boltzmann distribution there is nonequipartition and the rotational temperatures are as much as several hundred degrees in excess of thermochemical values, and (b) assuming the nonlinearity of log I_j/A_j versus E_j/kT with overpopulation of large J-values, there is a considerable excess of rotational energy with a non-Boltzmann distribution.

4. There seems to be a maximum "temperature" for both vibrational and rotational modes several millimeters beyond the reaction zone.

A possible explanation for the nonequipartition of energy between vibrational and rotational modes for CO molecules may lie in the fact that at flame temperatures the CO population consists of molecules formed by dissociation of CO_2 as well as of unreacted molecules. Whereas the latter may well be expected to be in thermal equilibrium, the former may well be in nonequipartition or even in nonequilibrium. This could come about if the reaction $CO_2^*+M \rightarrow CO^*+O+M$ is sufficiently probable. In this event, although the time between collisions ($\sim 10^{-8}$ to 10^{-9} sec) is very short compared with the radiative lifetime ($\sim 10^{-2}$ sec), collisions involving excited species may be sufficiently numerous to maintain on the average an excess of rotational energy. This point of view seems to be supported by the marked quenching action of added CO_2 and even N_2 molecules, accompanied by relatively little cooling of the flame.

With regard to so large a displacement of the region of maximum excitation beyond the reaction zone, this downstream displacement of several mm is equivalent to a time delay of about 1 to 2 $\times 10^{-2}$ sec. The radiative peak seems, therefore, to lag behind the peak of thermal excitation by a time interval equal to about one radiative lifetime.

Further work is being planned on the $CO+O_2$ reaction and it is hoped that more light will be shed on the tentative explanations set forth here.

In conclusion, the author expresses his appreciation to Dr. K. E. Shuler of this laboratory and to Prof. K. J. Laidler of the Catholic University of America for many stimulating discussions concerning this problem, and to Mr. R. K. Neumann of this laboratory, who performed the thermochemical calculations.

8. High-Resolution Spectra of Hydrocarbon Flames in the Infrared[1]

By W. S. Benedict [2] and Earle K. Plyler [3]

In this paper is presented a summary of recent work in which the spectra of hydrocarbon flames have been studied between 1 and 2.6 microns with considerably higher resolution than has hitherto been possible. (For the strongest regions of emission, resolution of 0.2 cm^{-1} has been achieved.) The improvement in resolution has resulted from the use of lead-sulfide photoconductive cells, which are sensitive detectors in that region, together with a 15000 lines-per-inch grating spectrometer of high optical quality. The results for the most part have been presented in greater detail elsewhere [1, 2, 3]*; the emphasis of the present paper will be to point out the similarities and the differences between flame spectra in the near-infrared and in the more familiar visible and near-ultraviolet regions.

1. Introduction

The most intense and characteristic spectra in the visible and ultraviolet, as summarized for example by Gaydon in his valuable book [4], are the electronic spectra of diatomic molecules or radicals. The upper energy levels are from 2 to 10 ev above the ground energy levels of the molecular species, so that if there is thermal equilibrium, characterized by the Boltzmann distribution, the emitting molecules are a very small fraction of the total. However, the radiation process in which transition occurs from one electronic state to another is often very efficient; that is, it is characterized by a high probability and a correspondingly short lifetime of the excited state, so that considerable radiant energy may be transferred by this very small fraction of molecules. In many cases it also appears that the upper states are populated in excess of a Boltzmann modulus; i. e., have an abnormally high "electronic temperature", thus increasing the radiant-energy transfer.

By contrast, the most characteristic spectra in the near-infrared are *vibration-rotation* spectra, of *all* the constituents of the flame, polyatomic as well as diatomic, except for the homopolar diatomic molecules, O_2, H_2, and N_2. The upper energy levels are only 0.5 to 2.0 ev above the ground level, so that they are well populated at flame temperatures. Except for the fundamental vibration-rotation bands, whose short wavelength limit is near 2.4 microns; that is, at the long-wavelength limit of the region here under study, the transition probabilities are low. Hence the larger proportion of radiating molecules does not result in much larger radiant transfer than in electronic transitions. Moreover, because the lifetimes of excited states of equal transition probability are proportional to the square of the wavelength, the lifetimes of such states for infrared radiation are very much longer than for electronic radiation, being, respectively, of

---

[1] Supported in part by the Office of Naval Research.
[2] Present address, The Johns Hopkins University, Baltimore, Md.
[3] National Bureau of Standards, Washington, D. C.
*Figures in brackets indicate the literature references on p. 72.

the order of 10^{-2} to 10^{-3} sec for the infrared and 10^{-6} to 10^{-8} sec for the near ultraviolet. In the former case, this is very much longer than the mean time between gas-kinetic collisions; in the latter, it is of the same order. Thus even though the collision process is often quite inefficient for the transfer of vibrational quanta (as is evidenced by the dispersion of high-frequency sound waves [5] and time lags in gas-dynamic processes [6]), infrared-radiating molecules are much more likely to be in thermal equilibrium within their vibrational and rotational energy modes than are the shorter lived electronically excited molecules.

In the course of our high-resolution studies of the spectral region 1 to 2.6 μ, from simple hydrocarbon flames (principally acetylene-oxygen burning in an ordinary blowtorch, we have identified and analyzed radiation from six molecular species; namely, H_2O, CO_2, CO, OH, C_2, and CN. The transitions for the first four were rotation-vibration spectra; for the last two they were infrared extensions of known electronic transitions. The first four could be observed in various portions of the flame with, in general, the more stable oxidized products, H_2O and CO_2, predominating in the outer cone, and the high-temperature-stable diatomic products, OH and CO, reaching a maximum of intensity just above the tip of the inner cone. C_2 and CN, just as with their more familiar visible spectra, occur only in the inner cone.

In the subsequent sections we shall discuss the spectra of the molecules just named in greater detail. There are two principal problems in the interpretation of the spectra; first, the identification of the energy states responsible for the appearance of spectral lines. This has been achieved to the extent that the general regions of emission are satisfactorily accounted for, and much of the detail, insofar as it has been resolved, is also understood. The second problem is the explanation of the intensity of each line in terms of the concentration of molecules in each such energy level. This has been only partially solved. In general, measurements of absolute intensity are difficult experimentally, because of problems connected with the finite width both of the spectral lines and of the slits of the measuring instrument. Such measurements were not attempted in this work. The relative intensity of resolved lines can be much more easily measured and interpreted, and some such measurements have been made, leading to the general conclusion that the radiation is predominantly thermal in origin. In the next section we will summarize the general theoretically calculable facts concerning the equilibrium concentrations and intensities of the molecules that we have identified in the flame, as well as of other molecules that may be present.

2. Equilibrium Concentrations and Intensities

If the radiation is thermal, all the energy states of all the molecular species must be in equilibrium; if nonthermal or chemiluminescent, some states of some species are preferentially excited. The equilibrium among the various energy levels of a particular molecule, as a function of temperature, is one aspect of this problem. Second is the question whether the various molecules are themselves in a state of chemical equilibrium with each other at a particular temperature. From a knowledge of the heats of formation and entropies of the various possible reactants, intermediates, and products in flames, it is possible to calculate the equilibrium concentrations of a large number of molecules under a large number of possible burning conditions.

For orientation purposes, table 8.1 presents the results of such a calculation for a hydrocarbon burned with the stoichiometric amount of O_2 containing 1 percent of N_2, at three values of the temperature, 3000°, 2600°, and 2200° K. The adiabatic temperature would depend upon the particular hydrocarbon; thus for C_2H_6 it would be slightly in excess of 3000° K; for $C_2H_2+2H_2$ it would be nearly 3200° K. The calculations were based principally upon the compilations of Hottel, Williams, and Satterfield [7], which give the concentrations of the major constituents of these particular flames. The minor constituents were then calculated from various other sources for the equilibrium constants, mainly taken from the tables of free energy published by the National Bureau of Standards. For some of the free radicals considered there are no reliable data concerning the free energies and heats of reaction. In this case the results can be considered as of only order-of-magnitude accuracy and are based upon estimates of the bond energy and the moments of inertia and vibrational frequencies.

Table 8.1. *Equilibrium composition of hydrocarbon flame gases*

Atomic composition, C:O=0.30; H:O=1.0; N:O=0.01

Molecule	Temperature, ° K		
	3000	2600	2200
H_2O[a]	0.3821	0.5131	0.5389
H_2	.0819	.0548	.0554
CO_2[a]	.1326	.2260	.2534
CO[a]	.2153	.1620	.1436
O_2	.0429	.0077	1.2×10^{-4}
OH[a]	.0704	.0195	0.0018
O	.0248	.0022	3×10^{-5}
H	.0451	.0090	0.0013
N_2	.0043	.0056	.0060
NO	.0018	.00046	2.8×10^{-5}
C_2[a]	5×10^{-14}	2.8×10^{-15}	6×10^{-16}
CN[a]	9×10^{-9}	1.2×10^{-9}	2.3×10^{-10}
CH	1.1×10^{-9}	6.5×10^{-11}	6×10^{-12}
CH_2	8×10^{-13}	4×10^{-14}	1×10^{-17}
CH_3	1.8×10^{-12}	3×10^{-13}	1.4×10^{-14}
CH_4	1.7×10^{-13}	1×10^{-13}	6×10^{-13}
C_2H_2	8×10^{-16}	1×10^{-16}	1×10^{-17}
H_2CO	1.8×10^{-8}	9×10^{-9}	8×10^{-9}
HCO	1.2×10^{-8}	1.8×10^{-9}	2.7×10^{-10}
HCN	2×10^{-9}	7×10^{-10}	6×10^{-10}
N	1.0×10^{-5}	1.0×10^{-5}	5×10^{-7}
NH	3.9×10^{-6}	7×10^{-7}	1×10^{-7}
NH_3	1.1×10^{-8}	9×10^{-9}	1.5×10^{-8}

[a] Molecular species observed in this work.

The species considered in table 8.1 include the main products of combustion, namely, H_2O and CO_2; the products of partial combustion and unutilized reactants, namely, CO, H_2, O_2, and N_2; the products of dissociation, which are principally free diatomic radicals, such as OH, C_2, CN, NH, and monatomic species O, H, and N. In addition, there are the polyatomic products of partial combustion, which may be present, CH_4, C_2H_2, CH_2O, HCN, and some hypothesized larger polyatomic radicals, namely, HCO, CH_3, CH_2, and NH_2, which have never been identified with certainty by their spectra, (except for NH_2, for which the evidence is quite convincing) and for which the data concerning the equilibrium constants are completely speculative. For these polyatomic free radicals, the concentrations may be in error by 1 or 2 orders of magnitude; for the other substances, the calculated equilibrium concentrations are probably accurate within ± 50 percent of the amount given for most of the species and are considerably more accurate for the well-known gases that are present in largest concentrations.

A study of table 8.1 shows that, with the exception of OH, the equilibrium concentrations of the molecular fragments that are not stable at room temperatures, namely, the free radicals OH, CH, C_2, CN, and NH, are very small. The reason why the spectra of these radicals may be observed with relatively high intensity in the visible and ultraviolet regions is that in that region the emission is electronic in origin and has a very high transition probability, together with the possibility that these excited electronic states are formed in excess of the equilibrium concentration (chemiluminescence). In the infrared region the spectra may be either electronic in origin, in which case the minor constituents may appear (and, in fact, C_2 and CN have appeared); or they may be due to vibration-rotation transitions without changes in the electronic quantum states. The transition probabilities for these are usually much smaller than for electronic transitions and therefore it has been possible to observe only those molecules that have the largest concentration, as shown in table 8.1.

Table 8.1 also reveals the relative changes in concentration of the various free radicals and molecules that are to be expected with changing temperature. The actual temperature of the flame, assuming that equilibrium conditions prevail (a necessary condition for the temperature to have meaning) will in general lie below that of the adiabatic flame temperature. The temperature may vary in the various regions of the flame depending on how far it is from the region where the reaction has taken place to the place where observations are made. It is to be expected that the actual equilibrium temperatures in the outer cone of flames may be from 100 to 200 deg below the calculated adiabatic flame temperatures and at greater distances from the luminous zone of the flame will fall toward room temperature. Table 8.1 shows how the free radical concentration drops in this intermediate region.

The second factor that determines the intensity of a spectral line or of the totality of spectral lines in an unresolved band, in addition to the equilibrium total concentration of the species which we have just discussed, depends upon the transition probability for the particular spectral line in question. This transition probability may be expressed in a variety of ways. Most fundamentally, it is given by the quantum-mechanical expression

$$|R'{}^{,}{}''|^2 = |\int \psi' n' v' j' e\vec{x} \psi'' n'' v'' j'' d\tau|^2,$$

where R is the dipole strength of the transition, ψ' and ψ'' are the wave functions of the two states, characterized by quantum numbers n (electronic), v (vibrational), and j (rotational), and $e\vec{x}$ is the electric dipole. $|R|^2$ may be separated into electronic, vibrational, and rotational parts corresponding to the factoring of the wave function into those parts, and the dipole strength of each part may be computed separately from the properties of the wave functions. The rotational transition probabilities are in general well-known and simple functions of the rotational quantum numbers. The $|R|^2_{v'v''}$ cannot be calculated so directly, but may be empirically determined if normalized to unity; for vibration-rotation transitions from the level $v=0$, it is nearly unity for $\Delta v=1$, much lower for $\Delta v=2$, and still lower for higher values of Δv. The remaining factor in $|R|^2$, namely, $|R|^2_{n'n''}$ depends upon the distribution of electric charge in the two states, and must usually be determined from experiment, although order-of-magnitude calculations have been made for certain electronic transitions. $|R|^2$ has the dimensions of g cm^5 sec^{-2}, or (electric charge × length)^2, and in what follows is expressed in units of (Debye)^2, or 10^{-36} esu.

Empirically, intensities are determined either in absorption or in emission. For thermal radiation, that is when the relative populations of upper and lower states are given by the Boltzmann distribution $N'/N''=g'/g''e^{-(E'-E'')/kT}$, the absorptivity α_ν, and emissivity ϵ_ν, are equal according to Kirchoff's law. α_ν is defined as $(I/I_0)_\nu$, the fraction of incident radiation I_0 absorbed at the frequency ν; ϵ_ν is the ratio of emitted intensity to that emitted by a Planck black body at temperature T and frequency ν. For line and band spectra, α is a rapidly varying function of ν. The variation across a single line depends upon the line width, a parameter which depends on such conditions of experiment as pressure, temperature, and composition, and which is difficult to determine by direct experiment under most conditions, since the line width is usually of the order of 0.1 cm^{-1} or less, whereas the effective slit width of all but the most highly dispersive spectrographs is much greater. Accordingly, it is more meaningful to discuss the integrated intensity of lines or bands, defined by $\int \alpha_\nu d\nu$. This quantity has the dimensions of cm^{-1}; it is proportional to the path length and the amount of gas, and hence the molecular parameter related to the transition probability is the *integrated absorption coefficient* $\int k_\nu d\nu=(1/pl)\int \alpha_\nu d\nu$, having dimensions cm^{-2}atm^{-1}. (Atmospheres refer to STP.) This quantity has been determined for a number of vibration-rotation bands, using pressures high enough to broaden the line width until the instrumental slit-width factor is eliminated. We may discuss it either for a single line, or for all the lines in a band or band system. The relation between the dipole strength and the integrated absorption coefficient is

$$|R'{,}''|^2=\frac{3hc}{8\pi^3_\nu N''}\int k_\nu d\nu,$$

where N'' is the number of absorbing molecules per cm^3 in the initial state. If we are considering the integrated absorption coefficient of an entire band system, N'' refers to the total number of molecules of a given species, i. e., is related to Loschmidt's number. For a single line, we must compute the fraction of molecules of that species in the initial state, by the usual quantum statistical methods, giving the result

$$\frac{N''}{N}=\frac{ge^{-E''/kT}}{\Sigma ge^{-E''/kT}}=ge^{-E''/kT}/Q,$$

Q being the sum of states or partition function.

Another way in which the transition probability is often expressed is in terms of the dimensionless *f-value.* This is given by the relation

$$f^{\prime,\prime\prime}=\frac{8\pi^2\mu c\nu}{3h\epsilon^2}\,|R^{\prime,\prime\prime}|^2,$$

where μ and ϵ are the mass and charge of the electron. The f-values are most commonly used in expressing probabilities of electronic transitions in atoms and molecules. For atoms, they are of the order of unity for resonance transitions. In some molecular transitions they approach unity, but they are generally of the order of 0.01.

The Einstein coefficients, expecially the Einstein coefficient for emission, are also of interest in discussing radiative transition probabilities. *The Einstein absorption coefficient,*

$$B^{\prime,\prime\prime}=\frac{8\pi^3}{3h^2c}\,|R|^2,$$

has the dimensions sec g^{-1}. The *Einstein emission coefficient*

$$A^{\prime,\prime\prime}=8\pi hc\nu^3B^{\prime,\prime\prime}=\frac{64\pi^4\nu^3}{3h}\,|R|^2,$$

has the dimensions of $\sec^{-1}$. The lifetime τ of an excited state is given by the relation $\tau'=1/\Sigma A',''$. The ν^3 term in A/B results in the emitted intensity being proportional to ν^4, since the absorbed intensity is proportional to the frequency.

The particular method of expressing the transition probability has differed with different investigators, because of the various interests of the researchers. The intensities of infrared vibration-rotation bands have usually been in terms of the integrated absorption coefficient $\int k_\nu d\nu$, or, when determined from the dispersion or the refractive index, in terms of the $|R|^2$ or an "effective charge". Electronic transition probabilities have generally been in terms of f-values. In discussing flame kinetics it is desirable to have the Einstein emission coefficients, which are simply related to the excited state lifetimes. To facilitate intercomparisons of electronic and rotational-vibrational probabilities and lifetimes, table 8.2 presents numerical factors derived from the relations just given. In using the table, it must be recalled the ν is always in wave numbers, and that atmospheres refer to the gas at 273.16° K. If it is desired to use the wavelength, λ, in microns, the substitution $\nu=10^4\lambda^{-1}$ may be made.

TABLE 8.2. *Conversion table for intensities and transition probabilities*

Use entry as multiplier to convert

To ⟶ From	$\int k_\nu d\nu$ (cm^2atm^{-1})	$[R]^2$ (Debyes)^2	f-value	B (sec g^{-1})	A ($\sec^{-1}$)
$\int k_\nu d\nu$ ($cm^{-2}atm^{-1}$)	1	$0.089359\nu^{-1}$	4.2037×10^{-8}	$5.6175\times10^{6}\nu^{-1}$	$2.8035\times10^{-8}\nu^{2}$
$[R]^2$ (Debyes)^2	11.1908ν	1	$4.7043\times10^{-7}\nu$	6.2865×10^{7}	$3.1373\times10^{-7}\nu^{3}$
f-value	2.3788×10^{7}	$2.1257\times10^{6}\nu^{-1}$	1	$1.3363\times10^{14}\nu^{-1}$	$0.66691\nu^{2}$
B (sec g^{-1})	$1.7801\times10^{-7}\nu$	1.5907×10^{-8}	7.4833×10^{-15}	1	$4.9906\times10^{-15}\nu^{3}$
A ($\sec^{-1}$)	$3.5670\times10^{7}\nu^{-2}$	$3.1874\times10^{6}\nu^{-3}$	$1.4995\nu^{-2}$	$2.0038\times10^{14}\nu^{-3}$	1

Existing data on transition probabilities for the molecules of interest in this paper, converted to a common basis, are collected together with other pertinent information in table 8.3. This lists at two temperatures, namely, 287.7° K and 2877° K, corresponding to room and flame conditions, for all the molecules whose spectra were observed in the course of this study, the following data: The state sum, Q, broken down into rotational and vibrational factors, as well as the fraction of molecules in some of the excited electronic states of interest. Q_R is of importance, since it is related to the number of rotational lines that will appear in any band, and Q_v is likewise related to the number of bands in any sequence of constant Δv. Under *transition* in table 8.3 are listed the most important transitions that have been found to contribute to the infrared emission from 1 to 2.7 microns, together with a few other important transitions outside this spectral region for the purposes of comparison and orientation. Next in table 8.3 is listed the probability of this transition in several of the forms just discussed. Under $\int k_\nu d\nu$ are listed values, first for the entire band or band system, second for the most intense line in the band, at the two temperatures in question. The f-value and the lifetime of the upper state, derived from the Einstein A, relate to the entire band transition, and are essentially independent of temperature.

The sources of the tabulated intensity data vary considerably in reliability, ranging from determinations of the integrated absorption coefficient that may be accurate to ± 10 percent, to outright guesses based on analogy with similar molecules. These should, however, be within a factor of 10 of the true value.

Two general conclusions may be drawn from table 8.3. First, if we are dealing with relatively thin burner flames, as we are in the experiments and studies reported at this time, the infrared emissivity from thermally excited radiation will be well below unity. The highest value of the integrated absorption coefficient appearing in table 8.3 for a single line of a rotation-vibration band at wave numbers greater than 3900 cm^{-1} is 0.17. This is for the strongest line in the ν_3 fundamental of H_2O, namely, the rotational transition $14_{-14}-13_{-13}$ at 3990 cm^{-1}. If the H_2O concentration is 75 percent at 2877°K and the flame thickness 2 cm, $pl=0.14$, and the line strength $S=pl\int k\nu d\nu=0.025\ \mathrm{cm}^{-1}$. Since the half-width of the line δ is not likely to be less than 0.02 cm^{-1} (and may be as high as 0.2 cm^{-1}), the peak value of the emissivity assuming a Lorentz line shape, given by $\epsilon=\alpha=S/\pi\delta$, will be considerably less than unity. Hence self-absorption effects will not be of importance. This is in accordance with the experimental finding that doubling the path length, by placing a mirror behind the source, very nearly doubled the emitted intensity at all wavelengths.

It will be noted from table 8.3 that the transition probabilities of the strongest lines in the electronic transitions are higher by 3 or 4 orders of magnitude than in the vibration-rotation bands. For C_2 and CN bands in our region, however, the thermal concentrations that were given in table 8.1 for equilibrium conditions are so low that self-absorption will still not occur. However, it will be clear that if the OH concentrations approach 10 percent, as they do under equilibrium conditions, as shown in table 8.1, the OH electronic transition at 3064 A will show in its strongest lines integrated absorption coeffi-

TABLE 8.3. *Lifetimes of molecules in flames and intensities of emission in the infrared*

Molecule	T	Q_R	Q_v	$ge^{-E_{el}/kT}$	Transition	ν	$\int k_\nu d\nu$ band	$\int k_\nu d\nu$ line		f	τ'
								287° K	2877° K		
	° *K*					cm^{-1}	$cm^{-2}atm^{-1}$	$cm^{-2}atm^{-1}$	$cm^{-2}atm^{-1}$		*sec*
CO	287.7	104.0	1.00001	----------	v–r 1–0	2143	259	12.3	2.3	1.09×10^{-5}	0.03
	2877	1046	1.521	----------	v–r 2–0	4260	1.79	0.085	0.016	7.5×10^{-8}	.015
OH	287.7	43.2/4	1.00000	10^{-7}	v–r 1–0	3568	100	----------	.9	4×10^{-6}	.03
	2877	435.8/4	1.2063	----------	v–r 2–0	6971	4	----------	.036	1.7×10^{-7}	.015
	--------	--------	--------	----------	$^2\Sigma$–$^2\Pi$ 0–0	32600	29000	----------	260	1.2×10^{-3}	1.2×10^{-6}
CN $^2\Sigma$	2877	2128/2	1.569	2	$^2\Pi$–$^2\Sigma$ 0–0	9117	500000	----------	3000	.02	9×10^{-7}
CN $^2\Pi$	2877	4732/4	1.705	0.00105							
C_2 $^3\Pi_u$	2877	3720/6	1.809	6	$^1\Pi_u$–$^1\Pi_g$ 0–0	8268	500000	----------	70	.02	1.1×10^{-6}
C_2 $^1\Sigma_g^+$	2877	553	1.676	0.0706	$^3\Pi_g$–$^3\Pi_u$	19378	700000	----------	600	.029	1.4×10^{-7}
C_2 $^1\Pi_u$	2877	1258/2	1.834	$.0013\times2$							
C_2 $^3\Pi_g$	2877	3450/6	1.721	$.00006\times6$							
CO_2	287.7	256.2	1.0768	----------	v–r 010–000	667	187	2.6	0.031	7.9×10^{-6}	0.43
	2877	2570	36.9	----------	v–r 001–000	2349	2700	74.	.88	1.14×10^{-4}	2.25×10^{-3}
	--------	--------	--------	----------	v–r 101–000	3715	39	1.1	.013	1.6×10^{-6}	2.1×10^{-3}
	--------	--------	--------	----------	v–r 201–000	4978	1.0	.027	.0003	4×10^{-8}	2×10^{-3}
H_2O	287.7	167.3	1.00035	----------	v–r 010–000	1595	300	10	.50	1.3×10^{-5}	0.045
	2877	5550	2.6231	----------	001–000	3755	100	3.3	.17	4.5×10^{-6}	.023
	--------	--------	--------	----------	011–000	5331	30	1.0	.05	1.3×10^{-6}	.018
	--------	--------	--------	----------	101–000	7250	20	0.7	.03	8×10^{-7}	.020
	--------	--------	--------	----------	111–000	8807	0.6	.02	.001	2.5×10^{-8}	.015

cients very much higher than unity and will therefore very readily give rise to self-absorption and self-reversal effects in its stronger lines, as discussed by Dieke and Crosswhite [8], Broida [9], and Penner [10].

Table 8.3 demonstrates quantitatively the point made earlier, namely, that the lifetimes involved in vibration-rotation transitions in the infrared are of the order of 10^{-3} to 10^{-1} sec, as contrasted with orders of 10^{-8} to 10^{-6} sec for electronic transitions in the ultraviolet and visible, and 10^{-6} for the C_2 and CN transitions in the near infrared. This comes about principally from the ν^2 factor, in the relation between f and A, as well as from the much smaller amplitude of electronic oscillation involved in vibration-rotation transitions. Its consequence is that molecules that radiate vibration-rotation energy will have survived many collisions, and hence will have a very great chance of being in or near a state of thermodynamic equilibrium, as contrasted with the molecules that emit electronic energy.

Further details of the spectra of individual molecules and radicals, as summarized in table 8.3, are given briefly in the following section.

3. Observed Spectra

8.1. CO

This molecule is abundant in flames and has a simple vibration-rotation spectrum. Our observations have been discussed fully elsewhere [1, 11]. Four bands of the first overtone sequence appear between 4360 and 4000 cm^{-1}. The R branches form heads at $J=50$, and are resolved out to $J=46$. The resolved spectra are suitable for making determinations of both rotational "temperatures" from the intensity distribution of lines in the R branch, and vibrational "temperatures" from relative intensities of corresponding lines or of heads in the 2–0, 3–1, 4–2, and 5–3 bands. These measurements are subject to some uncertainty, based on both experimental difficulties and incomplete knowledge of the transition probabilities, but nevertheless, should be among the more reliable determinations of temperature by spectroscopic methods. The absolute transition probability is known to an accuracy of ± 10 percent [12]; hence the figures quoted in table 8.3 should be reliable, and indicate that self-absorption should be negligible. The resulting temperatures appear slightly lower than the adiabatic, being in the neighborhood of 2600° K in measurements reported here. Silverman [11] has more closely followed the variation of CO temperature with position in the flame.

8.2. OH

We have observed bands of the 2–0 and 3–0 sequences as discussed in greater detail elsewhere [2]. Inasmuch as the ground state of the radical is $^2\Pi$, the rotational structure is not simple. The four strongest P branches are, however, well resolved in the region 5900 to 6700 cm^{-1}, and yield a very characteristic pattern, with one pair of lines (spin-doublets) coming closer together with increasing K, and a second pair (λ-doublets) separating with increasing K. The R branches which form heads fall in a region of strong H_2O emission, and have been recognized but cannot be used for intensity determinations.

The transition probability ($\int k_\nu d\nu = 4$ cm^{-2} atm^{-1} for 2–0) listed in table 8.3, is a rough estimate based on the relative intensity of CO, OH, and H_2O emission in our spectra, and on the assumption that these radicals were present in thermochemical equilibrium. It cannot, therefore, be used to test whether such equilibrium exists. However, it is a reasonable value, as compared with the same transition in the similar molecules HCl and HF, and with a value calculated [13] on assumptions concerning the distribution of electric charge.

Our measurements in the P branches of 2–0, 3–1, and 4–2 have been used to yield vibration-rotation temperatures which range from 2600 to 2400° K, depending on the values assumed for the relative rotational and vibrational transition probabilities. These temperatures are several hundred degrees lower than those observed for similar flames from the ultraviolet-band system, and point up the necessity for complete understanding of the effects of line shape and line reversal in the latter spectra, which as is seen from table 8.3, will be large.

8.3. CN

This radical has two intense electronic band systems, each with an f-value in the neighborhood of 0.02. The violet system ($^2\Sigma^+ — ^2\Sigma^+$) is a characteristic feature of carbon-rich flames burning in air; the red system ($^2\Pi_i – ^2\Sigma^+$) has also been observed in such sources, but less prominently, in the red and near infrared. The origin of this system has recently been found [14, 15] to lie farther in the infrared than was earlier believed. The (0,0) band, which extends from 9195.6 cm^{-1} to beyond 8500 cm^{-1}, has its origin at 9117.3 ± 0.1 cm^{-1}. This band was photographed with high resolution by Kiess [15], using a carbon arc in air as the source, and was observed with a low-resolution infrared spectrometer by Herzberg and Phillips [14] from a discharge through benzene vapor.

We have observed this band as a very prominent feature of the radiation from the inner cone of a fuel-rich oxyacetylene flame. In the radiation from the outer cone it may be present very weakly, but is masked by water-vapor emission in the same region. The slit width was about 1.5 cm^{-1}. Under these conditions the complex rotational structure, consisting of 6 strong branches and 2 weak satellite branches, is not fully resolved, but a number of the lines, especially in the strong Q branches, stand out clearly.

In view of the imperfect resolution, it does not seem feasible to use this band for a determination of the rotational temperature. It was, however, verified that the observed intensities are in rough agreement with the calculated intensity assuming $T = 2500°$ K. Hence one may conclude that there is no large deviation from thermal equilibrium involved in the excitation of the various rotational levels within this band.

The order of magnitude of the CN $^2\Pi$ concentration may be very roughly estimated. If we accept the estimate of Herzberg and Phillips [14], the integrated intensity of the entire red system corresponds to an f-value of 0.02. Assuming $T = 2876°$, the vibrational population places 59 percent of the molecules on the 0 level. Since we could not observe (0,2) at 5059 cm^{-1} and could barely recognize (0,1) at 7075 cm^{-1}, it would mean that at least 50 percent of the total radiation from the $v=0$ level is in (0,0). Hence $\int k_\nu d\nu$ for (0,0) $\sim 5 \times 10^5 \times$

$0.5\times0.6\sim1.5\times10^5$ cm^{-2}atm^{-1}. From a rough estimate based on the intensity of other thermally excited spectra, the average emissivity over the band width of 300 cm^{-1} is $\sim$0.01. Accordingly, $N_{\mathrm{CN}^*}=0.01\times300/1.5\times10^5=2\times10^{-5}$ cm atm. For the inner-cone thickness of 0.10 cm, this gives a concentration of CN* of 2×10^{-6} atm; if in thermal equilibrium with the ground state, the total concentration of CN$=2\times10^{-4}$ atm. This is 10^5 times greater than the estimated concentration at thermal equilibrium (table 8.1). If these very rough results are confirmed by more quantitative measurements of the emissivity, it means that the CN* is formed in some of the chemical reactions in the inner cone, and that the radiation is chemiluminescent in origin. Temperature measurements using these bands would then have little meaning, except to demonstrate whether the radical survives through enough collisions to attain thermal equilibrium within its rotational modes. This appears to be the case.

8.4. C_2

Several electronic band systems have been observed for this molecule in flames. The ground state is $^3\Pi_u$; the Swan bands in the visible spectrum are in transition from a $^3\Pi_g$ to the ground state. Two low-lying singlet states are also known; the transition between them, $^1\Pi_u$–$^1\Sigma_g^+$, was discovered by Phillips [16], who located the (2,0), (3,1), (3,0), (4,1), and (5,2) bands in a discharge. The same bands, lying between 7700 to 9000 A, were found by Hornbeck and Herman [17] in the photographic infrared in the oxyacetylene flame. Since the constants of both electronic states are accurately known ($^1\Sigma_g^+$ is the lower level of the Mulliken bands, and $^1\Pi_u$ the lower level of the Deslandres-D'Azumbuja bands), it is possible to calculate with good accuracy the positions of the lines of the (1,0), (0,0), and (0,1) bands, which should be the strongest bands of the system under conditions of thermal excitation. The f-value of the system has not been measured or calculated, but it should be of the same order as the Swan bands, and the other band systems involving similar electron-transfer spectra [18], namely, $\sim$0.02.

We have now observed the (1,0) and (0,0) bands, which are the most intense features of the emission from the inner cone of the fuel-rich oxyacetylene flame in the region of the spectrum where they occur. The (1,0) band has its head at 9865.7 cm^{-1}, (10107 A), and may be followed to beyond $Q40$, at 9491.5 cm^{-1}. The rotational structure is relatively open, there being only the three branches characteristic of a $^1\Pi_u$–$^1\Sigma_g^+$ transition; a strong Q branch, and P and R branches that are weaker by a factor of 2. Moreover, because of the zero spin of the C^{12} nucleus, only even values of J, for the lower state, appear. The spacing of the Q branch lines at the maximum, near $J=24$, is 22 cm^{-1}, which permits clear resolution of all three branches, even with the relatively wide slits of $\sim$1.5 cm^{-1} required. The (1,0) band, in our tracings, is overlapped by a strong violet-shaded band head at 10330 A. As the second-order visible radiation was not completely removed by filters this is clearly the (0,0) Swan band, strongest band in that system, in the second order. It is of interest that the ratio of intensity of the Swan-Phillips systems showed no significant variations with conditions of excitation.

The (0,1) band falls in the region of strong emission due to OH and moderately strong emission due to H_2O. A number of the stronger lines of the Q branch, from $J''=10$ to 30, may be identified by comparing tracings of the inner- and outer-cone radiation in this region; the inner cone favors C_2, the outer, H_2O. Considerable overlapping occurs, however, and, under the most favorable conditions, its intensity does not exceed 30 percent of that of the OH lines in the region.

The (0,0) band is quite free from overlapping under the conditions where it appears strongly. Hence the relative intensities of the resolved Q, P, and R lines may be used to determine a C_2 rotational "temperature." The rotational transition probabilities for $^1\Pi-^1\Sigma$ are well known [19]. Plotting log $I/S_J\nu^4$ against E' a fairly good straight line is obtained, whose slope corresponds to a temperature of 2,600 ±200° K.

While this "temperature" determination on C_2 is relatively rough, due to the necessity of using wide slits and the presence of a considerable background and noise level, it is certain that the rotational distribution yields a temperature of the same order as that given by CO and OH, for the outer cones, and indicated by CN, as well as what is calculated for overall thermal equilibrium in the reaction products. This is in marked contrast to findings in similar flames when the Swan bands of C_2 are observed [20] where "temperatures" in excess of 4000° K are indicated. This would appear to mean that the triplet states, involved in the Swan transition, are formed in the chemical reaction with excess rotational energy that they are not able to equilibrate through collisions in their radiative lifetime of $\sim 10^{-7}$ sec, whereas the singlet states involved in the Phillips transition are formed either by chemical reaction with no excess rotational energy, or by collisions efficient enough to bring their rotational mode in equilibrium with the rest of the flame in their lifetime of $\sim 10^{-6}$ sec.

The intensity (emissivity) of the strongest lines of the (0,0) and (1,0) bands is of the same order as that of CN (0,0); i. e., perhaps 0.03. Since most of the radiation coming from the 0 level is in (0,0) [(0,1) is less intense by a factor of 5 or thereabouts], we can, as with CN, estimate the concentration of excited $C_2(^1\Pi)$, if an f-value of 0.02 is assumed for the system. Because of the more open rotational structure, the result is about one order less than CN; i. e., about 10^{-7} cm atm for the excited state. The position of the singlet system relative to the ground state is not precisely known; Herzberg estimates 5300 cm^{-1} for the $^1\Sigma_g^+$. This would place the total C_2 concentration at about 10^{-4} atm, again very much in excess of the calculated equilibrium values, indicating a chemiluminescent rather than a thermal origin for this species.

8.5. CO_2

The vibration-rotation spectrum of this abundant constituent of flame gases has been extensively studied in absorption, so that its molecular constants are well known. A few features of the emission spectrum have been resolved [21, 22], but in general the infrared emission shows a structureless continuum, in several regions. In the region beyond 4000 cm^{-1} there is only weak emission between 4500 to 5100 cm^{-1}. In hydrocarbon flames this is much weaker than the H_2O emission in the same region and even when relatively hydrogen-free CO is burned the most prominent features superposed on the CO_2 background are due to H_2O lines.

The principal reason for the essentially continuous CO_2 emission is the low value of the quanta in the ν_2 vibration, 667 cm^{-1}. Hence at flame temperatures very many vibrational levels are excited. The Q_v, as listed in table 8.3, is 36.9. Combined with the facts that Fermi resonance increases the number of strong transitions in a given spectral region and that the vibrational transition probability increases with increasing v, this leads to a very large number of bands of nearly equal intensity in the 4900 cm^{-1} region. Table 8.4 lists the calculated origins, heads, and relative intensities at 2500° K of the bands whose lower levels have $v_2 \leq 2$. Very many more bands of nearly comparable intensity would arise from higher levels. There are a few structural features in the observed spectra as listed in table 8.5, that may possibly be identified with some of the strongest expected heads, but it is clear that even with improved resolution it would be impossible to observe structures well enough to check vibrational "temperatures".

TABLE 8.4. *Calculated CO_2 bands in 4900-cm^{-1} region*

v''_1	v''_2	l''	ν_0	ν_{head}	$I_{2500\,^\circ\mathrm{K}}$
			cm^{-1}	cm^{-1}	
0	0	0	4854.0	4924	18
0	0	0	4978.2	5019	60
0	0	0	5099.1	5154	22
0	1	1	4807.6	4866	26
0	1	1	4965.4	5008±1	70
0	1	1	5125	5178±4	40
1	0	0	4687.6	-----------	14
0	2	2	4757	4823±2	19
0	2	0	4790.4	-----------	11
1	0	0	4840.0	4882	38
0	2	0	4942.8	4981	31
1	0	0	4959.9	5000	42
0	2	2	4980	5022	46
0	2	0	5062.7	5100	34
1	0	0	5114.6	-----------	21
0	2	2	5147	5202±1	28
0	2	0	5217.4	5278	17

TABLE 8.5. *Observed* CO_2 *peaks in 4900-cm^{-1} region*

I	Character	ν, observed	ν, calculated
		cm^{-1}	cm^{-1}
10	R-head	5019	5019
7	R-head	5012	5009
12	R-head (+H_2O)	5007	5007
5	Broad line	4987	?
10	Head?	4971	4981?
8	Line?	4966	?
10	Line?	4962	?
18	R-head (+H_2O)	4952	4952
15	R-head	4925	4924
12	Line?	4911	?
8	Line?	4907	?
25	Broad line? (+H_2O)	4904	?
10	Head?	4898	?
10	Line	4894	?
12	Head?	4891	4882?
15	Broad line?	4865	4866
20	Broad line?	4858	?
8	Sharp line	4851	?
15	Head?	4838	4825?
8	Wide head	4804	?
10	Sharp line	4782	?

8.6. H_2O

This is the strongest emitter throughout the region 1 to 2.6μ. It is most intense near 2.5μ (4000 cm^{-1})at the maximum of the *R* branch of the ν_3 fundamental. This vibrational region extends with decreasing intensity to about 4250 cm^{-1}. The $\nu_3+\nu_2$ combination band, whose laboratory absorption extends from 5050 to 5500 cm^{-1}, is also very strong in emission, and contributes most of the radiation from 4400 to 5900 cm^{-1}. The absolute intensity at the maximum near 5000 cm^{-1} (*P* branch) and again near 5580 cm^{-1} (*R* branch) is almost as great as at 4000 cm^{-1}, and slits as narrow as 0.2 cm^{-1} may again be used. The $\nu_1+\nu_3$ combination band and its satellites, which in absorption extends from 6700 to 7450 cm^{-1}, emits strongly from 6300 to 7500 cm^{-1}. It is, however, not quite as intense as the 1.9μ band. A sharp gathering together of the *R* branch to form a head near 7500 is a characteristic feature of this region. Beyond this point the intensity is very much decreased. With wide slits (approximately 1 cm^{-1}) some emission due to H_2O may be observed all the way to 10000 cm^{-1} (1μ), most strongly near 8500 cm^{-1}. In this last region it is not possible to resolve the emission sufficiently to identify individual rotation-vibration lines. In the other regions, however, particularly in the 1.9μ band, the individual lines are quite well resolved, the strongest such lines having intensities approximately 20 times that of the essentially continuous background of weak lines. A rather satisfactory analysis of most of the lines with intensities 20 to 4 above the background has been made and will be reported in greater detail, elsewhere.

The analysis of the H_2O emission spectrum proceeds briefly as follows. From previous studies in absorption, a large number of vibration-rotation energy levels had been located. Forty-three vibrational states were known, all making transitions to the ground level. In the strongest of these e. g., $v_1v_2v_3=011$, $\nu_0=5331.2$ cm^{-1}, approximately 100 rotational levels, of which $2J+1$ exist for each integer J, had been located. The transitions between these and the ground vibrational level, of which some 200 rotational levels, ranging up to 4000 cm^{-1} have been located [23, 24], give rise to many of the most intense lines. At the emission temperatures, however, additional higher rotational levels are excited, and vibrational transitions also occur with the lower state a vibrationally excited one. The relative intensities of these new emission lines may be calculated; their approximate position may be estimated from the known levels of next lower J; and the resulting tentative identifications may be confirmed by combination relations. In this way nearly all of the strongest features in the 1.9μ region have been identified. The relative intensities again appear consistent with thermal equilibrium within both vibrational and rotational modes, with a temperature in the neighborhood of 2500° K.

The strongest vibrational transitions that should appear in the 1.9μ and 1.4μ regions are listed in table 8.6. Most of these have been observed. T_ν, the vibrational transition probability, is calculated on the harmonic-oscillator approximation and is given relative to 100 for the strongest transition in each region separately. As an example of the rotational analysis the combination relations for some of the strongest lines of the series with $\tau=-J$ are given in table 8.7. The difference $\Delta = R(J''+1) - P(J''-1)$ should be equal for the two emission bands 011–000 and 101–000, as well as for the absorption band 010–000 (last column). Within experimental accuracy, this is the case. The same combination differences and many additional ones, are also observed in H_2O emission bands in the photographic infrared, both for the ground vibrational level and for the lower excited states.

TABLE 8.6. *Calculated band origins and relative intensities, 2,876°, H_2O*

Spectral region	v'_1	v'_2	v'_3	v''_1	v''_2	v''_3	ν_0	T_v	$I_{2876°K}$
							cm^{-1}		
1.9μ	0	1	1	0	0	0	5331.2	100	100
	0	2	1	0	1	0	5277.0	200	90
	0	3	1	0	2	0	5221.8	300	62
	0	4	1	0	3	0	5166.9	400	39
	0	5	1	0	4	0	5112	500	23
	0	6	1	0	5	0	5067	600	12
	1	1	1	1	0	0	5149.9	100	16
	0	1	2	0	0	1	5244.3	178	28
	0	2	2	0	1	1	5192	355	25
	0	3	2	0	2	1	5139	531	16
	1	2	1	1	1	0	5093.7	200	15
1.4μ	1	0	1	0	0	0	7249.8	100	100
	1	1	1	0	1	0	7212.3	100	45
	1	2	1	0	2	0	7177.3	100	21
	2	0	1	1	0	0	6956.2	177	28
	2	1	1	1	1	0	6916.2	177	12
	1	0	2	0	0	1	7113.0	112	17
	3	0	0	0	0	1	6843.9	88	14
	0	2	1	0	0	0	6871.3	7	7
	0	3	1	0	1	0	6779.1	21	9
	0	4	1	0	2	0	6682.0	42	9
	0	5	1	0	3	0	6581.8	70	7

TABLE 8.7. *Combination differences in H_2O main series*

J'	$I^R_{2876°K}$	011–000			101–000			$\Delta(010)$
		$R(J+1)$	$P(J-1)$	Δ	$R(J+1)$	$P(J-1)$	Δ	
		cm^{-1}	cm^{-1}	cm^{-1}	cm^{-1}	cm^{-1}	cm^{-1}	cm^{-1}
10	24.2	5503.5	5096.6	406.9	7405.1	6998.1	407.0	406.9
11	23.4	5516.6	5073.3	443.3	7416.0	6972.7	443.3	443.3
12	22.3	5529.1	5049.3	479.8	7426.2	6946.5	479.8	479.7
13	20.9	5541.1	5025.5	515.6	7435.9	6920.0	515.9	515.8
14	19.4	5552.4	5000.0	552.4	7444.7	6892.8	551.9	552.1
15	17.6	5563.0	4975.7	587.3	7452.4	6865.5	586.9	587.4
16	16.0	5573.3	4950.5	622.8	7460.0	6837.1	622.9	623.0
17	14.3	5582.9	4924.7	658.2	7466.1	6808.2	657.9	------
18	12.6	5592.0	4898.5	693.5	7471.9	6778.7	693.2	------
19	10.8	5600.7	4872.2	728.5	7477.4	6748.8	728.6	------
20	9.4	5608.8	4845.3	763.5	7481.9	6717.7	764.2	------

4. Discussion and Conclusions

The observed infrared radiation from the outer cone of flames from 3700 to 10000 cm^{-1} has all been ascribed to the vibration-rotation spectra of the four most abundant species with such allowed spectra, namely, CO, OH, CO_2, and H_2O; in the inner cone the electronically excited CN and C_2 radicals also contribute. Search has been made for spectra from the other molecules and radicals listed in table 8.1, but with negative results. In the inner cone of oxyacetylene flames, electronic bands of CH are very intense. The *P* branch of the 2–0, and especially the 3–1 band of the vibration-rotation spectrum falls in the region of 4500 cm^{-1}, where other emission is relatively weak. The positions of the lines, which because of the $^2\Pi$ character of the state will split into close groups of 4, can be predicted with good accuracy. They have not been observed, even with very wide slits, and it can be stated with assurance that they are less than 1 percent as strong as the overtone bands of CO or OH. If as is reasonable the effective charge for vibration of CH is of the same order as in OH, concentration of nonelectronically excited CH in the inner cone is therefore less than 10^{-3}. But since a much lower concentration of excited radicals suffices to produce the electronic bands, and since the equilibrium concentration is very much lower still, the nonappearance of vibration-rotation CH was to have been expected. Even in the region of the fundamental, it will still be extremely unlikely that it could be found.

Analogous reasoning holds for such molecules as C_2H_2, HCN, CH_4, H_2CO, etc., whose spectra are known; the additional fact that all will have a very high vibrational *Q*, greater than that for CO_2, makes their nonappearance in the overtone region to be expected, and their future identification as fundamentals very dubious, unless they are present in very high concentrations at relatively low temperatures, such as might be the case if a very large excess of CH_4 or C_2H_2 were burned. Equally unlikely are the possibilities of detecting the radicals with unknown spectra, such as CH_3, CH_2, or HCO, although it is again conceivable that they might appear in the region of the C—H fundamental ($\sim 3.5\mu$) under the same conditions that produce the emission spectra of CH_4 or H_2CO.

The general finding of these studies, with regard to the intensity and energy distribution of the various emitters, is also in accordance with the discussion in section 2. In every case where a "temperature" could be measured from resolved spectra, the results were from 2400 to 2800° K, whereas visible and ultraviolet spectra from the same regions of comparable flames yield values $>$3000° K. The principal reason for the difference, as has repeatedly been mentioned, must be the greater lifetimes for radiation in the infrared, so that the lower lying excited states that are responsible for infrared emission show a much closer approach to complete thermodynamic equilibrium than states with higher amounts of electronic excitation. The distortion of the measurements by temperature gradients will likewise tend to give lower values at longer wavelengths, where the cooler regions contribute relatively more to the total emission. Distortion by self-absorption should be less important in the infrared.

References

[1] E. K. Plyler, W. S. Benedict, and S. Silverman, J. Chem. Phys. **20,** 175 (1952).
[2] W. S. Benedict and E. K. Plyler, J. Chem. Phys. **21,** 398 (1953).
[3] W. S. Benedict, NBS Report #1123, Appendix 1A (1951).
[4] A. G. Gaydon, Spectroscopy and Combustion Theory (Chapman & Hall Ltd., London, 1948).
[5] R. N. Schwartz, Z. I. Slawsky, and K. F. Herzfeld, J. Chem. Phys. **20**, 1591 (1952).
[6] A. Kantrowitz, J. Chem. Phys. **14**, 150 (1946).

[7] H. C. Hottel, G. C. Williams, and C. N. Satterfield, Thermodynamic Charts for Combustion Processes (Wiley & Sons, New York, N. Y., 1949).
[8] G. H. Dieke and H. M. Crosswhite, Progress Reports for Contract NOrd 8036 (1948–51).
[9] H. P. Broida, J. Chem. Phys. **19,** 1383 (1951); H. P. Broida and K. E. Shuler, J. Chem. Phys. **20,** 168 (1952); H. P. Broida and G. T. Lalos, J. Chem. Phys. **20,** 1466 (1952).
[10] S. S. Penner, J. Chem. Phys. **20,** 507 (1952).
[11] S. Silverman (see paper No. 7, p. 51).
[12] S. S. Penner and D. Weber, J. Chem. Phys. **19,** 807, 817 (1951).
[13] Heaps and G. Herzberg, Z. Physik (1952).
[14] G. Herzberg and J. G. Phillips, Astrophys. J. **108,** 163 (1948).
[15] C. C. Kiess, Astrophys. J. **109,** 551 (1949).
[16] J. G. Phillips, Astrophys. J. **107**, 389 (1948).
[17] G. A. Hornbeck and R. C. Herman, J. Chem. Phys. **19,** 512 (1951).
[18] G. Stephenson, Proc. Phys. Soc. [A] **64**, 99 (1951).
[19] G. Herzberg, Molecular Spectra and Molecular Structure I: Diatomic Molecules, p. 208 (D. Van Nostrand, New York, N. Y., 1950).
[20] A. G. Gaydon and H. C. Wolfhard, Proc. Roy. Soc. [A] **201,** 570 (1950).
[21] W. S. Benedict, R. C. Herman, and S. Silverman, J. Chem. Phys. **19,** 1325 (1951).
[22] E. K. Plyler and J. J. Ball, J. Chem. Phys. **20,** 1178 (1952).
[23] W. S. Benedict, H. H. Claassen, and J. H. Shaw, J. Research NBS **49,** 91 (1952).
[24] J. Taylor, W. S. Benedict, and J. Strong, J. Chem. Phys. **20,** (1952).
[25] G. Hornbeck and R. C. Herman (see paper No. 2, p. 9).

9. Infrared Emissivity of Diatomic Gases[1]

By S. S. Penner[2]

An outline is presented of the basic theoretical relations which are used to calculate the infrared emissivity of diatomic gases. Next the measurement of absolute values for the integrated absorption, together with the determination of rotational half-widths resulting from collision broadening, is described. The experimental results are useful for the calculation of the infrared emissivity of diatomic gases at low pressures, where overlapping between rotational lines may be neglected, and at very high pressures, where complete overlapping occurs. Calculations at elevated pressures are believed to yield reasonable approximations for the conditions existing in rocket combustion chambers. The theoretical calculations have been found to be in satisfactory agreement with available empirical emissivity data for CO.

1. Introduction

A gas emits radiation as the result of electronic, vibrational, and rotational transitions from excited energy levels to lower energy levels. The emitted radiant energy corresponding to these transitions is distributed over a well-defined wavelength region. In general, the radiation emitted as the result of electronic transitions is concentrated in the visible and ultraviolet regions of the spectrum, whereas vibration-rotation bands are responsible for the emission of light in the near infrared. Pure rotational transitions give rise to absorption bands at long wavelengths (i. e., 30μ and more) in the infrared. As the temperature of the emitter is raised, the discrete emission lines or bands occurring at progressively shorter wavelengths make the more important contributions to the emitted radiant energy. At the temperatures of interest in connection with studies of equilibrium radiant-heat transfer in combustion chambers, only the transitions corresponding to the infrared vibration-rotation bands make significant contributions to the observed energy flux. Accordingly, the present discussion will be concerned with an outline of the experimental and theoretical work that must be done in order to calculate the infrared emissivity of diatomic gases from spectroscopic data.

Section 2 contains a summary of basic relations used for heat-transfer calculations. Before these expressions can be applied to practical problems, it is necessary to obtain quantitative integrated absorption and line-width data, in addition to the more usual type of information on frequencies and energy levels. Recent work on the determination of physical constants for diatomic gases is reviewed in section 3. Representative applications of the theoretical and experimental results are described in section 4.

---

[1] This paper presents the results of one phase of research carried out at the Jet propulsion Laboratory California Institute of Technology, under Contract No. DA-04-495-ORD 18, sponsored by the Department, of the Army, Ordnance Corps.

[2] Jet Propulsion Laboratory, California Institute of Technology, Pasadena, Calif.

2. Basic Physical Laws [2a]

The volume density of radiant energy $\rho^0(\nu)d\nu$ emitted in the frequency range between ν and $\nu+d\nu$ by a black-body radiator is given by the Planck distribution law

$$\rho^0(\nu)d\nu=(8\pi h\nu^3/c^3)\,[\exp\,(h\nu/kT)-1]^{-1}\,d\nu, \tag{1}$$

where h denotes Planck's constant, c is the velocity of light, and T represents the absolute temperature of the black-body emitter. The radiant energy emitted per unit area of black body per unit time into a solid angle of 2π steradians in the indicated frequency range is then given by the relation

$$R^0_\nu d\nu=c\rho^0(\nu)d\nu/4. \tag{2}$$

According to the basic law for the absorption of monochromatic radiation, under conditions where emission is negligible, the fractional decrease in spectral light intensity is proportional to the optical density, i. e.,

$$-(1/R_\nu)\,(dR_\nu/dX)=P_\nu, \tag{3}$$

where X represents the optical density (viz, the product of partial pressure of absorber p and optical path length l), and P_ν is the spectral absorption coefficient.

Consider the absorption of radiation produced by energy transitions from the lower energy level E_l of statistical weight g_l to the upper energy level E_u of statistical weight g_u. The frequencies of radiation absorbed as the result of these energy changes are not infinitely sharp but are distributed over a finite frequency range as the result of various line-broadening effects, the most important of which are collision and Doppler broadening. The frequency at the center of a region of absorption is calculated from the Bohr frequency rule, that is,

$$\nu_{lu}=(E_u-E_l)/h.$$

According to the Einstein theory [1] for emission and absorption of radiation, it follows that

$$-\int_{\Delta\nu_{lu}}(d\,\mathrm{lu}\,R_\nu/dX)d\nu=(N_lB_{l\rightarrow u}-N_uB_{u\rightarrow l})h\nu_{lu}/c, \tag{4}$$

where the integral in eq 4 must be extended over all of the frequencies associated with the indicated energy transition. The quantities N_l and N_u represent, respectively, the number of molecules per unit volume in the lower and upper energy states, $B_{l\rightarrow u}$ is the Einstein coefficient of induced absorption, and $B_{u\rightarrow l}$ is the Einstein coefficient of induced emission. The term corresponding to induced emission must be included because induced emission is known [2] to occur in the direction of the incident radiation. Comparing eq 3 and 4, the following well-known result is obtained:

$$S_{lu}=\int_{\Delta\nu_{lu}}P_\nu d\nu=(N_lB_{l\rightarrow u}-N_uB_{u\rightarrow l})h\nu_{lu}/c. \tag{5}$$

[2a] Most the material of section 2 was prepared in 1948 and published in Progress Report No. 9-37 issued by the Jet Propulsion Laboratory in May 1949.

The Einstein coefficients are related [3] through the expression

$$N_u A_{u\to l} = (N_l B_{l\to u} - N_u B_{u\to l})\rho^0(\nu_{lu}), \tag{6}$$

where $A_{u\to l}$ is the Einstein coefficient of spontaneous emission. From eq 5 and 6, the following basic relation is obtained:

$$S_{lu} = N_u A_{u\to l} h\nu_{lu}/c\rho^0(\nu_{lu}). \tag{7}$$

Theoretical calculation of radiant energies rests on the assumption of validity of a relation that can be obtained from the classical expressions for the intensity of radiation emitted from an oscillating dipole by the use of Bohr's correspondence principle [4, 5, 6], viz,

$$A_{u\to l} h\nu_{lu} = (16\pi^4/3)(\nu_{lu}^4 q_{lu}^2/c^3), \tag{8}$$

where q_{lu}, the matrix element corresponding to transitions between the lower and upper energy states, is given by the relation

$$q_{lu} = \int \psi_l^* q \psi_u \, d\tau$$

if ψ_l^* and ψ_u are the appropriate wave functions for the qauntum mechanical system under study and $d\tau$ denotes a volume element in the phase space of the oscillating dipole. Since, classically, the term q_{lu} is replaced by an electrical moment, q_{lu} may be set equal to the product of an effective charge ϵ and an amplitude of oscillation α.[3]

Hence, combining eq 7 and 8, it follows that

$$S_{lu} = (16\pi^4/3)N_u \nu_{lu}^4(\epsilon\alpha)^2/c^4\rho^0(\nu_{lu}) \tag{9}$$

It is known from statistical quantum mechanics that, at equilibrium,

$$N_u = N_T g_u \exp(-E_u/kT)/Q, \tag{10}$$

where N_T represents the total number of molecules per unit volume, and Q is the complete partition function. For anharmonic vibrating-rotating diatomic molecules the amplitudes of oscillation α have been obtained by Oppenheimer [7] for transitions between the vibrational ground level and the first excited state for molecules with P and R branches. Thus

$$(\alpha_{j\to j-1}^{0\to 1})^2 = (h/2\pi^2\mu\nu_e)[j/(2j-1)]F \tag{11}$$

and

$$(a_{j-1\to j}^{0\to 1})^2 = (h/2\pi^2\mu\nu_e)[j/(2j+1)]F', \tag{11a}$$

where

$$F = 1 + 4\gamma j[1 + (5\gamma j/8) - (3\gamma/8)], \tag{12}$$

$$F' = 1 - 4\gamma j[1 - (5\gamma j/8) - (3\gamma/8)], \tag{12a}$$

and where ν_e is the frequency corresponding to an infinitesimal oscillation at the equilibrium internuclear distance, μ equals the reduced mass of the molecule, and $\gamma = h/4\pi^2 I\nu_e$, with I representing the equilib-

---

[3] In more precise terminology, ϵ represents the rate of change of electric moment with internuclear distance

rium moment of inertia of the molecule. The upper subscript to α indicates the vibrational transitions involved; and the lower subscript, the changes in rotational quantum number. Combining eq 9 through 12a and using eq 1 leads to the results

$$S^{0\rightarrow 1}_{j\rightarrow j-1}=(\omega^*/\omega_e)(N_T\pi\epsilon^2/3\mu cQ)[\omega^{0\rightarrow 1}_{j\rightarrow j-1}/\omega^*)j\{\exp\ [-E(0,j)/kT]\}FG] \quad (13)$$

and

$$S^{0\rightarrow 1}_{j-1\rightarrow j}=(\omega^*/\omega_e)\,(N_T\pi\epsilon^2/\mu cQ)\ [(\omega^{0\rightarrow 1}_{j-1\rightarrow j}/\omega^*)j\{\exp\ [-E(0,\ j-1)\,/kT\}F'G'] \quad (14)$$

where ω^*=wave number corresponding to the (forbidden) transition $j=0\rightarrow j=0$ and $n=0\rightarrow n=1$, with n denoting the vibrational quantum number; $\omega=\nu/c$; $E(n,j)$=energy of the nth vibrational and jth rotational level;

$$G=1-\exp(-hc\ \omega^{0\rightarrow 1}_{j\rightarrow j-1}/kT);\ G'=1-\exp(-hc\ \omega^{0\rightarrow 1}_{j-1\rightarrow j}/kT);$$

$$g_u=2j-1 \text{ for } j\rightarrow j-1,$$

$n=0\rightarrow n=1$; $g_u=2j+1$ for $j-1\rightarrow j$, $n=0\rightarrow n=1$. Equations 13 and 14 differ from the corresponding relations obtained by Crawford and Dinsmore [8] only through the factors F and F', which are nearly equal to unity for small values of j.

It is well known that, to a very close approximation [8, 9],

$$\sum_j S^{0\rightarrow 1}_{j\rightarrow j\pm 1}=\alpha_F=(\omega^*/\omega_e)\,(N_T\pi\epsilon^2/3\mu c). \quad (15)$$

Experimental methods for the determination of α_F are described in section 3.1. After α_F has been measured, the quantities $S^{0\rightarrow 1}_{j\rightarrow j-1}$ and $S^{0\rightarrow 1}_{j-1\rightarrow j}$ can be calculated by the use of eq 13 to 15.

In order to determine completely the radiant intensity emitted from the region of the spectrum corresponding to the fundamental vibration-rotation band, it is necessary to know also the values of $S^{n\rightarrow n+1}_{j\rightarrow j-1}$, $S^{n\rightarrow n+1}_{j-1\rightarrow j}$. As a first approximation, it may be assumed that

$$S^{n\rightarrow n+1}_{j\rightarrow j\pm 1}/S^{0\rightarrow 1}_{j\rightarrow j\pm 1}=\sum_j S^{n\rightarrow n+1}_{j\rightarrow j\pm 1}/\sum_j S^{0\rightarrow 1}_{j\rightarrow j\pm 1} \quad (16)$$

where the ratio of the sums appearing on the right-hand side of eq 16 is well known for a harmonic oscillator. This approach leads to the relation: [4]

$$S^{n\rightarrow n+1}_{j\rightarrow j\pm 1}/S^{0\rightarrow 1}_{j\rightarrow j\pm 1}=(n+1)(\omega^{n\rightarrow n+1}_{j\rightarrow j\pm 1}/\omega^{0\rightarrow 1}_{j\rightarrow j\pm 1})\ \exp\{[-E(n,j)+E(0,j)]/kT\}$$

$$[1-\exp\,(-hc\omega^{n\rightarrow n+1}_{j\rightarrow j\pm 1}/kT)]\,[1-\exp\,(-hc\omega^{0\rightarrow 1}_{j\rightarrow j\pm 1}/kT]^{-1}. \quad (17)$$

An alternate expression to that given in eq 17 is obtained from the treatment of Scholz [10], whose results can be shown to lead to eq 17,

---

[4] Equation 17 is identical with the corresponding relation derived from the treatment of Crawford and Dinsmore [8].

with the factor $n+1$ replaced by $f(n,n+1)$, where

$$f(n,n+1)=(n+1)\ [(k'-2n-1)(k'-2n-3)(k'-n-1)^{-1}(k'-3)^{-1}], \tag{18}$$

and k' is the nearest integer less than $4D/h\nu_e$, with D representing the dissociation energy. For small values of n, $f(n,n+1)\simeq n+1$.

Explicit relations for the integrated absorption of rotational lines of upper harmonics are readily obtained from the treatment of Crawford and Dinsmore [8]. These relations involve empirically determined parameters, such as

$$\sum_j S^{0\rightarrow 2}_{j\rightarrow j\pm 1}=\alpha_0,$$

etc. To a good approximation it is found that

$$S^{0\rightarrow 2}_{j\rightarrow j\pm 1}/S^{0\rightarrow 1}_{j\rightarrow j\pm 1}=\alpha_0/\alpha_F.$$

For the ratios $S^{n\rightarrow n+2}_{j\rightarrow j\pm 1}/S^{0\rightarrow 2}_{j\rightarrow j\pm 1}$, expressions similar to eq 17 may be obtained.

Calculation of radiant intensities requires knowledge not only of the integrated absorption for each rotational line but also of the actual values of the spectral absorption coefficients P_ν or P_ω. Simple expressions can be given for these quantities for collision broadening [11 to 15] and for Doppler broadening [11]. For collision broadening it is found, for example, that

$$P^{0\rightarrow 1}_{j\rightarrow j\pm 1}=(b/\pi)S^{0\rightarrow 1}_{j\rightarrow j\pm 1}\ [(\omega-\omega^{0\rightarrow 1}_{j\rightarrow j\pm 1})^2+b^2]^{-1}, \tag{19}$$

where b represents an empirically determined value of the rotational half-width, which is usually assumed to be the same for each of the rotational lines of a given vibration-rotation band (see sec. 3.2 for a discussion of experimental methods used to determine b). For Doppler broadening it is readily shown, for example, that

$$P^{0\rightarrow 1}_{j\rightarrow j\pm 1}=S^{0\rightarrow 1}_{j\rightarrow j\pm 1}\,[m/2\pi kT(\omega^{0\rightarrow 1}_{j\rightarrow j\pm i})^2]^{1/2}\times \\ \exp\{-[mc^2/2kT(\omega^{0\rightarrow 1}_{j\rightarrow j\pm 1})^2](\omega-\omega^{0\rightarrow 1}_{j\rightarrow j\pm 1})^2\}, \tag{20}$$

where m represents the mass per molecule. Thus the spectral absorption coefficient for Doppler-broadened lines can be calculated as a function of temperature (being independent of pressure) if the value of the integrated absorption is known. Other broadening effects have been discussed by Margenau and Watson [11], and the superposition of Doppler and collision broadening has been treated, for example, by Minkowski and Bruck [16]. For the calculation of infrared emissivities at moderate temperatures and, particularly, at elevated pressures, Doppler broadening is generally unimportant, although it represents the principal cause of line broadening in the visible and ultraviolet regions of the spectrum at high temperatures and at low pressures.

The problem of calculation of infrared emissivities is solved, in principle, after the values of the spectral absorption coefficients corresponding to given energy transitions are known. Consider a uniform volume distribution of molecules, and let R_ω be the incident intensity of radiation in the wave-number interval between ω and $\omega+d\omega$ in a given direction. The change in R_ω in a layer of optical density dX is then,

$$dR_\omega=(I_\omega-P_\omega R_\omega)dX,$$

where I_ω represents the emitted intensity of radiation in the indicated wave-number interval by the emitters present in dX. From eq 7 it is evident that I_ω is to be identified with $c\rho^0(\omega)P_\omega/4=R^0_\omega P_\omega$, whence, after integration between $X=0$, where $R_\omega=0$ and $X=X$, where $R_\omega=R_\omega$, the following well-known relation is obtained

$$R_\omega=R^0_\omega\,[1-\exp\,(-P_\omega X)]. \tag{21}$$

The total intensity of radiation emitted over all wavelengths is

$$\int_0^\infty R_\omega d\omega=\int_0^\infty R^0_\omega\,[1-\exp(-P_\omega X)]\,d\omega. \tag{22}$$

Because of the rapid variation of P_ω with ω, it is convenient, in practice, to divide the infinite integration interval in such a way as to obtain separately the contributions from each of the spectral regions for which P_ω is sensibly different from zero. In evaluating the integral appearing in eq 21, particular care must be taken to add correctly the numerical values of P_ω arising from various independent transitions. Under certain conditions this addition may be complicated by the occurrence of mutual perturbations between lines in the same spectral range.[5]

3. Experimental Determination of Integrated Absorption and of Rotational Line Widths

It was shown in section 2 that the problem of calculating the infrared emissivity of diatomic gases is solved, in principle, provided integrated absorption and line-width data are available. Experimental measurement of these quantities will now be considered.

3.1. Measurement of Integrated Absorption

Most of the recently published measurements on integrated absorption of diatomic and polyatomic gases involve the use of an extrapolation method introduced by Wilson and Wells in 1946 [19]. Representative measurements have been described by several authors [20 to 24]. Reliable experimental results are obtained if particular care is taken to pressurize the gases sufficiently and minimize the curvature that is usually observed in the Wilson-Wells extrapolation plots [24]. In addition, suitable precautions must be exercised in order to eliminate errors arising from imperfect mixing or selective adsorption of gases on the walls of infrared absorption cells.

The integrated absorption for the fundamental vibration-rotation band is

$$\alpha_F=\sum_j S^{0\to 1}_{j\to j\pm 1}=\int_{\Delta\nu_F} P_\nu d\nu, \tag{23}$$

---

[5] Benedict and Plyler [17] have observed abnormal intensities in members of the ν_1R branches of H_2O, which they ascribe to a perturbation induced by Coriolis forces interacting between vibration and rotation, according to the discussion of Wilson [18]. Problems of this sort will not be considered in the present review.

and for the first overtone is

$$\alpha_0 = \sum_j S^{0\to 2}_{j\to j\pm 1} = \int_{\Delta\nu_0} P_\nu d\nu, \tag{24}$$

where the integrals appearing in eq 23 and 24 must be extended over the entire effective widths $\Delta\nu_F$ and $\Delta\nu_0$ of the respective vibration-rotation bands. According to the treatment of Crawford and Dinsmore [8], it is readily shown that

$$\alpha_F \simeq (4\pi^3 N_T/3hc)\,\gamma(p_e')^2\omega_e(1-2x_e) \tag{25}$$

and

$$\alpha_0 \simeq (2\pi^3 N_T/3hc)\,\gamma^2(p_e')^2\omega_e(1-3x_e)(\rho_e''+\alpha_1^2) \tag{26}$$

where $p_e' = (dp/d\xi)_{\xi=0} = \epsilon r_e$; $p_e'' = (d^2p/d\xi^2)_{\xi=0}$; p=electric moment of the molecule; $\xi = (r-r_e)/r_e$; r=internuclear distance; r_e=equilibrium internuclear distance; x_e=mechanical anharmonicity constant; $\rho_e'' = p_e''/p_e'$; and α_1=coefficient of the cubic term in the expansion of the potential energy as a power series in ξ. A somewhat simplified version of eq 26 was used in the discussion on integrated absorption of individual rotational lines presented in section 2.

Representative experimental results [24] obtained for the fundamental of CO have shown that broadening by the infrared-inactive gas H_2 at total pressures below 100 psia is insufficient to remove the curvature in the Wilson-Wells extrapolation plot, whereas excellent results are obtained at a total pressure of 700 psia. Quantitative estimates of integrated absorption can also be obtained by the judicious use of self-broadening [24], as shown by data on the first overtone of CO [24]. For the successful use of this method it is essential that the cell length is chosen sufficiently small to permit accurate measurements at pressures which make P_ν a slowly varying function of ν. Under these conditions the apparent transmission is independent of total pressure and a function only of the optical density. By using sufficiently high total pressures it is possible also to determine absolute values of P_ν directly [24] and to obtain the integrated absorption as the integral of the spectral absorption coefficients. This method has also been used for CO.

The results obtained on α_F and α_0 for CO by use of the three separate techniques outlined in the preceding paragraphs were found to agree within the limits of experimental error. The numerical values for CO are

$$\alpha_F = 237 \pm 12 \text{ cm}^{-2} \text{ atm}^{-1} \text{ at } 297 \pm 2^\circ\text{K} \tag{27a}$$

and

$$\alpha_0 = 1.67 \pm 0.05 \text{ cm}^{-2} \text{ atm}^{-1} \text{ at } 297 \pm 2^\circ\text{K}. \tag{27b}$$

Integrated absorption data have also been obtained for HCl, HBr, and NO [25].

3.2. Measurement of Rotational Half-Widths

As was stated in section 2, the principal broadening effect in the infrared region of the spectrum is the result of collision broadening, which requires the experimental determination of optical collision diameters [11 to 15]. For infrared spectra, rotational line widths are customarily obtained by using indirect methods based on Elsasser's treatment [26] for equally spaced and equally intense rotational lines [27 to 29]. A detailed consideration of this problem shows, however, that the simplified analysis yields valid functional forms for the dependence of absorption on optical density, total pressure, etc., but cannot yield quantitative estimates of rotational half-width [30]. This deficiency arises from the fact that there is no satisfactory method for estimating, a priori, the appropriate value that should be used for the integrated absorption $\overline{S}$ of each of the equally spaced and equally intense rotational lines. Empirical measurements [30] suggest use of the relations

$$\overline{S}_F = \alpha_F / 2(\Delta\nu_F / q), \tag{28}$$

where q represents an average spacing between the rotational lines. At elevated temperatures one would expect [31] $\overline{S}_F$ to approach the value $\alpha_F/(\Delta\nu_F/q)$.

Rotational half-widths can be calculated from experimental data on collision-broadened lines by a straightforward application of the basic relations given in section 2. Thus if $R_{0\omega}$ represents the incident intensity of radiation in the wave-number interval between ω and $\omega + d\omega$, it follows from eq 3 that the spectral intensity of radiation R_ω absorbed by molecules distributed uniformly through a region of optical density X is

$$R_\omega = R_{0\omega}[1 - \exp(-P_\omega X)] \tag{29}$$

Thus, for the fundamental vibration-rotation band,

$$\int_{\Delta\omega_F} R_\omega d_\omega = \int_{\Delta\omega_F} R_{0\omega}[1 - \exp(-P_\omega X)] d\omega, \tag{30}$$

where P_ω is given by eq 19 and $S^{0\to1}_{j\to j-1}$, $S^{0\to1}_{j-1\to j}$ are obtained from eqs 13 and 14, respectively.

The precise evaluation of the integral appearing in eq 30 is a difficult computational problem except under conditions in which overlapping between rotational lines can be neglected [26, 32, 33]. Under these conditions it can readily be shown [33] that, at room temperature, eq 30 takes the form

$$\begin{aligned} \int_{\Delta\omega_F} R_\omega d\omega = 2\pi b \sum_{j=1}^{\infty} \{ & R_{0\omega_j} X_j \exp(-X_j)[I_0(X_j) + I_1(X_j)] \\ & + R_{0\omega_{j-1}} X_{j-1} \exp(-X_{j-1})[I_0(X_{j-1}) + I_1(X_{j-1})] \} \end{aligned} \tag{31}$$

where $R_{0\omega_j}$ = incident intensity of radiation evaluated at the wave number $\omega^{0\to1}_{j\to j-1}$, $R_{0\omega_{j-1}}$ = corresponding quantity evaluated at $\omega^{0\to1}_{j-1\to j}$; I_0 and I_1 represent modified Bessel functions of the first kind; and

$$X_j = S^{0\to1}_{j\to j-1} X / 2\pi b, \quad X_{j-1} = S^{0\to1}_{j-j\to j} X / 2\pi b. \tag{32}$$

Since $\int_{\Delta\omega_F} R_\omega d\omega$ is determined experimentally and $R_{0\omega_j}$, $R_{0\omega_{j-1}}$ are known, the only unknown quantity appearing in eq 31 is the rotational half-width b. In practice it is usually permissible to replace $R_{0\omega_j}$ and $R_{0\omega_{j-1}}$ by an average value $\overline{R}_0$ without introducing an error of more than a few percent.[6] The rotational half-width b is then adjusted [30], by trial and error, until the calculated value of $\int_{\Delta\omega_F} (R_\omega/\overline{R}_0)d\omega$ equals the observed value. Rotational half-widths determined by use of this method are essentially empirical fits of the experimental data to a dispersion formula. Valid results will be obtained for small values of X and at low pressures, where overlapping between rotational lines can be ignored, provided it is known that a dispersion formula applies to the line shape and that the half-widths are uniform across the rotational lines composing the vibration-rotation band under study. Since neglect of overlapping between rotational lines maximizes the value of the integral appearing on the right-hand side of eq 30 for any given value of b, it follows that the suggested procedure will yield lower limits for b. For CO it was found [30] that b had a value of 0.077 $\mathrm{cm}^{-1}\mathrm{atm}^{-1}$ for broadening by hydrogen and 0.040 $\mathrm{cm}^{-1}\mathrm{atm}^{-1}$ for broadening by argon.

The procedure just described for the calculation of rotational half-widths can be applied also to upper harmonics. For the first overtone the rotational half-widths have been found to have numerical values similar to those observed for the fundamental [30].

The conditions under which eq 31 applies are such as to render its use particularly attractive for half-width determinations on molecules with distant rotational spacing such as HCl and HBr. For application to these molecules the calculations can be simplified materially by utilizing an approximate closed form for the sum appearing in eq 31, which was obtained by H. S. Tsien [34] by using asymptotic forms for the modified Bessel functions, as has also been done by Elsasser [26] for a simplified representation of the vibration-rotation band.

4. Applications to Radiant Heat Transfer

The formulation of the basic relations given in section 2 and the experimental results described in section 3 can be used to calculate the equilibrium emission of radiation from carbon monoxide. Calculations can be carried out without difficulty for two special cases, namely, (a) heat transfer at sufficiently low pressures to justify a treatment for nonoverlapping rotational lines [34], and (b) heat transfer at elevated pressures where overlapping between rotational lines is so extensive that average absorption coefficients can be used for the effective widths of entire vibration-rotation bands [35].

The engineering emissivity E is defined as

$$E=\int_0^\infty R_\omega d\omega \Big/ \int_0^\infty R_\omega^0 d\omega$$

or, using eq 22,

$$E=\int_0^\infty R_\omega^0\,[1-\exp(-P_\omega X)]\,d\omega/\sigma T^4 \tag{33}$$

---

[6] Experimental errors from this source can be eliminated completely by performing experiments with automatic slit drive keeping R_0 constant over the range $\Delta\omega_F$.

where σ represents the Stefan-Boltzmann constant. The determination of E for two special cases will now be described.

4.1 Emissivity Calculations for Nonoverlapping Rotational Lines

For nonoverlapping rotational lines with a Lorentz distribution and of uniform half-width b, the emissivity E is given by a relation [33] analogous to eq 31, that is,

$$E=(\pi bc/2\sigma T^4)\sum_{n}\sum\sum_{n'},\rho^0(\omega_{j\to j\pm1}^{n\to n'})X_{j\to j\pm1}^{n\to n'}\times$$
$$\exp(-X_{j\to j\pm1}^{n\to n'})[I_0(X_{j\to j\pm1}^{n\to n'})+I_1(X_{j\to j\pm1}^{n\to n'})], \quad (34)$$

where

$$X_{j\to j\pm1}^{n\to n'}=S_{j\to j\pm1}^{n\to n'}X/2\pi b.$$

For optical densities at which the approximation of nonoverlapping between rotational lines applies, the values of n' that need to be considered normally are $n+1$ (fundamental vibration-rotation band) and $n+2$ (first overtone). At room temperature, eq 34 reduces to the relation

$$E=(\pi bc/2\sigma T^4)\sum_{j}\{\rho(\omega_{j\to j\pm1}^{0\to1})X_{j\to j\pm1}^{0\to1}\exp(-X_{j\to j\pm1}^{0\to1})[I_0(X_{j\to j\pm1}^{0\to1})+I_1(X_{j\to j\pm1}^{0\to1})]$$
$$+\rho^0(\omega_{j\to j\pm1}^{0\to2})X_{j\to j\pm1}^{0\to2}\exp(-X_{j\to j\pm1}^{0\to2})[I_0(X_{j\to j\pm1}^{0\to2})+I_1(X_{j\to j\pm1}^{0\to2})]\}. \quad (35)$$

Equation 35 has been used for calculating the overall emissivity of CO at 300° K and at atmospheric pressure. Excellent agreement was obtained with empirically determined emissivities for optical densities less than about 2-cm atm, for which eq 35 can be shown to be applicable [34].

4.2. Emissivity Calculations at Elevated Pressures

At elevated pressures an average absorption coefficient can be used for the entire effective width of the vibration-rotation bands [35]. Thus eq 33 becomes

$$E=[1-\exp(-\overline{P}_F X)]\int_{\Delta\omega_F}R^0(\omega)\,d\omega/\sigma T^4+$$
$$[1-\exp(-\overline{P}_0 X)]\int_{\Delta\omega_0}R^0(\omega)\,d\omega/\sigma T^4+\ \ldots, \quad (36)$$

where $\overline{P}_F$ and $\overline{P}_0$ represent, respectively, average absorption coefficients for the fundamental and first overtone, and $\Delta\omega_F$ and $\Delta\omega_0$ are the corresponding effective bandwidths. The numerical values of $\Delta\omega_F$ and $\Delta\omega_0$ can be approximated [35] by noting that the dependence of S on j is primarily determined by the factor $j\exp(-E/kT)$. In first approximation the values of $\overline{P}_F$ and $\overline{P}_0$ are given by the relations [31, 35]

$$\overline{P}_F=(\alpha_F/\Delta\omega_F)(300/T)\quad\text{and}\quad\overline{P}_0=(\alpha_0/\Delta\omega_0)(300/T) \quad (37)$$

for fixed values of the optical density X [35] if α_F has been determined from experimental measurements at 300° K. In accord with the analysis of Crawford and Dinsmore [8], it appears to be desirable to introduce slight corrections into the preceding relations, particularly at elevated temperatures.

Equation (36) has been used for the calculation of approximate high-pressure emissivities of diatomic gases. The theoretical relations predict the dependence of emissivity on temperature with remarkable accuracy and also yield very reasonable absolute values for the emissivity [35]. At the present time eq 36 represents the only available relation which can profitably be used for estimating equilibrium emissivities of diatomic gases under the conditions existing in rocket combustion chambers.

References

[1] A. Einstein, Phys. Z. **18,** 121 (1917).
[2] W. Heitler, Quantum theory of radiation, p. 102 (Oxford University Press, London, 1936).
[3] See, for example, L. Pauling and E. B. Wilson, Jr., Introduction to Quantum Mechanics, p. 301 (McGraw-Hill Book Co., Inc., New York, N. Y., 1935).
[4] R. C. Tolman, Phys. Rev. **23,** 693 (1924).
[5] E. C. Kemble, Phys. Rev. **25,** 1 (1925).
[6] D. M. Dennison, Phys. Rev. **31,** 503 (1928).
[7] J. R. Oppenheimer, Proc. Camb. Phil. Soc. **23,** 327 (1926).
[8] B. L. Crawford, Jr., and H. L. Dinsmore, J. Chem. Phys. **18,** 983, 1682 (1950).
[9] J. L. Dunham, Phys. Rev. **34,** 438 (1929); **35,** 1347 (1930).
[10] K. Scholz, Z. Physik **78,** 751 (1932).
[11] H. Margenau and W. W. Watson, Revs. Mod. Phys. **8,** 22 (1936).
[12] J. H. Van Vleck and V. F. Weisskopf, Revs. Mod. Phys. **17,** 227 (1945).
[13] A. Jablonski, Phys. Rev. **68,** 78 (1945).
[14] E. Lindholm, dissertation (Uppsala, 1942).
[15] P. W. Anderson, Phys. Rev. **76,** 647 (1949).
[16] R. Minkowski and H. Bruck, Z. Physik **95,** 274, 284 (1935).
[17] W. S. Benedict and E. K. Plyler, J. Research NBS **46**, 246 (1951).
[18] E. B. Wilson, Jr., J. Chem. Phys. **4,** 313 (1936).
[19] E. B. Wilson, Jr., and A. J. Wells, J. Chem. Phys. **14,** 578 (1946).
[20] A. M. Thorndike, A. J. Wells, and E. B. Wilson, Jr., J. Chem. Phys. **15,** 157 (1947).
[21] A. M. Thorndike, J. Chem. Phys. **15,** 868 (1947).
[22] S. A. Francis, J. Chem. Phsy. **18,** 861 (1950); **19,** 942 (1951).
[23] D. Z. Robinson, J. Chem. Phys. **19,** 881 (1951).
[24] S. S. Penner and D. Weber, J. Chem. Phys. **19,** 807, 817, 974 (1951).
[25] S. S. Penner and D. Weber, J. Chem. Phys. **21,** 649 (1953).
[26] W. M. Elsasser, Harvard Meteorological Studies No. 6 (Blue Hill Observatory Milton, Mass., 1942).
[27] A. M. Thorndike, J. Chem. Phys. **16,** 211 (1948).
[28] J. Strong and K. Watanabe, Phys. Rev. **57,** 1049 (1941).
[29] M. Summerfield and J. Strong, Phys. Rev. **60,** 162 (1941).
[30] S. S. Penner and D. Weber, J. Chem. Phys. **19,** 1351 (1951).
[31] S. S. Penner and D. Weber, J. Appl. Phys. **22,** 1164 (1951).
[32] R. Landenburg and F. Reiche, Ann. Phys. **42,** 181 (1913).
[33] S. S. Penner, J. Chem. Phys. **19,** 272 (1951).
[34] S. S. Penner, M. H. Ostrander, and H. S. Tsien, J. Appl. Phys. **23,** 256 (1952).
[35] S. S. Penner, J. Appl. Phys. **21,** 685 (1950); J. Appl. Mech. **18,** 53 (1951).

10. Infrared Spectra of Thermally Excited Gases[1]

By Richard H. Tourin[2]

Instrumentation has been developed for the measurement of infrared emission and absorption spectra of gases heated under controlled conditions of temperature, pressure, and composition. The setup now in use consists of a specially made quartz gas cell heated by a tube furnace, and an optical system which illuminates the entrance slit of a monochromator with radiation from the gas sample or the globar source. Spectra are measured with a modified Perkin-Elmer Infrared Spectrometer. Some preliminary results have been obtained on carbon dioxide in both emission and absorption.

In recent years a considerable amount of work has been reported on the spectra of flames and explosions. On the other hand, a relative paucity of information exists regarding the spectra of heated gases. In this connection we distinguish between a heated gas, by which we mean a gas brought to equilibrium at a high temperature by purely thermal means, and a flame, in which the excitation of the gas molecules is due partly to thermal and partly to chemical effects.

Thermal radiation from gases was studied by a number of investigators around 1900, about the time the theory of black-body radiation was being developed. Infrared spectra of heated gases were measured by Paschen[3] and by Schmidt,[4] to verify that gases do, in fact, emit radiation as a result of temperature alone. More recently Daly and Sutherland [5] measured the emission from hot carbon dioxide in the form of a jet of gas issuing from a steel tube.

The present paper is a preliminary report on a project which is under way in this laboratory to measure the infrared emission and absorption spectra of heated gases under controlled conditions. The object of this work is to obtain quantitative information on the relations between the spectrum of a hot gas and some of its thermodynamic variables. In this work, in addition to measuring a given spectrum, it is necessary to know the temperature, pressure, and composition of the gas at the time the spectrum is obtained. These quantities, for a stream of hot gas, such as that issuing from a burner, are in a continued state of flux, and are difficult to determine precisely. Consequently, in order to make the desired measurements it has been necessary to develop means for heating a known sample of gas in a closed container, which can be kept at constant temperature in a furnace. At present a quartz gas cell is being used for this purpose. This gas cell has thin quartz windows, which are sufficiently transparent to permit measurements to about 4.8 microns. Connections to vacuum and gas supplies are made through quartz tubes.

When in use, the gas cell is placed in the center of an electric furnace. The furnace temperature is sensed by a chromel-alumel thermocouple

---

[1] Supported by Air Materiel Command.

[2] Industrial Scientific Company, New York, N. Y.

[3] F. Paschen, Wied. Ann. **52,** 209 (1894).

[4] H. Schmidt, Ann. d. Physik **42,** 415 (1913).

[5] E. F. Daly and G. B. B. M. Sutherland, Third Symposium on Combustion and Flame and Explosion Phenomena (University of Wisconsin, 1948).

and maintained constant by a potentiometer-type controller. The gas temperature is also measured directly, using the infrared monochromatic radiation (IMRA) method.[6]

The furnace is located in relation to the optical system used in such a manner that radiation from the sample gas, or a continuous source, or both, can be focused on the entrance slit of the spectrometer. The spectrometer used is a Perkin-Elmer model 12–C,[7] which has been modified to permit use of other detectors in addition to the thermocouple.

Figure 10.1 shows the apparatus being used in this work. The furnace is to the left of the spectrometer, and the connections to the gas cell can be seen protruding from the furnace tube. Air is pumped out of the gas cell and gas admitted through these connections. The pressure in the system is indicated on the mercury manometer. The furnace control and the power-supply unit are on the left, behind the furnace. In this picture, the setup is arranged for absorption measurements, so that the 13-cycle radiation chopper is located in front of the globar, ahead of the furnace. The optics on the furnace platform are used to focus images of the globar in the gas cell and at the normal globar position on the spectrometer. For emission measurements, the 13-cycle chopper is located in front of the second image point. This image is then focused on the spectrometer slit in the usual way. The platform in front of the entrance slit of the monochromator is for mounting high-speed choppers, which are used in conjunction with lead sulfide detectors. The thermocouple amplifier is in the bottom

---

[6] M. Grossman, W. S. Tandler, and R. H. Tourin, Air Force Technical Report 6064 (May 1950).

[7] R. B. Barnes, R. S. McDonald, V. Z. Williams, and R. F. Kinnaird, J. Appl. Phys. 16, 77 (1945).

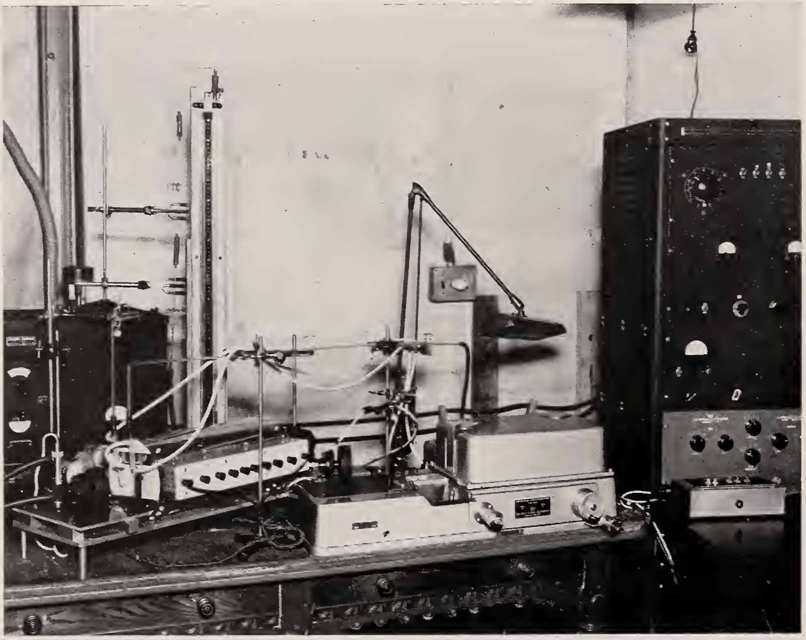

Figure 10.1. *Experimental setup, showing gas cell in position in the furnace.*

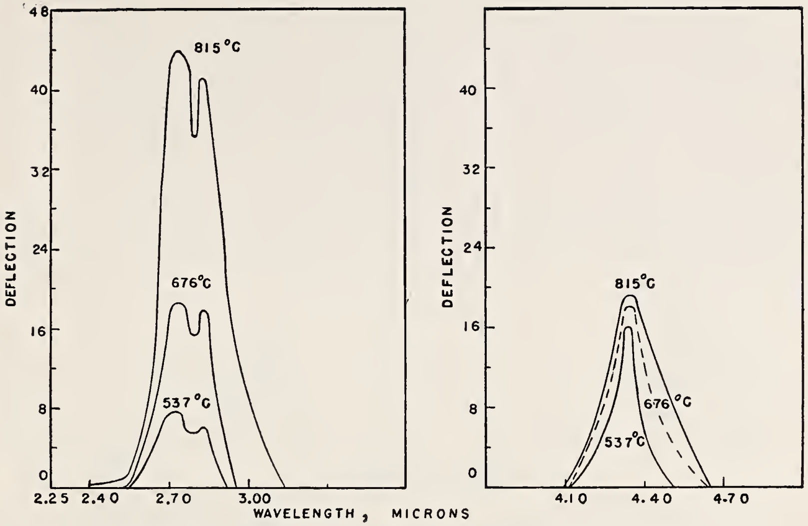

Figure 10.2. *Emission spectrum of heated carbon dioxide.*

panel of the relay rack, on the right. The other three panels contain amplifiers for the lead sulfide detector, globar power supply, and miscellaneous controls. Detector output is indicated on a Speedomax recorder, not visible in this photograph.

In figure 10.2 we show an example of the emission from carbon dioxide in the 2.8- and 4.3-micron regions, measured with the setup described above, using a rock-salt prism. The gas cell was filled to a pressure of 62 mm of mercury, with commercial, 99.96-percent pure "bone-dry" carbon dioxide, having water vapor as a trace impurity. This spectrum has been corrected for the effect of atmospheric absorption. However, no correction has been made for the fact that quartz absorbs more strongly in the 4.3-micron than the 2.7-micron region, and the intensities in the two sets of curves are therefore not comparable. The 3716 cm^{-1} and 3609 cm^{-1} combination bands of carbon dioxide appear at the left. These are the bands which are difficult to observe in flame spectra, due to overlapping by the water-vapor fundamental bands at 3652 cm^{-1} and 3756 cm^{-1}. In these measurements the slit width was about 50 cm^{-1}. On the right in figure 10.2 we have the 2349 cm^{-1} CO_2 fundamental, which is not resolved into its two branches. The slit width used here was about 30 cm^{-1}. The data indicate a slight shift of the spectra toward lower frequencies as the temperature is increased, although this effect does not show up very well in this particular drawing. An absorption spectrum of hot carbon dioxide appears in figure 10.3, measured under the same conditions as the emission. Broadening of the bands and a shift towards lower frequencies with increasing temperature are evident for the 2.7-micron bands. As in figure 10.2, the 4.3-micron band is not very clear. This is due to the fact that the data were not completely corrected for the effects of atmospheric absorption and absorption in the quartz windows.

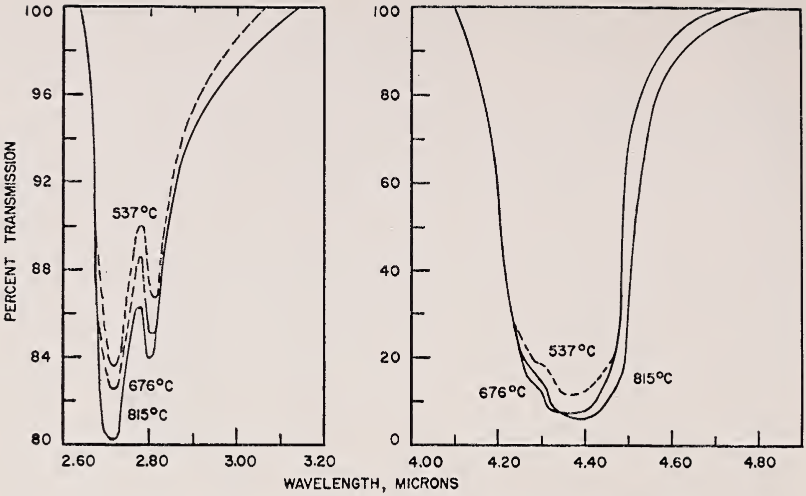

Figure 10.3. *Absorption spectrum of heated carbon dioxide.*

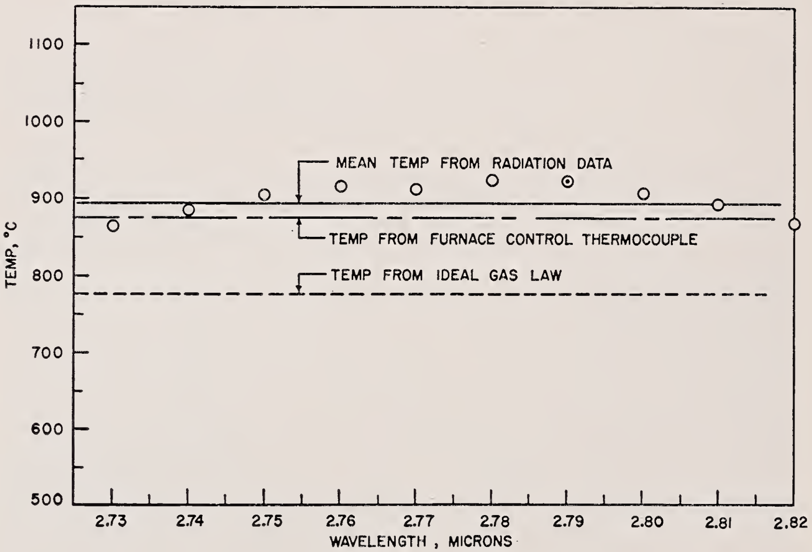

Figure 10.4. *Temperature comparison.*

Figure 10.4 is a comparison of three methods of measuring the temperature of the gas in the furnace. The uppermost horizontal line shows the mean temperature calculated by the IMRA method, using the data of the previous two figures for various wavelengths in the 2.7-micron region. The mean value here is 895° C. During these measurements the indicated temperature of the furnace was 876° C as shown by the centerline in figure 10.4. The difference between the two values is within the experimental error.

The experimental points in figure 10.4 appear to fall on a smooth curve, with the exception of one point. As these measurements are not very precise, this apparent regularity may not be significant. These temperature values were obtained in the following way. We can write the Planck radiation law for a black body as

$$d_\lambda = K_\lambda [\exp(C_2/\lambda T) - 1]^{-1},$$

where K_λ is a constant incorporating wavelength, slit width, detector sensitivity, etc., so that d_λ is the observed deflection on the output indicator. For a nonblack body this becomes

$$d_\lambda / e_\lambda = K_\lambda [\exp(C_2/\lambda T) - 1]^{-1},$$

where e_λ is the emissivity at wavelength λ. By Kirchhoff's law, e_λ equals the absorptivity a_λ. Making this substitution and solving for T we get

$$T = \frac{C_2}{\lambda \log (1 + K_\lambda a_\lambda / d_\lambda)}.$$

The values of a_λ were obtained from the absorption spectra, and the values of d_λ from the emission spectra. The constants K_λ were calculated from measured values of d_λ and T for the globar source, correcting for the emissivity of globar.

Using the ideal gas law a value of 777° C was calculated from the pressure change observed when the sample was heated up from room temperature. This corresponds to the lowermost line in figure 10.4.

Work on the spectrum of heated carbon dioxide is now being continued with higher resolution, using a lithium fluoride prism, and a lead sulfide detector for the 2.7-micron region. With the technique described here, which provides control of the temperature and composition of a hot gas while its spectrum is being measured, it is expected that much new information will be obtained, particularly with regard to gas-temperature measurement and the absorption laws for hot gases.

The assistance of Mr. Leonard Goodwin is acknowledged in measuring the spectra. Mr. Morris Grossman contributed valuable suggestions and criticism.

11. Present Position of the Theory of Flames

By Bernard Lewis [1]

The organizers of this Symposium have asked me to talk on the subject of this paper and to indicate areas where further basic studies are needed. I shall show how judicious emphasis on one or another transport process is broadening, conceptualwise, our understanding of flame phenomena.

Within the scope of this Symposium we may focus our attention on three principal combustion phenomena: (a) Combustion waves, (b) detonation waves, and (c) flames of fuel jets. My remarks will be concerned mainly with the first of these topics. Combustion waves are formed in explosive gases. We note that explosive gases are not always mixtures of two reactants—fuel and oxygen. Some gases, such as ozone, acetylene, hydrazine, and others, are explosive in themselves and support combustion waves.

We are concerned with two aspects of the combustion wave. One I should like to refer to as its macrostructure and the other its microstructure. The macrostructure determines the shape of the wave, such as the inner cone of the Bunsen burner or the approximately paraboloidal shape of the wave traveling in a tube or fluctuating distortions imposed by large-scale turbulence. Problems of macrostructure seem, in general, to be fairly well analyzable from the assumption of constant burning velocity, this being the preferred term for the propagation rate with respect to the unburned medium, and from considerations of the dynamics of gas flow. There are some cases that have not been sufficiently treated. Among these may be mentioned particularly the propagation of a combustion wave in a confining channel. This involves consideration of the movement of the gases ahead of and behind the flame. We believe that the steady state that is experimentally observed in tubes of moderate diameter is critically controlled by the viscous drag of the gas at the wall. Although the gas may be initially quiescent, flow is nevertheless induced by the thermal expansion of the burning gas. This flow is modified by friction at the wall in such a way that in the burned gas the stream tubes contract toward the axis, and in the unburned gas the stream tubes expand from the axis outward. There is certainly room here for experimentation and theoretical analysis, which should bring about an understanding of many complex phenomena exhibited by flames in ducts. The effect of large-scale turbulence, which was first discussed by Damköhler, has since been and is still being investigated by Karlovitz, Scurlock, Williams and Bollinger, Wright, Wohl, and others. This active field seems to be, therefore, well covered by able investigators.

The microstructure of the wave—that is, the gradients of temperature and concentration of various molecular species, the distribution

---

[1] Chief, Explosives and Physical Sciences Division, Bureau of Mines, Pittsburgh, Pa. Now President, Combustion and Explosives Research, Inc., Pittsburgh, Pa.

of reaction rate, and the mass flow through the wave—has long been known to present problems of great complexity; but gradual inroads have been made in determining the governing factors in the treatment of various problems under various sets of conditions. We note that there are two transport processes—heat conduction and diffusion. The former transports heat from the burned gas in the direction of the unburned gas. This transport process is well defined with respect to its direction and with respect to the property that is being transported. The diffusion process does not possess this simplicity. Thus, the reaction products diffuse in the direction of the heat flow, while the reactants diffuse against it. We see that as the reactants carry with them their chemical enthalpy, there is an enthalpy current opposing the heat flow from the burned gas. Another aspect of the diffusion process is the initiation of chemical reaction by active species, such as atoms and free radicals, that diffuse into the unburned gas.

It is possible to set up the system of hydrodynamic equations, as has been done by Hirschfelder and Curtiss, Boys and Corner, Manson, and others. However, it is not easy by this means to arrive at conceptual understanding of the various phenomena in which the microstructure of the wave plays the determining role. On the other hand, much has been accomplished by introducing suitably simplified models of the combustion wave. The model must be chosen to incorporate the principal features of the process that one wishes to study. Thus, if it is desired to derive theoretical equations for the burning velocity, it may well be justified to assume that the principal rate-determining process is the diffusion of chemical chain carriers into the unburned gases. The model, therefore, should attempt to reflect the diffusion of such particles as accurately as possible, while license may be taken with the heat transfer equations. On such basis, von Elbe and I in 1934 developed a model of the combustion wave in mixtures of ozone and oxygen in which we assumed a constant enthalpy distribution throughout the wave and which yielded burning velocities of the right order of magnitude. One may thus assume that the various calculated concentration gradients are also of the right order and are fairly realistic, whereas the temperature distribution is less so. Another model in which emphasis is placed on the diffusion process may be found in Tanford and Pease's treatment of combustion waves in mixtures containing hydrogen or hydrogen compounds. This is a semiempirical treatment that has yielded excellent correlations of the relative change of burning velocity with mixture composition.

However, investigators of flame phenomena should bear in mind that the problem of calculating burning velocities and microscopic structure from fundamental physical and chemical kinetic data is only one phase of fundamental research on combustion waves. There are other phases in which quite different problems arise and which, therefore, require quite different model simplifications. In the first instance I refer to the problem of ignition. Let us suppose that the enthalpy flow by diffusion of reactants, which was mentioned earlier, is negligible compared to the flow of heat. It is easily seen in such a case that the mixture of reactants now contains a substantial amount of heat over and above the chemical enthalpy it possesses. That is, if an element of gas within the wave were to burn adiabatically, its final temperature would substantially exceed the adiabatic combustion temperature of the fresh mixture, which of course is the temperature of the burned gas behind the wave, unless a heat sink is close by. We see, therefore, that an enthalpy wave is associated with the combustion wave; and the question immediately arises as to where this excess enthalpy in the wave originates. It is a small step from this question to the concept of the critical energy of the ignition source. To be sure, the ordinary ignition source, such as a spark, presents a problem of three-dimensional propagation of flame; that is, the area of the wave continually grows, and, therefore, the total excess enthalpy stored in the wave also grows. However, it is not difficult to see that after the wave area has grown to a certain size, that is, after the flame diameter has grown to a certain magnitude, the wave can satisfy its additional enthalpy requirement at the expense of the burned gas by retaining part of the chemical enthalpy released within it. We thus have the additional concept of a minimum wave surface; and the minimum ignition energy appears simply as the product of that surface and the excess enthalpy per unit area of the wave. That is,

$$H \simeq \pi d^2 h,$$

where H is the minimum ignition energy; d, the critical flame diameter; and h, the excess enthalpy per unit area of the wave. Neglecting enthalpy transport by diffusion, one obtains from the energy equation of the combustion wave approximately

$$h \simeq (\mu / S_u)\ (T_b - T_u),$$

where μ is the coefficient of heat conductivity of the mixture; S_u, the burning velocity; T_b, the temperature of the burned gas; and T_u, the temperature of the unburned gas. All these quantities are known or measurable. Diameter d may be identified approximately with the distance within which two solid surfaces, on approaching the incipient flame, have the effect of increasing the ignition energy. In other words, d may be identified approximately with the quenching distance. The experiment is readily realizable because the electrodes of a spark circuit provide such probing surfaces. The d and h being approximately known, it becomes possible to calculate the minimum ignition energy and compare the calculated values with experimental values of the minimum ignition energy of electric sparks. Such work performed at the Bureau of Mines has given excellent agreement except in cases that I shall discuss later. Calcote, at Experiment, Incorporated, has reported similar good agreements with many fuels.

Thus, here we have a field of study of combustion waves in which the successful working model purposely neglects diffusion, but only in the sense that transport of enthalpy by diffusion is assumed to be negligible. We cannot expect this model to carry over to other problems under other conditions.

Another important problem I wish to discuss is that of quenching distance. This problem by no means refers only to flame trapping in small channels but also to the important problems of flame stabilization and of flashback and blowoff of burner flames. The simplified model must provide a system of equations from which the decrease of burning velocity near a solid body may be calculated. One notes that such a body acts as a heat sink and also as a sink for chain carriers that are transported to its surface by diffusion. Success has been achieved by setting up the problem as one of heat conduction, with auxiliary assumptions concerning the change of a characteristic temperature, something of the nature of an ignition temperature. The exact form of the assumption was found to be quite uncritical, and the treatment permits the calculation of quenching distances and flashback and blowoff limits in excellent agreement with the experiment, from data of burning velocity and other data unrelated to experimental values of quenching distance, blowoff, and flashback. Thus, we see that, to describe conditions near a heat sink, a model that emphasizes heat flow has successfully replaced the model that had been used previously for calculating burning velocities from fundamental data in adiabatic combustion waves on the basis primarily of diffusion of chain carriers. It would seem, therefore, that near a heat sink the process of heat flow is of greater consequence than diffusion of chain carriers.

Diffusion phenomena again come into prominence when the two reactants of an explosive mixture possess widely different diffusivities and when the more rapidly diffusing component is stoichiometrically deficient. Such is the case in lean mixtures of hydrogen and also methane with air, and rich mixtures of heavy hydrocarbons and other organic fuels with air. Since the latter group includes the important technical fuels, gasoline, kerosine, etc., we deal here with phenomena that are occasionally of considerable practical interest. I mentioned earlier that there are certain exceptions to the good agreement found between calculated and experimental minimum ignition energies. These exceptions are found with rich mixtures of heavy hydrocarbons and similar compounds and they are readily explainable. In such mixtures the chemical enthalpy is associated primarily with oxygen since the fuel is in excess. The relatively high diffusivity of oxygen causes an enthalpy flow from the unburned to the burned side of the wave that materially reduces the net enthalpy flow from burned to unburned gas. Hence, it reduces the excess enthalpy h substantially below the value calculated from the equation given above. The discrepancies are due to the fact that minimum ignition energies of rich mixtures are remarkably low and the effect is more pronounced the larger the molecular weight, and therefore, the smaller the diffusivity, of the fuel.

In mixtures of this kind the macroscopic structure of the combustion wave is characteristically altered. The wave is always broken by folds that give rise to cell structure. Such flame cells generally wander and fluctuate in size; but in burner flames under carefully controlled conditions, it is possible to maintain perfectly stationary cells, which are bounded by ridges that extend from the tip to the base of the cone; these are the polyhedral flames that were reported many years ago by Smith and Pickering at the Bureau of Standards. When an electric spark is passed in a quiescent mixture of this type, the flame does not propagate spherically with uniform velocity but nonisotropically with variable velocity over its surface. Instantaneous schlieren pictures taken by Manton at the Bureau of Mines show the development of cells in such mixtures that in every respect resemble the cells that have been studied in considerable detail by Markstein. The experimental facts that have become available about such effects clearly point to the role of mixture change by diffusion in curved parts of the combustion wave. Here we have a field of study that should be continued both experimentally and theoretically. The phenomenon described may not be the most important one, as there is no question in my mind but that the effect of diffusional mixture change plays a primary role in the modification of the limits of flammability by variation of experimental conditions.

The subject of the limits of flammability should become one of the major fields of combustion research in the future. Many questions have been left open thus far. In the first place, it may be asked under what conditions a heat-evolving medium ceases to support a combustion wave. In other words, the existence of limits of flammability is an empirical fact rather than a theoretical necessity. Second, in the studies of limits of flammability, more and more knowledge should be accumulated about experimental conditions that modify the limits. I mention not only the effect of gravitational buoyancy on a flame in tubes or of induced turbulence, but I have in mind particularly the various complex phenomena that occur in rich mixtures of heavy fuels that seem to be the result of two processes—the diffusional mixture change mentioned and the existence of two regimes of chemical reaction, one of which we may designate the normal flame and the other the cool flame. This is a challenging field of study, and we would have been rather helpless in interpreting the observed phenomena without the pioneering work of Prettre and Laffitte in France, Townend and his associates in England, and Aviazov and Neumann in Russia. I also want to mention the careful observations of Egerton and Powling on the limits of flammability and the interesting research tool, namely the flat-burner flame, that they have developed. In this field, the study of flame as a flow phenomenon must be combined with chemical kinetic studies in the cool flame. The results should be both interesting and important, since normal and cool flames have a way of coalescing. As, on the one hand, the phenomena are modified strongly by pressure, and, on the other hand, it is precisely in aviation that fuels of high molecular weight are used over a wide range of pressure, the subject appears to possess elements of importance.

This concludes my remarks on combustion waves. Before closing, I want to remind you briefly that a combustion wave may transform into a detonation wave if the mixture lies within the limits of detonability and if suitable conditions are provided, namely confinement generally in a channel in which pressure pulses emanating from the combustion wave may telescope into a shock wave. Studies in this field offer various interesting problems connected with the interpretation of non-steady-state phenomena such as spin. Furthermore, the problem of limits of detonability exists analogous to, but perhaps more readily approachable than, the problem of limits of flammability.

Valuable theoretical and experimental information has been obtained in recent years on burning fuel jets. I mention the work of Wohl and coworkers, and of Hottel and Williams and coworkers. Nevertheless, in many respects this is a virgin field. I am thinking particularly of liquid-fuel sprays, which are used in jet engines, and the problems of flame stabilization connected with them. About this I have least to say because the systematic facts available are not sufficient to guide theoretical concepts. However, I believe that even a moderate research effort would prove rewarding and might lead to discovery of principles of considerable practical importance.

12. Detailed Mechanism of Elementary Reactions: Production of OH ($^2\Sigma^+$) in the H_2—O_2 Flame*

By Kurt E. Shuler**

Abstract

The mechanism of elementary reactions can best be studied in detail by constructing the relevant potential energy surfaces and investigating their properties and interactions.[1] In order to carry out such a program it is necessary to know the correlations between the internal states of reactants, intermediate reaction complexes and products so that the resulting term manifold may be determined from the states of the separated chemical species (reactants). These correlation rules are well known for diatomic and linear polyatomic molecules (Wigner-Witmer rules), but have not yet been developed explicitly for nonlinear polyatomic molecules.

Correlation rules for nonlinear polyatomic molecules can be formulated, without specific reference to detailed electronic configurations, by means of group theoretical arguments based on the symmetry of the nuclear configurations. This procedure utilizes an a priori configurational specification of the intermediate reaction complex from which one can obtain the necessary correlations by means of species resolution tables analagous to those developed by Mulliken.[2] A knowledge of the electronic and vibronic species of the reaction surfaces then permits a more detailed investigation of their behavior (optical transitions, predissociations, perturbations).

To give a concrete example, these correlation rules are applied to a study of the reaction $H+O_2 \rightarrow OH^*+O$ which may be of importance in the hydrogen-oxygen flame. The detailed mechanism of this reaction via both linear and nonlinear HO_2 surfaces is investigated with special reference to the OH($^2\Sigma^-$) state postulated by Gaydon and Wolfhard [3] and Broida and the author.[4] It is pointed out that the interactions and consequent radiationless transitions between the HO_2 surfaces are probably much more effective in producing OH($^2\Sigma^+$) than are the extremely weak interactions and radiationless transitions between the OH($^2\Sigma^-$) and OH($^2\Sigma^+$) states themselves.[5]

---

*This work was supported by the U. S. Navy, Bureau of Ordnance, under Contract NOrd-7386.

**Applied Physics Laboratory, The Johns Hopkins University, Silver Spring, Md.

[1] K. J. Laidler and K. E. Shuler, Chem. Rev. **48,** 153 (1951).

[2] R. S. Mulliken, Phys. Rev. **43,** 279 (1933).

[3] A. G. Gaydon and H. G. Wolfhard, Proc. Roy. Soc. A**208,** 63 (1951).

[4] H. P. Broida and K. E. Shuler J. Chem. Phys. **20,** 168 (1952).

[5] For a detailed discussion of these correlation rules see K. E. Shuler, J. Chem. Phys. **21,** 624 (1953).

13. Some Reactions of Atomic Hydrogen in Flames

By J. R. Arthur and D. T. A. Townend [1]

Methods of detecting the presence of atoms in flames are summarized. Particular attention is given to the chemiluminescence observed when hydrogen flames are brought into contact with certain promoted oxides. Proof that this luminescence is due to the recombination of hydrogen atoms is furnished by experiments with the oxides in a hydrogen discharge. The influence of various gaseous additives in extinguishing the chemiluminescence induced by hydrogen flames is examined; and the suppression of the sodium *D* lines is observed at the same additive concentration. An apparent expansion of flames which occurs when sodium salts are added to them is also described, the expansion depending on the fuel, the mode of combustion and the nature of the sodium salt. It is suggested that additives suppress the chemiluminescence by inducing the recombination of hydrogen atoms and that these atoms are mainly responsible for the formation of sodium atoms ($NaX+H \rightarrow Na+HX$) when sodium salts are present in flames. The latter process also appears to provide a basis for explaining the expansion phenomena.

It has become increasingly obvious over recent years that many chemical reactions involve the participation of atoms and free radicals; and the intensive study of chain reactions has contributed materially to the demonstration of the vital role played by these simple bodies. The most certain evidence relates to those reactions which can be carried out sufficiently slowly for the course of the reaction to be followed. Flame reactions are far too rapid to apply experimental methods which are suitable for slower reactions, and their investigation requires special methods. Considerable use has been made of the fact that, by definition, a flame is a chemical reaction emitting light; by examining the quality of the light, the presence of certain species excited in the flame such as OH, C_2 and CH has been demonstrated. By burning flames at low pressures (4 to 10 mm Hg) rather than at atmospheric pressure, it has been possible to widen considerably their reaction zones with the result that emission spectra measurements are more informative [1]. More recently, use has also been made of absorption spectra to demonstrate quantitatively the concentration of certain species (OH, O_2, C_2, etc.) in "flat" diffusion flames [2].

In combustion reactions, particular interest centers in the reactions of hydrogen and oxygen atoms. It is known, for example, that both of them are involved in the chain-branching reactions occurring during the slow combination of hydrogen and oxygen:

$$H+O_2 \rightarrow HO+O$$

$$O+H_2 \rightarrow HO+H.$$

Similar equations are thought to apply to the carbon monoxide-oxygen reaction when it occurs in the presence of hydrogen-containing species,

---

[1] The British Coal Utilization Research Association, Leatherhead, Surrey, England.

but insufficient information is known about the later stages of the reactions of hydrocarbons with oxygen to speculate upon the mechanisms involved.

There are few techniques actually detecting the presence of H and O atoms in flames, the best known being: (a) The addition of nitric oxide to flames containing oxygen atoms gives rise to a yellow-green continuous spectrum due to the association reaction

$$NO+O \rightarrow NO_2+h\nu.$$

The color is particularly well developed with CO flames [3]. (b) The formation of sulfuric acid mists in the products from flames to which sulfur compounds have been added indicate the presence of oxygen atoms [4]. The responsible reaction is believed to be

$$SO_2+O \rightarrow SO_3$$

It is uncertain whether this association takes place in the flame zone or slightly after it; equilibrium considerations make the latter alternative the more likely. (c) Crone [5] found that S_2 bands are very strongly emitted in the reversed hydrogen/oxygen flame containing sulfur and suggested that the excitation is due to the three-body reaction

$$\begin{array}{l} S_2+H+H \rightarrow S_2^{*}+H_2 \\ \qquad\qquad\qquad\;\; \downarrow \\ \qquad\qquad\qquad\;\; S_2+h\nu. \end{array}$$

In support of this, Crone pointed out that the hydrogen atom association reaction generates sufficient energy just to excite the low vibrational levels of the excited state of S_2 which are evolved in the emission. This observation has a parallel in the phenomenon reported by Brinsley and Stephens [6], who showed that the appearance of a blue calyx (which is due to S_2 emission) in coal-gas air flames containing sulfur can be used to judge when the mixture of gas and air is stoichiometric. (d). Kondratiev and coworkers [7] have used a thermoelectric method which is claimed not only to detect but also to measure the concentration of hydrogen atoms in flames. This consists of measuring the gradual heating of a thermocouple coated with the mixed oxides ($ZnO.Cr_2O_3$), an uncoated thermocouple being used as a control. The catalytic surface is said to bring about the combination of hydrogen atoms, and the method was applied with positive results to the flames of hydrogen, carbon monoxide, and acetylene. Attempts were also made to detect atomic hydrogen in cool flames of diethyl ether and acetaldehyde, but the results were negative.

This paper deals with the detection of atomic hydrogen in flames. The main technique to be described concerns the chemiluminescence observed when certain flames are brought into contact with promoted oxide surfaces. The pioneer work with this technique was carried out be E. C. W. Smith, and his earlier experiments have been described in the second Arthur Duckham Research Fellowship Report published in 1940 by the Institution of Gas Engineers.

It may be recalled that in his preliminary experiments Smith investigated the claim of Nichols and coworkers [8] that certain solid substances exist which, when in contact with flames, emit visible radiation in excess of that expected from the laws of radiation. Nichols had also suggested that, in favorable circumstances, visible radiation is emitted when such substances are at a temperature below that at which thermal radiation can be emitted. However, Smith found no evidence at all that at high temperatures any radiation is emitted which is other than purely thermal in origin; but in regard to the low temperature luminescence, he showed clearly that while it is not emitted by pure substances, a definite emission takes place when an impurity (activator) is present in the parent lattice, the emission then being characteristic of the activator. The oxides of calcium, strontium, barium, and beryllium were found to be suitable parent substances, and the following elements were found to be effective activators, giving rise to the colors indicated when a hydrogen flame was brought in contact with them: bismuth (violet), manganese (golden yellow), lead (blue), antimony (bright blue), and praeseodymium (pink). The luminescence was at a maximum with a concentration of activator of about 1 percent. The method of preparation of the specimens was also important, the most satisfactory being the coprecipitation of the carbonates of the two elements followed by ignition to the oxides.

The luminescence was observed most strongly in the outside edges of the flames and diminished in intensity as the specimen was heated to approach redness. A spectroscopic examination of the colors showed continuous spectra covering considerable portions of the visible spectrum, and proved conclusively the luminescent nature of the emission. The emission was in all cases strongest in hydrogen flames, very much less and somewhat erratic in town's gas flames, and probably nonexistent with CO flames.

Some further very significant results obtained by Smith are so far unpublished. These relate particularly to studies with low-pressure hydrogen flames, and to an examination of the effects of exposing the activated oxides to a hydrogen discharge. The experiments are described below and are followed by an account of further experiments carried out in the British Coal Utilization Research Association Laboratories; the latter work has been briefly referred to in earlier publications [9].

Smith's Experiments With Hydrogen Flames at Low Pressures

The effect of low pressures on the intensity of the luminescence was examined in a simple glass apparatus in which the hydrogen could be burned at a silica jet at any pressure down to the limit of flammability. The axis of the jet could be turned through a small angle so that the flame could be made to impinge on a refractory disk coated with the activated oxide. The results obtained were very striking: as the pressure was reduced with the hydrogen rate maintained constant, not only did the size of the flame increase, but in addition the intensity of the luminescence became greater. When the pressure was reduced to below about 100 mm Hg, the glow was produced on any part of the surface of the oxide which was within 3 to 5 mm of the visible flame. This striking effect of pressure reduction is presumably due to a decrease in the number of three body collisions which limits the intensity of the luminescence at ordinary pressures.

Exposure of the Oxides to a Hydrogen Discharge

The obvious test to decide whether the luminescent effects were associated with the presence of hydrogen atoms was to expose the active oxides to the products of an electric discharge in hydrogen at low pressures.

A simple diagram of the discharge tube used is shown in figure 13.1, and is similar to that used by H. G. Poole[10]. The tube was made of pyrex glass and consisted of a straight tube 46 in. long and 1 in. internal diameter. Small side tubes, approximtaely 4 in. from each end, served to admit the hydrogen, the flow being controlled by capillary taps. At approximately 6 in. from each end, large side tubes were fitted carrying cylindrical aluminum electrodes. The lead in wires were of tungsten, and were sealed into the base of the electrode chambers. From the center of the main tube a side tube of the same diameter and about 50 in. long, led directly to a rotary oil pump having a speed of 2 cu. ft. per minute. Sixteen in. from the main tube this exit tube carried a side arm which served to admit the specimens to be tested.

The whole of the interior surface of the tube with the exception of the electrode chambers was coated with glacial metaphosphoric acid, while the hydrogen was saturated with water vapor. Both these precautions were intended to reduce the tendency for hydrogen atoms to recombine on the walls of the tube. The tube was fed from a transformer with a maximum output of 7,500 volts with 200 volts on the primary. A stabilizing resistance of 10,000 ohms was connected in series with the tube, while a variable resistance in series with the primary of the transformer enabled the secondary current to be varied between 20 and 40 milliamperes with the tube running at the usual pressures. The tube was run at pressures between 1 and 5 mm Hg, and under these conditions gave a bluish-purple emission. According to Lunt, Meek, and Smith[11], this is the optimum condition for the production of atoms.

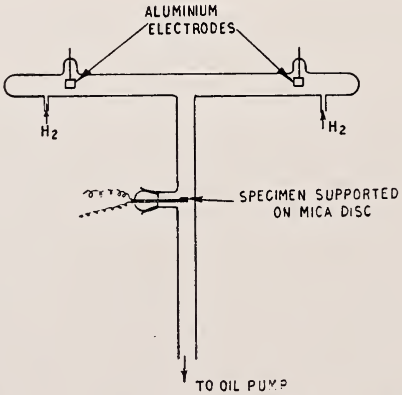

Figure 13.1. *Discharge tube used by E. C. W. Smith*

Specimens of activated oxide were coated on a small mica plate about $\frac{1}{2}$ in. sq and inserted into the stream of exit gases from the discharge through the side tube shown in figure 13.1. In all cases a luminescence was produced on the surface when the discharge was running under conditions suitable for the production of atoms, and its intensity varied in the way that the H atom concentration varied due to changes of operating pressure.

It was found that the color of the luminescence observed in the discharge tube was different from that which had been seen in the flames. Thus, bismuth and antimony specimens showed a yellowish luminescence in the discharge while with manganese the color was red. By heating the oxide support electrically, however, the colors of the luminescence approached that observed in the flame, suggesting that the differences arose from the varying surface temperature of the oxides in the two cases.

The experiments seemed, therefore, to show clearly that the luminescence observed in the flames had its origin in the recombination of hydrogen atoms on the oxide surfaces. This reaction is exothermic to the extent of 103 kcal, and assuming a quantized process, would be sufficient to produce light of wavelength 2,800 A. Actually the observed emissions corresponded to much smaller quanta, and the following discharge-tube experiments were devised with a view to ascertaining the mode of dissipation of the remainder of the energy.

Three thermocouples (Pt—Pt/Rh, 0.002 in. diameter) were arranged so as to project a height of 0.25 inch above the surface of an uncoated mica strip which was placed in the gases streaming from the discharge. The couples were connected in opposition so that assuming the junctions with the three leading-in wires were at the same temperature, the emf produced between any two of the wires would be a measure of the difference in temperature between the appropriate pair of couples. One couple was coated with metaphosphoric acid in order to prevent the recombination of hydrogen atoms on its surface. The second was left bare; platinum is known to be a most effective catalyst for the same reaction. The third was coated with a luminescent oxide. When hydrogen atoms were produced in the tube, the surface of the third couple was observed to luminescence. The second couple was found to be 66° C. hotter than either the first or the third, there being no appreciable temperature difference between these two.

The results indicate strongly that the excess energy referred to above is not liberated as heat, and also that when the hydrogen atoms recombine on the active oxides, very little of the energy liberated appears as heat energy.

On the fundamental side, the most interesting point about Smith's work is that it afforded the first direct demonstration of the existence of hydrogen atoms in flames. From the applied point of view, the low efficiency of light production by this means, and also the difficulty of bringing sufficient area of the flame in contact with the solid surface, have prevented a direct application in the gas industry. The more recent work undertaken in the British Coal Utilization Research Association laboratories has been concerned with using the luminescence to further fundamental knowledge of flame reactions.

British Coal Utilization Research Association Experiments

Preparation of Active Oxides

The activators used mainly have been manganese, antimony, and bismuth, the parent oxide being calcium oxide in every case. The preparation of the activated oxides was essentially the same as that recommended by Smith, but as no details have previously been published, these are given below in full: (a) *Manganese activated lime*—Amounts of "Analar" hydrated calcium chloride ($CaCl_2.6H_2O$) and manganese dioxide were taken to give 1 percent of Mn in the final product. 27.3 g of $CaCl_2.6H_2O$ were dissolved in the minimum quantity of distilled water, and to this was added the solution obtained by dissolving 0.079 g MnO_2 in sufficient HCl to liberate on warming all available chlorine. This solution was treated with very strong (Analar) sodium carbonate until all the calcium and manganese were precipitated as carbonates. The latter was filtered off, dried, and strongly ignited. (b) *Antimony activated lime*—Amounts of "Analar" hydrated calcium chloride ($CaCl_2.6H_2O$) and antimony trioxide (Sb_2O_3) were taken to give 1 percent of Sb in the product finally obtained. 19.6 g $CaCl_2.6H_2O$ were dissolved as above. 0.059 g Sb_2O_3 were dissolved in HCl and added to the $CaCl_2$ solution. The calcium and antimony were precipitated as carbonates with sodium carbonate (as above), filtered, dried, and strongly ignited. (c) *Bismuth activated lime*—Amounts of "Analar" hydrated calcium chloride and bismuth nitrate ($Bi(NO_3)_3\ 5H_2O$) were taken to give 1 percent of Bi in the final product. 19.6 g of $CaCl_2.6H_2O$ were dissolved as above. 0.116 g $Bi(NO_3)_3\ 5H_2O$ were dissolved in water containing a little nitric acid. The solutions were mixed, the carbonates precipitated (as above), filtered, dried, and strongly ignited.

Design of Flame Support

Diffusion flames were supported on a burner similar to, but simpler than, that described by Smith. The flame was burnt on the top face of a block of soft refractory brick, the combustible gas being led in at the base. The other five faces were sealed with cold-setting sillimanite cement. The activated oxide was smeared as a very thin layer on the top face and the combustible gas allowed to diffuse through the block and through the oxide layer. If the gas rate was low, the gas burned in air as a number of very small separated flames. At higher gas rates (those normally used), the flames coalesced in one flame.

Appearance of the Luminescence

Using a diffusion flame of hydrogen, the characteristic luminescence was observed as a circular annulus on the brick surface. This is illustrated in figures 13.2 and 13.3, which relate to an experiment in which manganese was used. In these figures the whole of the light emission from the surface of the block is due to the chemiluminescence. The thickness of the annulus was about 3 to 4 mm; and it presumably gives an indication of the extent of the reaction zone at the base of the flame. If the hydrogen rate were decreased (not sufficient to

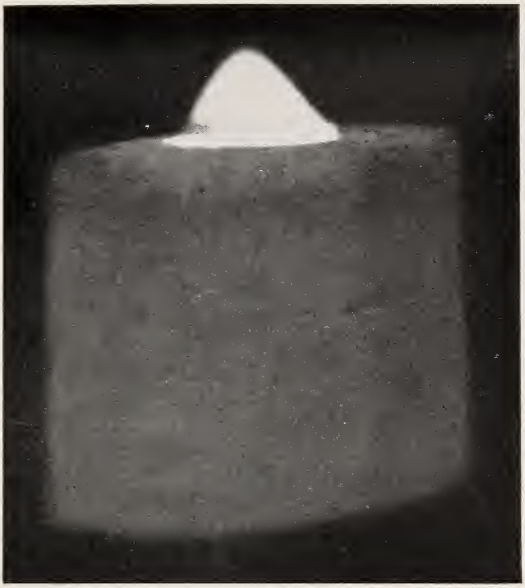

FIGURE 13.2. *Chemiluminescence exhibited by hydrogen flame.*

FIGURE 13.3. *Chemiluminescence exhibited by hydrogen flame (alternative view).*

produce the separate small flames described above), the luminescent annulus was degraded to a circle of smaller radius. Such a flame is presumably "solid," the larger flame being "hollow." The hydrogen flame is visible in figure 13.2 mainly because of emission from the sodium *D* lines, the sodium arising from the refractory support.

Chemiluminescence in Flames Other Than Hydrogen

Smith reported that no chemiluminescence could be observed with carbon monoxide and that some—but not all—specimens glowed satisfactorily in town's gas. We have confirmed the result with CO and our work with town's gas too shows that with no specimen could anything but the faintest glow be obtained. In the case of pure hydrocarbons (CH_4 and C_2H_4) we have also found that no luminescence could be observed either at atmospheric pressure or at reduced pressures (down to 10 cms mercury).

The Extinction of the Chemiluminescence by Gaseous Additions to the Hydrogen Stream

Systematic experiments were carried out to determine the amounts of various gases and vapors which were required completely to suppress the chemiluminescence exhibited by a specimen activated by manganese. A constant hydrogen rate of 400 cm^3/min was used. Permanent gases were mixed with the hydrogen at a T-junction;

FIGURE 13.4. *Reduced chemiluminescence exhibited by hydrogen flame containing added carbon dioxide (compare fig. 13.2).*

vapors of liquids were introduced by bubbling a portion of the hydrogen through the liquid maintained at constant temperature. Only one additive (argon) was found which did not, in adequate concentration, suppress the chemiluminescence. The extinction point was not easy to judge in all cases; it was much easier to define in the case of heavy molecules (e. g., hydrocarbon vapors) than smaller molecules (e. g., some of the permanent gases). The extinction was found to be reversible in all cases of addition except sulfur trioxide and carbon tetrachloride. These latter compounds presumably exerted some permanent deactivation effect on the solid surface of the oxides. In table 13.1 are given the quantities of additive (*P*) which were just sufficient to completely suppress the chemiluminescence. *P* is the percentage by volume of the total gas. When *P* is greater than cir. 4.0, the values given are approximate. In general, most of the chemiluminescence was suppressed by an amount of additive which was a small fraction of the quantities given in table 13.1. Figure 13.4 shows the reduced luminescence when 4 percent of carbon dioxide was added to the hydrogen. The last traces of luminescence were usually due to individual "bright spots" on the surface, and by comparison with the remainder of the surface they appeared difficult to extinguish. The insensitivity of the luminescence to such very large quantities of argon appears particularly significant.

TABLE 13.1. *Critical concentration of additives required to suppress the chemiluminescence*

Additive	P (percent by volume)	Additive	P (percent by volume)
$C_6H_5C_2H_5$	1.8	CO_2	6.2
$C_6H_5CH_3$	2.4	N_2O	29.0
$n C_6H_{14}$	2.7	N_2	37.0
C_6H_6	2.9	CO	15.4
C_2H_4	3.6	NH_3	19.4
CH_4	6.6	Air	34.0
SO_2	2.3	A	>79.0

In the experiments, sodium from the refractory support was a persistent impurity in the hydrogen flames which were clearly visible by their bright orange color. It was observed that when sufficient additive was present in the flame to suppress the chemiluminescence at the base of the flame, the sodium light was extinguished; *D* lines could then be only very faintly observed through a spectroscope. This observation suggested that hydrogen atoms are involved in some stage of the overall process of sodium excitation. Further support for this view is described below.

These simple experiments have also been extended to include useful observations on the mechanism of carbon formation in flames. It is well known that the latter may be suppressed by addition of foreign gases to hydrocarbon flames; it is noteworthy that the *D* line emission is also quenched at a concentration of additive (CO_2 for example) at which carbon formation is almost completely inhibited; this suggests that a stage in the process of carbon formation involves reactions of H atoms. A detailed discussion of this subject is, however, outside the scope of the present paper.

An Apparent Expansion of Flames Colored by Sodium Salts

When flames are contaminated with sodium salts, there is an expansion in size of the visible luminous envelope of gas [12]. The extent of the expansion depends on the fuel and on the mode of combustion. Thus, when simple diffusion flames of the following fuels burning in air were examined, the expansion decreased in the order

$$\text{Hydrogen} > \text{methane} > \text{ethylene} > \text{calor gas} > \text{carbon monoxide}.$$

The following figures show the relative increases in length of the luminous envelopes of gas which were measured using normal diffusion flames in air which were about 3 to 5 cm in height when uncontaminated, sodium chloride being vaporised into the flames:

	Fuel				
	H_2	CH_4	C_2H_4	Calor gas	CO
Percentage increase in length	102	55	25	18	13

The extent of the expansion was also found to depend on the nature of the sodium salt. Thus with the hydrogen diffusion flame the order with three sodium salts was found to be $NaI > NaCl > Na_2SO_4$. It appeared from experiments with the hydrocarbon flames that the extra height was due to an emission of the *D* lines; thus the tip of the envelope containing the luminous carbon appeared to be of the same height whether or not the flame was contaminated.

The expansion was found to be very much greater for reversed flames (of air burning in fuel) than for normal flames, this difference also being accompanied, in the case of hydrocarbon flames, by a widely differing tendency of these flames to deposit carbon.

The expansion phenomenon can be demonstrated in an even more spectacular way by using premixed flames in which the inner and outer cones are separated with a Smithells separator. When the separated flames of coal gas were contaminated with sodium chloride, the lower cone showed an increase in height of 500 to 600 percent. Methane flames showed an even greater expansion, whereas carbon monoxide flames showed no expansion. The *D*-line emission from the outer cone of the flames was feeble by comparison with that from the inner cone. When small quantities of hydrogen were added to the interconal gases, there was a substantial increase in the emission in the upper cone: corresponding quantities of carbon monoxide had very little effect.

Discussion

Since the chemiluminescence at the promoted oxide surfaces (S) is shown by Smith's work to have its origin in the process

$$H+H+S \rightarrow H_2+S+h\nu,$$

it is probable that its suppression by added gases is due to new reactions which remove hydrogen atoms. The exact nature of these new reactions is uncertain, but the most likely suggestion is that the additives (A) act as third bodies in the recombination of hydrogen atoms:—

$$H+H+A \rightarrow H_2+A.$$

The improbability of such a three-body collision could be decreased by the reaction occurring as two consecutive two-body collisions, the first collision being a "sticky" one:

$$H+X \rightarrow H\ .\ .\ .\ X,\ H\ .\ .\ .\ X+H \rightarrow H_2+X.$$

The data given in table 13.1 are consistent with the view that the additives act as targets on which the hydrogen atoms recombine. Thus it is obvious that large polyatomic molecules are the most effective and that the only monatomic gas used (argon) is the least effective. Differences in the critical quantities of the additives required exist which would not be anticipated on the basis of molecular diameters and velocities. Molecules containing nitrogen are a case in point; they are rather less effective than would be expected on simple collision considerations.

The coincidence between the suppression of the chemiluminescence and of the sodium light from the hydrogen flames is particularly interesting. It has often been suggested that the excitation of sodium in flames is a chemiluminescent rather than a thermal phenomenon, but this does not accord with the fact that the measurement of flame temperature by the sodium line reversal method is reckoned to give quite reliable results. The extreme sensitivity of hydrogen flames, compared to others, to the presence of sodium is a further relevant observation. The observations reported above certainly suggest that hydrogen atoms are involved in some stage of the over-all process of sodium atom excitation; the most likely suggestion [13], which is consistent with all the facts, is that hydrogen atoms are responsible for the generation, rather than the excitation, of the sodium:

$$NaX+H \rightarrow Na+HX.$$

If X is halogen, this reaction is near to being thermally neutral, whereas the dissociation reactions

$$NaX \rightarrow Na+X$$

are very strongly endothermic.

The expansion phenomena reported are consistent with the participation of hydrogen atoms. The observations which require interpretation are: (a) for a given fuel, greater expansions are observed in the order: normal diffusion, reversed diffusion, separated premixed; (b) the fuel and the type of sodium salt influence the degree of expansion; (c) there is only a feeble emission of *D* lines from the upper one of separated flames.

With all three types of flame, sodium is excited in regions which were not emitting visible light in the uncontaminated flames; this is because the lifetime of the excited atoms is too short to permit of excitation in the main flame envelope followed by emission of the *D* lines in the outer, originally dark, regions. The extent of the expansion and its variation with fuel type suggest that sodium atoms are also formed in the originally dark regions. It is accordingly suggested that the degree of expansion would be related to the tendency for free hydrogen atoms to diffuse from the reaction zone into the dark region surrounding the flames, the expansion depending mainly on the number of hydrogen atoms diffusing out and on the rate at which they are removed by chemical reaction. The large expansion of the hydrogen flame would then be expected because of the large concentration of hydrogen atoms in its reaction zone. The extent of expansion of the different types of flame can also be explained; thus the premixed flame is the hottest of the three, so that the concentration of hydrogen atoms is largest. Moreover, because the original flame envelopes in both the separated premixed and the reversed diffusion flames are surrounded by an oxygen-free atmosphere, a relatively long lifetime for the hydrogen atoms outside the original flame envelope is likely. The nature of the sodium salt is important because of the variable tendency for the reaction

$$NaX+H \rightarrow HX+Na$$

to occur in the originally dark region outside the flame. Lastly, the weak emission of *D* lines in the upper cone of separated flames is probably due to the low concentration of hydrogen atoms in the presence of the combustion products from the lower cone.

Conclusions

Both the techniques described above afford evidence of the reactions of hydrogen atoms in flames. Further application of them requires a means of calibration so that actually concentrations of atoms might be measured.

The authors are indebted to Dr. M. S. Iyengar for help with some of the chemiluminescent work and to Mr. R. F. Littlejohn for making some of the separated flame observations.

References

[1] A. G. Gaydon and H. G. Wolfhard, Third Symposium on Combustion, Flame and Explosion Phenomena, p. 504 Williams and Wilkins Co., Baltimore, Md., (1949).
[2] H. G. Wolfhard and W. G. Parker, Proc. Phys. Soc. [A] **65,** 2 (1952).
[3] A. G. Gaydon, Proc. Roy Soc. [A] **183,** 111 (1944).
[4] A. Dooley and G. Whittingham, Trans. Faraday Soc. **42,** 354 (1946).
[5] H. G. Crone, quoted by A. G. Gaydon, Spectroscopy and Combustion Theory, 2d. ed., p. 91 Chapman and Hall, Ltd., London, (1948).
[6] F. Brinsley and A. G. Stephens, **157,** 622 (1946).
[7] V. Kondratiev et al., J. Acad. Sci. U. S. S. R., **51,** 607 (1946); J. Phys. Chem., **21,** 769 (1947); **17,** 453 (1921).
[8] E. L. Nichols et al., Phys. Rev. [2] **17,** 453 (1921).
[9] J. R. Arthur, Nature **165,** 557 (1950); D. T. A. Townend, Fuel **29,** 64 (1950).
[10] H. G. Poole, Proc. Roy. Soc. **163,** 404, (1937).
[11] R. W. Lant, C. A. Meek, and E. C. W. Smith, Proc. Roy Soc. **158**, 729 (1937).
[12] J. R. Arthur and R. F. Littlejohn, Nature **169,** 288 (1952).
[13] J. R. Arthur, D. H. Bangham, R. H. Baulk, and G. Whittingham, Nature **166,** 358 (1950).

14. Temperature of the Hydrogen-Fluorine Flame

By R. H. Wilson, Jr., J. B. Conway, A. Engelbrecht, and A. V. Grosse [1]

The high exothermicity of the combination of hydrogen with fluorine combined with the excellent stability of the reaction product results in a very high flame temperature. The maximum theoretical flame temperature is calculated to be 4,300° K at 1 atm pressure. After preliminary experiments indicated that this maximum temperature must be higher than that of any man made radiator, a new technique was developed using the sun as a comparison source. The actual flame temperature, measured by means of the line-reversal method using the lithium line, is 4,300° K ±150°.

Introduction

The combination of hydrogen with fluorine is both very rapid and highly exothermic. The heat of the reaction is 128.0 kcal/mole of hydrogen [1]. In addition, the product of the reaction—hydrogen fluoride—is an extremely stable molecule. These factors combine to produce a very high flame temperature, higher than either the oxyhydrogen flame (2,700° C) or the oxyacetylene flame (3,100° C).

The hydrogen-fluorine torch, a device designed to produce a hydrogen-fluorine flame, has already been described by Priest and Grosse [2]. This torch produces a diffusion-type flame due to the inability to premix the two reactants. All attempts to premix the two gases within the torch without ignition have so far been unsuccessful.

The torch used in the measurements to be described below was made of nickel and was similar in construction to the torch described by Priest and Grosse [2]. The fluorine flowed through the center tube and the hydrogen through the annular space surrounding this tube. The inside diameter of the central tube was 0.128 inch; the width of the annular space was 0.019 inch. The fluorine flow rate varied from 2.0 to 17.0 liters per minute while that of the hydrogen varied from 3.4 to 15.0 liter/min. The hydrogen flow rate was measured with a small rotameter, while that of the fluorine was measured with an orifice and manometer assembly. The orifice was made of brass and the manometer was made of Kel-F tubing and filled with Kel-F oil. The orifice was calibrated with oxygen against a wet-test meter.

Fluorine and hydrogen combine giving a bluish-white flame. The fluorine forms a dark inner cone of varying length depending on the flow rate. For a fluorine rate of 4.0 liter/min, the inner cone is about 2.5 mm in length; for a rate of 8.0 liter/min, this length is about 8.5 mm. As the fluorine flow rate increases, the inner cone becomes less and less discernible until the flame seems to be almost homogeneous. The total length of the flame depends, of course, on the flow rates of the two gases. Flames have been obtained varying from 5 to 50 cm in length. The hottest portion of the flame seems to be a few mm above the tip of the inner cone.

Theoretical Flame Temperatures

The relationship between the theoretical flame temperature and the composition of the hydrogen-fluorine mixture fed to the torch was calculated according to the method described in Wenner [3]. In these

---

[1] The Research Institute of Temple University, Philadelphia, Pa.

calculations the latest thermodynamic data were employed. These data were obtained as follows:

(a) the free energy data for the dissociation of molecular hydrogen from [4];
(b) the free energy data for the dissociation of molecular fluorine from [5];
(c) the free energy data for the dissociation of hydrogen fluoride into hydrogen and fluorine atoms from [6];
(d) the heat of dissociation of hydrogen from [4];
(e) the heat of dissociation of hydrogen fluoride from [4];
(f) the heat of dissociation of fluorine from [7];
(g) all heat capacity data from [4].

It is to be noted that the new value of the dissociation energy of fluorine (36.4 kcal/mole) has been used as reported by Evans, Warhurst, and Whittle [7]. The original value of 63.5 kilocalories per mole of fluorine due to von Wartenberg [8] has been found to be considerably in error.

The following discussion deals with the way in which the method of Wenner [3] for calculating theoretical flame temperatures was applied to the hydrogen-fluorine reaction. The discussion will be concerned with the case in which 1 mole of fluorine and 1 mole of hydrogen are being mixed and allowed to react. The reaction is taking place at a constant pressure of 1 atmosphere. In applying this method it was first assumed that the mole of H_2 and the mole of F_2 were dissociated at 298° K; there the atoms combined to form HF. Thus

$$H_2(g) \rightarrow 2H(g) \tag{1}$$

$$F_2(g) \rightarrow 2F(g) \tag{2}$$

$$2H(g) + 2F(g) \rightarrow 2HF(g) \tag{3}$$

At the high temperatures attained in this reaction we must take into account the dissociation of the reaction products. In other words, we must consider the dissociation of HF into atoms and also the combination of atomic hydrogen and fluorine into the molecular form.

The following reactions then must be considered at the high temperature:

$$2HF(g) \rightarrow 2H(g) + 2F(g) \tag{4}$$

$$2H(g) \rightarrow H_2(g) \tag{5}$$

$$2F(g) \rightarrow F_2(g) \tag{6}$$

Let

x=fraction of HF moles dissociated at the flame temperature.
y=fraction of H atoms combining to form H_2 at the flame temperature.
z=fraction of F atoms combining to form F_2 at the flame temperature.

Then at equilibrium we have the following:

Moles of HF dissociated$=2x$
Moles of H_2 formed$=(2xy/2)=xy$
Moles of F_2 formed$=xz$

The mixture then will consist of the following:

$$\begin{aligned}
&\text{Moles of HF} = 2-2x\\
&\text{Moles of } H_2 = xy\\
&\text{Moles of } F_2 = xz\\
&\text{Moles of H} = 2x-2xy = 2x(1-y)\\
&\text{Moles of F} = 2x-2xz = 2x(1-z)\\
\hline
&\text{Total moles} = 2+2x-xy-xz
\end{aligned}$$

Using the relationship for equilibrium constants described in Hougen and Watson [9], it is possible to write the following expressions for reactions (4), (5), and (6):

for eq (4)

$$\frac{[2x(1-y)]^2[2x(1-z)]^2}{(2-2x)^2(2+2x-xy-xz)^2}=K_4 \tag{7}$$

for eq (5)

$$\frac{xy[2+2x-xy-xz]}{[2x(1-y)]^2}=K_5 \tag{8}$$

for eq (6)

$$\frac{xz[2+2x-xy-xz]}{[2x(1-z)]^2}=K_6 \tag{9}$$

These equations contain three unknowns, but cannot be solved for x, y, and z, because the flame temperature is still unknown and therefore K_4, K_5, and K_6 are as yet undetermined. Another relationship may be determined by considering the heat evolved in these reactions. When the feed gases enter the flame they may be considered to dissociate at 298° K. according to reactions (1) and (2); the atoms then combine to form HF at 298° K. according to reaction (3). The net heat release for these reactions is the heat of reaction (3) minus the sum of the heats of the other two reactions. This calculation yields 128,000 cal as the overall exothermic heat release. This quantity, however, is not all available to raise the temperature of the reaction mixture because of the dissociation and recombination which occurs at the high temperature. The HF is dissociated as the temperature increases reducing this amount of available heat; on the other hand, the recombination of hydrogen and fluorine atoms increases this amount of heat. In connection with the symbols employed in this discussion, the actual amount of heat available for raising the temperature of the reaction mixture is as follows:

$$128{,}000-269{,}600x+104{,}200xy+36{,}400xz$$

This quantity of heat is available for increasing the enthalpy of the reaction mixture. The correct expression is as follows:

$$\begin{aligned}
&128{,}000-269{,}600x+104{,}200xy+36{,}400xz\\
&\quad=(2-2x)\int_{298}^{T}C_{p_{\mathrm{HF}}}\,dT+xy\int_{298}^{T}C_{p_{\mathrm{H}_2}}\,dT+xz\int_{298}^{T}C_{p_{\mathrm{F}_2}}\,dT+\\
&\quad 2x(1-y)\int_{298}^{T}C_{p_{\mathrm{H}}}\,dT+2x(1-z)\int_{298}^{T}C_{p_{\mathrm{F}}}\,dT
\end{aligned} \tag{10}$$

The upper limit on the integral is the theoretical flame temperature.

Substituting average C_p values we obtain:

$$128{,}000-269{,}600x+104{,}200xy+36{,}400xz$$
$$=(2-2x)\int_{298}^{T}7.5\,dT+xy\int_{298}^{T}8.0\,dT+xz\int_{298}^{T}8.0\,dT+$$
$$(2x-2xy)\int_{298}^{T}5.0\,dT+(2x-2xz)\int_{298}^{T}5.44\,dT \qquad (11)$$

Integration gives

$$128{,}000-269{,}600x+104{,}200xy+36{,}400xz$$
$$=(T-298)[15+5.88x-2xy-2.88xz] \qquad (12)$$

The four eq (7),(8),(9), and (12), containing four unknowns, can now be solved simultaneously for x, y, z, and T. In solving these equations for the necessary variables the following procedure is employed:

1. Assume a value of T and calculate the values of the equilibrium constants for reactions (4), (5), and (6) at this temperature;
2. Substitute these values of the equilibrium constants in eq (7), (8), and (9), respectively;
3. Solve eq (7), (8), and (9), simultaneously for x, y, and z; (this is a trial-and-error solution);
4. Substitute the values of x, y, z, and T in eq 12 to see if this equation is satisfied. A check here indicates a correct solution. If eq (12) is not satisfied, a new temperature T must be selected and the process repeated.

The calculations just described were extended to various feed compositions of fluorine and hydrogen. The following theoretical temperatures were obtained:

Feed composition		Theoretical flame temperature at 1 atm
Mole percent of F_2	Mole percent of H_2	
		° K
10. 0	90. 0	1, 900
33. 3	66. 7	3, 550
50. 0	50. 0	4, 300
66. 7	33. 3	3, 800
90. 0	10. 0	1, 200

These values are plotted in figure 14.1.

Experimental Flame Temperatures

The spectrum line-reversal method was used in measuring the flame temperature. The standard setup for this measurement has been described by Lewis and von Elbe [10] and also by Jones, Lewis, Friauf, and Perrott [11]. A 6-volt, tungsten-ribbon-filament lamp was first employed as the comparison source, but it was soon found that this was inadequate for measuring the maximum flame temperature. Reversal could not be obtained with this particular source because the maximum flame temperature was above that of the lamp (melting point of tungsten=3,640° K.). The ordinary carbon arc could not be used as the comparison radiator for the same reason (sublimation point of carbon=3,810° K. at atmospheric pressure.) In addition, it was found difficult to obtain the necessary radiation stability with the carbon arc.

The preliminary investigations described above indicated that in order to measure the maximum flame temperature it would be necessary to have a comparison radiator whose spectral distribution approached Planckian continuity, at least in the region including the spectral lines to be used and the pyrometer filter band, for temperatures above 4,000° K. No such simple radiator made by man seemed to be available. Hence attention was turned to the sun as a radiator possessing the desired characteristics.

The effective temperature of the sun has been found by other investigators [12, 13], to be about 6,000° K. This temperature, by definition, is approximately the mean of the brightness temperature for all wavelengths, with the atmospheric absorption assumed to be negligible. This temperature is also the mean of the distribution of radiation at all distances from the sun's limb, whereas actually the apparent brightness temperature varies from nearly 6,700° K. at the center to less than 5,400° K. at the limb of the sun's disk [12]. Similarly, the atmosphere of the earth will cut down the brightness temperature almost without limit, depending on the sun's zenith distance and the dustiness and haziness of the air mass through which the observation is made. Thus, only in the clearest weather can the actual brightness temperature of a point on the sun's disk for a certain wavelength at a given time and place on the earth's surface be deduced from the general knowledge of solar temperature and atmospheric transmission.

However, the latter complication in using the sun as a standard radiator was here avoidable by the fact that the Pyro optical pyrometer, using its "Filter II," can be set on a temperature as high as that of the sun for a band of 6,650 A. (Tables for use with our particular filter were specially prepared by the National Bureau of (Standards). Such a reading of effective temperature, taken simultaneously with a line-reversal setting, can thus be made to include all agents of absorption, including any instrumental agent such as mirrors and absorbing material introduced into the optical train for the purpose of equalizing the effective radiator temperature to that of the flame.

In using the sun as a comparison radiator, the element to be introduced into the flame for observation of reversal of its persistent spectral line must be given special consideration. For an artificial radiator, having a perfectly continuous spectrum, many elements are satisfactory and sodium is usually chosen for the convenient observability and easy excitability of its yellow pair of persistent lines. However, the latter characteristic also causes the sodium in the solar atmosphere to display itself as conspicuous dark absorption lines, the so-called *D* lines of the solar spectrum. Thus much of the line from sodium in the flame would be superposed on the line originating in the "reversing layer" of the sun and the reversal effect would give comparison of the flame only with the less definite temperature of the sun's atmosphere.

Such complication was avoided in the present procedure by introducing the element lithium into the flame. A recent publication by Greenstein [14] indicates that for all practical purposes lithium does not appear in the solar spectrum. The lithium was introduced into the flame by dipping a small glass rod into a solution of lithium chloride and then holding this in the base of the flame.

The essential variation of the present method from standard line-reversal procedure is that radiation from the sun replaces that of the artificial radiator in the optical setup. In addition, a two-mirror heliostat was used in keeping the sun's image (about ⅛ in. in diameter) focused on the spectroscope slit. Since the sun's effective temperature decreases by over 1,000° K from center to limb, it is necessary to know the exact position of the sun's image on the slit, so, usually an exactly central position would be simplest. With this arrangement the width of the observed spectrum would correspond to a diametral distribution of solar radiation with central disk temperature at the center of the line segment. Then the two points along the lithium line where it is reversed will correspond to the radius on the solar disk at which flame temperature equals apparent solar temperature. An optical pyrometer, carefully set at such a radius, then gives the temperature desired.

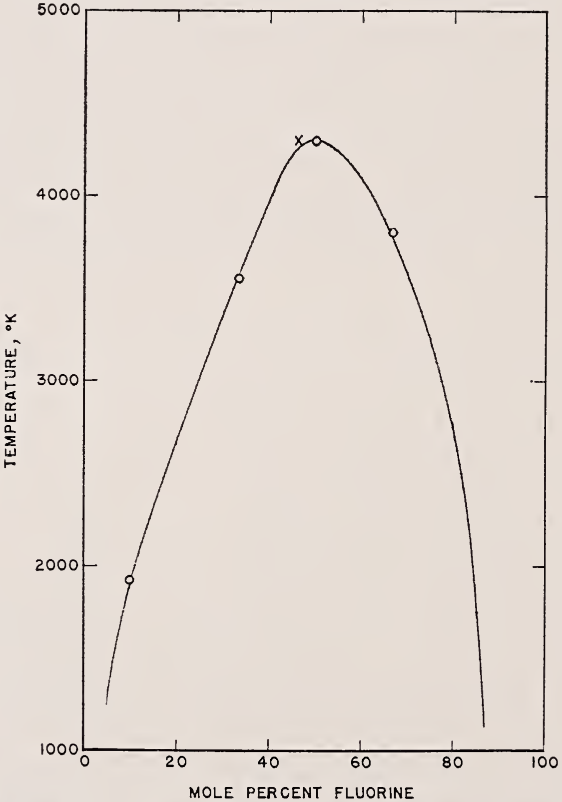

FIGURE 14.1. *Flame temperatures versus percent fluorine for the hydrogen-fluorine torch.*

O, theoretical; X, experimental.

The brightness of the sun was varied by introducing a neutral, variable absorbing agent of good optical quality so that it intercepts the whole solar beam before it passes through the flame. The absorption is increased until reversal is obtained and an optical pyrometer reading of the sun was taken through the same filter setting. This temperature is thus the flame temperature and represents the average of nine readings.

The maximum flame temperature was measured as 4,300° K ± 150°. This point is plotted in figure 14.1. The close agreement between the theoretical and experimental temperature is admittedly fortuitous.

The Effect of Pressure

The effect of pressure on the theoretical flame temperature has also been calculated. The following values were obtained using a feed composition of 50 mole percent of hydrogen and 50 mole percent of fluorine:

Pressure (atm)	Theoretical flame temperature, ° K
1	4, 300
10	4, 900
100	5, 400

The apparatus shown in figure 14.2 has been used to operate a hydrogen-fluorine flame under pressure. It consists essentially of a water-cooled copper pipe, 85 cm long, with an adjustable flourine jet, passing through a stuffing box. The main difficulty is one of observing the flame. This has been accomplished by using a crosspiece with two sight glasses made out of silica-free glass, as described previously by one of us [15]. The pressure was observed through a standard gage.

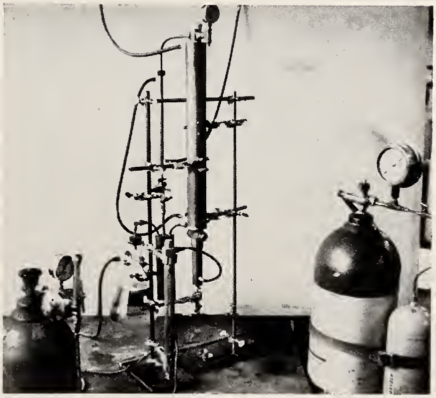

Figure 14.2. *Apparatus used to operate a hydrogen-fluorine flame under pressure.*

The hydrogen flow was measured through a regular pressure flowmeter, while the fluorine flow from a commercial fluorine cylinder was controlled by means of two small Hoke valves.

The fluorine flame was started in an atmosphere of hydrogen at atmospheric pressure and then both the hydrogen and fluorine pressure raised to the desired value. A flame was successfully maintained at a pressure of 5.0 atm. At this pressure the calculated flame temperature should correspond to 4,750° K (8,080° F). Work is underway to measure this increase in temperature due to pressure.

We should like to acknowledge the cooperation of Dr. Michels, of the Physics Department of Bryn Mawr College, in lending us the heliostat.

The donation of a cylinder of fluorine is also acknowledged from the Pennsylvania Salt Manufacturing Co.

This work was partially supported by ONR Project N9–onr–87300.

References

[1] F. Bichowsky and F. Rossini, Thermochemistry of Chemical Substances (Reinhold Publishing Corp., New York, N. Y., 1936).
[2] H. F. Priest and A. V. Grosse, Ind. Eng. Chem. **39,** 431 (1947).
[3] R. R. Wenner, Thermochemical Calculations (McGraw-Hill Book Co., New York, N. Y., 1941).
[4] A. P. I. Research Project 44, NBS.
[5] G. M. Murphy and J. E. Vance, J. Chem. Phys. **7,** 806 (1939).
[6] W. M. Latimer, MDDC–1462, U. S. Atomic Energy Commission, Declassified Document, Nov. 13, 1947.
[7] M. G. Evans, E. Warhurst, and E. Whittle, J. Chem. Soc. London, 1524 (1950).
[8] H. von Wartenberg, Z. Phys. Chem. Bod Fest, p. 61 (1931).
[9] O. A. Hougen and K. M. Watson, Chemical Process Principles, vol. II (John Wiley & Sons, Inc., New York, N. Y., 1947).
[10] Temperature, Its Measurement and Control in Science and Industry, p. 707 (Reinhold Publishing Corp., New York, N. Y., 1940).
[11] C. W. Jones, B. Lewis, J. B. Friauf, and C. St. J. Perrott, J. Am. Chem. Soc. **53,** 869 (1931).
[12] W. Bernheimer, Handbuch der Astrophysik IV, p. 5.
[13] O. Struve, Stellar Evolution, p. 9, 14, 64 (Princeton University Press, Princeton, N. J., 1950).
[14] J. L. Greenstein, Astrophys. J. **113,** 532 (1951).
[15] Aristid V. Grosse, Note on the use of silica-free glasses for handling anhydrous hydrogen fluoride and uranium hexafluoride, MDDC–1040, U. S. Atomic Energy Commission, Declassified Document, June 13, 1947.

Since this article was submitted for publication some new thermodynamic data have appeared which are considered to be more reliable. These data have been reviewed recently (Cole, Farber and Elverum, J. Chem. Phys. **20,** 4, 586, 1952) and include a value for the dissociation energy of fluorine and free energy data for the dissociation of fluorine and hydrogen fluoride into atoms. These data indicate fluorine and hydrogen fluoride to be less stable than the data used in the present article. The new value for the dissociation energy of fluorine is so close to the one used in this paper that it would have no direct effect on the calculated flame temperatures. However, some of the theoretical flame temperatures calculated using the new free energy data for the stability of fluorine and hydrogen fluoride are appreciably lower than those reported above. The flame temperatures at 1 atmosphere as a function of feed composition are changed as follows: 1,900° K to 1,900° K, (no change); 3,550° K to 3,500° K; 4,300° K to 4,000° K; 3,800° K to 3,600° K; and 1,200° K to 1,100° K.

The calculated flame temperatures at 10 and 100 atmospheres are changed to 4,400° and 5,100° K, respectively.

15. Effect of Flame-Generated Turbulence on Heat Transfer From Combustion Gases[1]

By Bela Karlovitz[2]

As a diversion from the fundamental papers presented at this symposium, I should like to talk on some practical possibilities which result from the studies of turbulent flames.

In our studies of turbulent flames we developed a theory of turbulent burning velocity in explosive mixtures with large-scale turbulence. Measurements carried out to test the validity of this theory showed that much higher intensity turbulence was required by the theory to account for the measured turbulent burning velocity than was present in the approach flow. This result led to the realization that turbulent flames generate additional turbulence.

The mechanism of turbulence generation by the turbulent flame can be easily understood from the following simple picture.

As shown in figure 15.1, the instantaneous flame front moves with velocity S_u into the unburned gas mixture. The burned gas moves away with velocity $[(V_2-V_1)/V_1]\ S_u$, relative to the unburned gas. Therefore the instantaneous flame front is a source of an additional velocity of magnitude $[(V_2-V_1)/V_1]\ S_u$. In the case of a laminar flame the orientation of this additional flame-introduced velocity vector is constant in time. In the case of a turbulent flame, as shown in figure 2, the instantaneous flame front fluctuates within the thick, diffuse, turbulent flame front. The orientation of every small portion of the instantaneous flame front changes constantly and with it the orientation of flame-introduced velocity vector $[(V_2-V_1)/V_1]S_u$. In the average this velocity vector of constant magnitude but fluctuating orientation will have an average forward velocity component $\overline{U}$ normal to the turbulent flame front. After this average forward velocity component is subtracted from the fluctuating velocity vector, the remaining velocity is distributed truly at random in magnitude as well as in orientation; therefore it constitutes turbulence generated by the turbulent flame.

By simple calculation we get for the average forward velocity the value

$$\overline{U}=\frac{V_2-V_1}{V_1}\,S_u\,\frac{S_u}{S_T},$$

where V_2 is the specific volume of the burned gas, V_1 the specific volume of the unburned gas, and S_T the turbulent burning velocity.

---

[1] This research is a part of the work being done at the Bureau of Mines on Contract NA–onr–25–47, NR–090–117, (33–038) 51–4151, supported by the Office of Naval Research and the Air Materiel Command.

[2] Physicist; head, Flame Research Section, Explosives and Physical Sciences Division, Bureau of Mines, Pittsburgh, Pa.

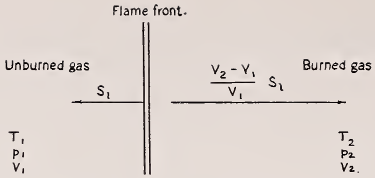

FIGURE 15.1. *Laminar flame front in an explosive mixture.*

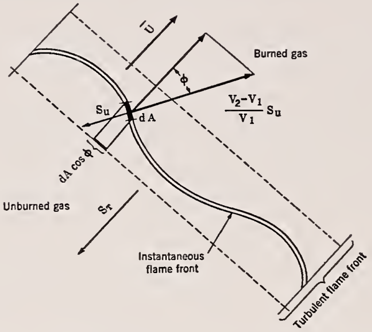

FIGURE 15.2. *Turbulence generation by the turbulent flame.*

The intensity of the flame-generated turbulence can be calculated from the energy equation

$$\bar{u}+\bar{v}+\bar{w}=\left(\frac{V_2-V_1}{V_1}S_u\right)^2-\left(\frac{V_2-V_1}{V_1}S_u\frac{S_u}{S_T}\right)^2,$$

where u, v, and w are the turbulent velocity components.

The first term on the right side is $2g$ times the kinetic energy of the flame-introduced velocity; the second term, $2g$ times the kinetic energy of $\bar{U}$, average forward velocity, all measured relative to the unburned gas. If turbulent burning velocity S_T is a few times larger than normal burning velocity S_u, the second term on the right side becomes negligible, and we obtain for the maximum value of the flame-generated turbulence:

$$\bar{u}^2+\bar{v}^2+\bar{w}=\left(\frac{V_2-V_1}{V_1}S_u\right)^2.$$

If uniform energy distribution is assumed among the three turbulence components, the intensity of the flame-generated turbulence is given by the formula:

$$u'=v'=w'=\frac{1}{\sqrt{3}}\left(\frac{V_2-V_1}{V_1}\right)S_u.$$

It was found that this maximal value of the flame-generated turbulence intensity agreed well with the turbulence intensities required by the theory to explain the measured turbulent burning velocity data for natural gas-air and for acetylene-air flames. These experimental results seem to substantiate the theories of turbulent burning velocity and of flame-generated turbulence. For a final test of these theories, direct measurement of the turbulence intensity in the flame will be necessary. At present, work is in progress to develop an electronic probe method for direct measurement of turbulence intensity in turbulent flames for this purpose.

At flow velocities up to a few hundred feet per second the flame-generated turbulence by far outweighs the turbulence of the approach flow, and therefore it has decisive influence on the turbulent-flame propagation. Similarly, the high-intensity turbulence generated by the turbulent flame has large influence on every mixing and heat transport phenomenon behind the flame.

Using the notation of the mixing-length theory the turbulent heat conductivity is

$$\lambda = c_p \rho l w',$$

where λ is turbulent heat conductivity; c_p, specific heat; ρ, density; l, mixing length; w', turbulence intensity. It follows that, under similar conditions, heat transport is proportional to turbulence intensity. Therefore, immediately behind the turbulent flame the heat-transfer rate is increased several times above the value that would be expected from the approach flow turbulence. This should be taken into account when heat transfer from flames or combustion gases is studied. Also it may be advantageous to apply premixed turbulent flames in industrial processes where heating at high temperatures is desired.

The turbulence generated by the flame is put into the gas flow only once. Therefore its intensity decays with increasing distance from the flame and it has probably negligible influence on the transmission of the heat content of the combustion gases at lower temperatures.

16. Astrophysicist's Concept of Temperature

By Hari K. Sen

The paper gives an account of deviations from thermodynamic equilibrium in stars, which have made the astrophysicist revise his concept of "temperature." Temperature of the solar and stellar atmospheres is now an "operational" concept, critically dependent on the method used to obtain it. Theoretical extensions of thermodynamic concepts designed to meet the nonthermodynamic cases are discussed, together with a recent investigation (unpublished) by the author on the effect of the non-Maxwellian electron velocity distribution in a shock front on certain apparent temperature anomalies in giant stars and in the solar chromosphere.

Perhaps no concept has proved so fruitful to the astrophysicist as the thermodynamic concept of the black body. Of course, stars cannot radiate as ideal black bodies. The very fact that we receive radiation from them proves that their radiation is not enclosed. Further, an isotropic and homogeneous radiation field cannot give rise to absorption or emission lines.

So, the astrophysicist, like any other scientist, had to proceed by plausible approximations to the ideal black body. The first important step in this direction was taken by Milne [1] who, in his own words, "got the best of both worlds" by introducing the concept of "local thermodynamic equilibrium," which is to say, in effect, that under favorable circumstances, sufficiently small elements of an extended material may be taken to enclose the radiation within it; e. g., on account of the high opacity of stellar material, small portions of the stellar interior may be taken to be isothermal and to radiate as a black body at the local temperature, though there is a temperature gradient in the star as a whole, which drives the radiation outwards.

Local thermodynamic equilibrium is found to hold suprisingly well in the reversing layers of stars as well, which give rise to absorption lines. Stars are found to radiate as black bodies if account is taken of the radiation dammed back in the absorption lines and reradiated to the photosphere. Fowler and Milne applied the thermodynamic Saha equation of ionization, and from the observed maxima of spectral-line intensities arranged the stars of different spectral types on a definite temperature scale.

Difficulties, however, soon appeared in attempts to fit a Planckian curve to the stellar radiation. These so-called "color temperatures" did not fit in with the Fowler-Milne scale for stars of certain spectral types. Closer home, ionospheric observations and rocket-borne spectra indicated that the sun does not radiate as a black body, particularly in the ultraviolet. The situation becomes worse as we ascend into the solar chromosphere, which shows the high potential lines of hydrogen and helium that could not possibly be excited by the low temperature ($\simeq$6,000° K) photospheric radiation field. And, to cap it all, the solar corona shows emission spectra of highly ionized atoms, which would demand a temperature of the order of a million degrees.

Speaking of the chromosphere in particular, measurements of the widths of emission lines indicate a temperature $\simeq$30,000° K, the Boltzmann distribution among the excited levels of helium and the metals indicates a temperature $\simeq$5,000° K, and the intensity distribution in the Balmer continuum, a temperature $\simeq$10,000° K. No further proof is needed of the fact that the solar chromosphere is not in thermodynamic equilibrium. Presumably other extended stellar atmospheres would show a similar behavior.

The astrophysicist, thus being forced to abandon the simple picture of black-body radiation, has come to regard temperature as an "operational" concept. The stellar atmosphere has no unique temperature. The temperature derived is critically dependent on the method used to measure it. Thus he speaks of the effective temperature as that obtained by matching the total radiation with that from a black body, the color temperature as obtained from the fitting of a Planckian curve, the excitation temperature as determined from the Boltzmann distribution among the excited levels, the ionization temperature as obtained from the maxima of spectral lines, and so forth. It is only in the case of complete thermodynamic equilibrium that all these temperatures are *one and the same*, and we can properly speak of *the* temperature of the stellar atmosphere.

Once it had been clearly recognized that solar and stellar atmospheres do show considerable deviations from thermodynamic equilibrium, attempts were made to find the counterparts of the thermodynamic concepts and equations in media not in equilibrium with the transmitted radiation. Rosseland [2], gave up the principle of detailed balancing, but retained the assumption of the statistical equilibrium of the different quantum states, and from this basis built his "theory of cycles," which explained the presence of bright lines in stellar spectra and fluorescence in dilute stellar radiation of planetary nebulae.

Most workers have confined themselves to the consideration of a medium whose particles have a Maxwellian velocity distribution at a temperature T_1, traversed by a radiation field, Planckian in intensity, at a temperature T_2 (diluted by a factor W, when necessary.)[1] The thermodynamic equations are modified by factors b_n, that are theoretically computed from statistical steady state considerations and observationally determined from line intensities. Menzel [3] has determined the chromospheric temperature and electron concentration by this method from measurements of the intensity in the Balmer continuum. He finds the b_n's converge toward unity with increasing n, as the higher electronic states tend to merge into the continuum.

Menzel obtains a temperature $\simeq$10,000° K for the electrons of the chromosphere, a value which is in agreement with Hagen's [4] estimate from observations of the radio intensity of the quiet sun in the centimetric range of wavelengths. Redman's [5] observations, however, of the widths of chromospheric lines indicate a kinetic temperature $\simeq$30,000° K. This is also the temperature required in order that the chromosphere may be in hydrostatic equilibrium at the observed low density gradient [6]. We see here, again, a failure of the black-body temperature concept. Since it is not known with certainty that the two phenomena originate at the same level, it is

---

[1] When $T_1 = T_2 = T$, we have the case of thermodynamic equilibrium at temperature T.

possible that the existence of different local temperatures may suffice to explain the observations. In the author's opinion, however, the difficulty lies deeper.

As the optical and the radio observations indicate two different electron temperatures, may this not be a case, not of departure from thermodynamic equilibrium only, but of departure from Maxwellian velocity distribution as well? The chromosphere seems to simulate in a mysterious fashion a medium which has at once a high and a low temperature. Now, the medium in a shock front acts precisely as such a bimodal atmosphere, partaking of the temperatures both before and behind the shock [7]. The stronger the shock, the greater is the departure from the Maxwellian distribution [8].

In a recent investigation (unpublished) the author has attempted to show that the shocks caused by the photospheric granules would be of sufficient frequency in the chromosphere to overcome the tendency of collisions to restore the Maxwellian distribution. The velocity distribution in the shock front would be non-Maxwellian, ultimately developing a hump that would accentuate with the shock strength, M. (See fig. 16.1.) This, so to say, "two temperature atmosphere" should qualitatively explain both the optical and the radio data: the Doppler widths should indicate the higher temperature, whereas the radio intensity,[2] the lower one. Detailed investigation of the absorption and emission effects in a shock front supports this conjecture.

---

[2] The intensity depends on the absorption coefficient that increases inversely as some power of the temperature.

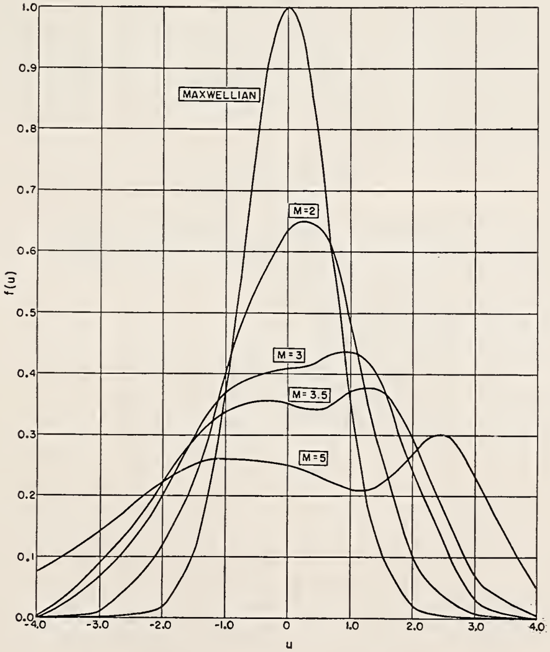

FIGURE 16.1. *Velocity distribution at center of shock front.*

If the above picture be correct, we would have to abandon the currently accepted view of the hydrostatic equilibrium of the chromosphere at a kinetic temperature of 30,000° K, and return to McCrea's [9] suggestion of support of the chromosphere by turbulent pressure.

The present method seems to the author to be capable of explaining some of the other anomalies in the solar chromosphere and the atmospheres of giant stars. We need an extension to non-Maxwellian velocity distributions of the Boltzmann and Saha equations of thermal equilibrium. As we ascend from the solar photosphere into the chromosphere, we see more granules; the shock frequency therefore increases, whereas the collision frequency decreases. Conditions are therefore more favorable for departure from Maxwellian distribution, the higher up we ascend into the chromosphere. According to this picture, the anomalies should increase with increasing height in the solar chromosphere and stellar atmospheres. This is precisely what is observed [5].

Regarding giant stars, we may note an interesting anomaly first pointed out by Struve [10]. The conventional curve of growth of δCMa indicated a turbulent motion ($\simeq$5 km/sec) much smaller than that obtained from line profiles ($\simeq$30 km/sec). Struve and Unsöld [11] explained this in terms of motions of turbulent elements much greater than the optical mean free path, which would affect the line profile but not the curve of growth. The author submits that, as a non-Maxwellian distribution in a shock front shows more pronounced Doppler broadening than absorption effects, it may make the curve of growth behave differently from the line profile, as observed.

The author would wish to conclude with the remark that the astrophysicist's preoccupation with solar and stellar atmospheres in his revision of the temperature concept is not purely academic. The solar chromosphere and corona, and the highly turbulent atmospheres of giant stars, are Nature's gigantic laboratories for the testing of new physical theories of turbulence, shock waves, and departures from thermodynamic equilibrium.

References

[1] E. A. Milne, Handbuch der Astrophysik **III/1,** 65, 1930.
[2] S. Rosseland, "Theoretical Astrophysics", 1936, p. 140.
[3] Menzel and Cillie, Harv. Circ. **410,** 1935; Ap. J. **85,** 88, 1937.
[4] J. P. Hagen, Ap. J. **113,** 547, 1951.
[5] R. O. Redman, M. N. **102,** 140, 1942.
[6] R. Wildt, Ap. J. **105,** 36, 1947.
[7] H. M. Mott-Smith, Phys. Rev. **82,** 885, 1951.
[8] J. F. Denisse and Y. Rocard, J. de Phys. et le Rad., **12,** 893, 1951.
[9] W. H. McCrea, M. N. **89,** 718, 1929; **95,** 80, 1934.
[10] O. Struve, Ap. J. **104,** 138, 1946.
[11] A. Unsöld and O. Struve, Ap. J. **110,** 454, 1949.

U. S. GOVERNMENT PRINTING OFFICE: 1954